

ISTANBUL TECHNICAL UNIVERSITY ★ GRADUATE SCHOOL OF SCIENCE
ENGINEERING AND TECHNOLOGY

***IN VITRO* SKELETAL MUSCLE MODEL DEVELOPMENT THROUGH CO-
CULTURE OF CELLS**



Ph.D. THESIS

Ayşe Burcu ERTAN

Department of Molecular Biology-Genetics and Biotechnology

Molecular Biology-Genetics and Biotechnology Programme

JUNE 2017

ISTANBUL TECHNICAL UNIVERSITY ★ GRADUATE SCHOOL OF SCIENCE
ENGINEERING AND TECHNOLOGY

***IN VITRO* SKELETAL MUSCLE MODEL DEVELOPMENT THROUGH CO-
CULTURE OF CELLS**

Ph.D. THESIS

**Ayşe Burcu ERTAN
(521092061)**

Department of Molecular Biology-Genetics and Biotechnology

Molecular Biology-Genetics and Biotechnology Programme

**Thesis Advisor: Assoc. Prof. Dr. Fatma Neşe KÖK
Thesis Co-Advisor: Prof. Dr. Gamze TORUN KÖSE**

JUNE 2017

İSTANBUL TEKNİK ÜNİVERSİTESİ ★ FEN BİLİMLERİ ENSTİTÜSÜ

***IN VITRO* İSKELET KAS MODELİNİN ORTAK-KÜLTÜR ARACILIĞIYLA
GELİŞTİRİLMESİ**

DOKTORA TEZİ

**Ayşe BurcuERTAN
(521092061)**

Moleküler Biyoloji-Genetik ve Biyoteknoloji Anabilim Dalı

Moleküler Biyoloji-Genetik ve Biyoteknoloji Programı

**Tez Danışmanı: Doç. Dr. Fatma Neşe KÖK
Eş Danışman: Prof. Dr. Gamze TORUN KÖSE**

HAZİRAN 2017

Ayşe Burcu ERTAN, a Ph.D. student of İTÜ Graduate School of Science Engineering and Technology student ID 521092061, successfully defended the thesis entitled “In Vitro Skeletal Muscle Model Development Through Co-Culture of Cells”, which she prepared after fulfilling the requirements specified in the associated legislations, before the jury whose signatures are below.

Thesis Advisor : **Assoc. Prof. Dr. Fatma Neşe KÖK**
ISTANBUL Technical University

Co-advisor : **Prof.Dr. Gamze TORUN KÖSE**
Yeditepe University

Jury Members : **Prof. Dr. Ayten YAZGAN KARATAŞ**
ISTANBUL Technical University

Prof. Dr. Zeynep Petek ÇAKAR
ISTANBUL Technical University

Prof. Dr. Nevin GÜL - KARAGÜLER
ISTANBUL Technical University

Assoc. Prof. Dr. Halime KENAR
Kocaeli University

Assist. Prof. Dr. Deniz YÜCEL
Acıbadem University

Date of Submission : 29 May 2017

Date of Defense : 21 June 2017





To my family,



FOREWORD

First of all, I would like to thank my supervisors Assoc. Prof. Dr. Fatma Neşe K k and Prof. Dr. Gamze Torun K se. This thesis would not be completed without their mentorship and commitment. Their willingness to provide guidance and assistance at anytime is something that I will always be thankful for.

I would also express my sincere gratitude to Assoc. Prof. Dr. Halime Kenar for her guidance to me. Her dedication and passion for science always gave me an inspiration.

I also would like to acknowledge members of Yeditepe University Tissue Engineering Group (YUTEG) Semih Arbatlı, G rke G rel Pek zer, A. Ceren  alıkođlu Koyuncu, Ay eg l Atasoy Zeybek, G rkem Cemali, Nergis Abay, Ezgi İrem Bekta , Asli Karacan and other colleagues; Dr. Dil ad Yurdakul, Ergi Terziođlu, Dr. Esra  oban, Binnur Kıratlı, Bur in Asutay for their support and motivation during my studies.

I would like to thank to Prof. Dr. Ayten Yazgan Karata  and Prof. Dr. Zeynep Petek  akar as my jury members during the thesis and their guidance and sincere understanding.

I would like to thank to my family members who always bring sunshine and pure happiness to my life. I will always be gratefull to my parents for their precious support and inspiration for me. This thesis also dedicated to their souls and my grandmother who passed away last year.

June 2017

Ay e Burcu ERTAN

TABLE OF CONTENTS

	<u>Page</u>
FOREWORD	ix
TABLE OF CONTENTS	xi
ABBREVIATIONS	xiii
LIST OF TABLES	xv
LIST OF FIGURES	xvii
SUMMARY	xxi
ÖZET	xxv
1. INTRODUCTION	1
1.1 Muscle Tissue	4
1.1.1 Smooth Muscle	5
1.1.2 Cardiac Muscle.....	6
1.1.3 Skeletal Muscle horizontally.....	6
1.2 Muscle Contraction	7
1.3 The Control of Muscle Contraction	12
1.3.1 The Role of Ca ⁺⁺ in Contraction.....	12
1.3.2 Nerves Stimulate Contraction	13
1.3.3 Motor Units and Recruitment.....	14
1.4 Types of Muscle Fibers	15
1.5 Muscle Metabolism during Rest and Exercise	16
1.6 Stem Cells	17
1.6.1 Embryonic Stem Cells	17
1.6.2 iPSCs.....	18
1.6.3 Adult Stem Cells	19
1.7 Aim of the Thesis	25
2. MATERIALS AND METHODS	27
2.1 Human Skeletal Muscle Stem Cell Isolation	27
2.2 Human Skeletal Muscle Stem Cell Characterization by Flow Cytometry	28
2.3 Myotube formation	28
2.4 Neuron-like Cell Differentiation	29
2.5 Neuron-like Cell Characterization by Immunostaining	29
2.6 Isolation of HUVECs	30
2.7 Co-Culture of hSkMSCs and HUVECs	30
2.8 <i>In vitro</i> human skeletal muscle model: co-culture of myotubes, neuron-like cells and the capillary network	31
2.9 Real-Time PCR	32
2.10 Live cell imaging	33
2.11 Electrophysiological Study	35

2.12 Study Summary Schema.....	35
3. RESULTS AND DISCUSSION	37
3.1 Human Skeletal Muscle Stem Cell Characterization.....	37
3.2 Neuron-like Cell Differentiation and Characterization.....	40
3.3 Characterization of HUVECs by Immunocytochemistry.....	43
3.4 Co-Culture of hSkMSCs and HUVECs	44
3.5 <i>In vitro</i> human skeletal muscle model: co-culture of myotubes, neuron-like cells and the capillary network	49
3.6 Real-Time PCR.....	52
3.7 Live cell imaging.....	53
3.8 Electrophysiological Study	59
4. CONCLUSIONS	61
REFERENCES	63
APPENDICES	73
CURRICULUM VITAE	735



ABBREVIATIONS

3D	: Three dimensional
ACh	: Acetylcholine
ADP	: Adenozin difosfat
ATP	: Adenozin trifosfat
ATPase	: Adenozin trifosfatase
BF	: Brightfield
bFGF	: Basic fibroblast growth factor
Ca⁺⁺	: Calcium ion
cDNA	: complementary deoxyribonucleic acid
CFDA, SE	: carboxyfluorescein diacetate succinimidyl ester
CFSE	: 5(6)-Carboxyfluorescein diacetate N-succinimidyl ester
CM-DiI	: Chloromethylbenzamido
c-Myc	: Cellular Myc
dH₂O	: Distilled water Reverse transcription
DMEM/F12	: Dulbecco's Modified Eagle's Medium/Nutrient F-12
DMSO	: Dimethylsulfoxide
ECM	: Extracellular matrix
EGM-2	: Endothelial cell growth medium-2
ENO2	: Enolase 2
ESC	: Embryonic stem cell
FBS	: Fetal bovine serum
FSC	: Fetal stem cells
GAPDH	: Glyceraldehyde-3-phosphate dehydrogenase
GCSF	: Granulocyte colony-stimulating factor
GF	: Growth factor
GFAP	: Glial fibrillary acidic protein
GM	: Growth medium
GvHD	: Graft-versus-host disease
HBSS	: Hank's balanced salt solution
HSC	: Hematopoietic stem cell
hSkMSCs	: Human skeletal muscle stem cells
HUVECs	: Human umbilical vein endothelial cells
ICM	: Inner cell mass
iPSCs	: Induced pluripotent stem cells
Klf4	: Kruppel-like factor 4
M-CSF	: Macrophage colony stimulating factor
MHC	: Major histocompatibility complex
mRNA	: Messenger ribonucleic acid
MSC	: Mesenchymal stem cells
MYOG	: Myogenin
NEFH	: Neurofilament, heavy polypeptide

NEFL	: Neurofilament, light polypeptide
Oct4	: Octamer-binding transcription factor 4
PBS	: Phosphate buffered saline
PCR	: Polymerase chain reaction
Pi	: Inorganic phosphate
PSA	: Penicillin-Streptomycin-Amphotericin
RT-PCR	: Reverse transcription polymerase chain reaction
Sox2	: Sex determining region Y)-box 2
SR	: Sarcoplasmic reticulum
TNF-α	: Tumor necrosis factor alpha
VEGF	: Vascular endothelial growth factor



LIST OF TABLES

	<u>Page</u>
Table 1.1: Muscle tissues localization, function, characteristic cell types.	5
Table 2.1: Media types tested in the co-culture of hSkMSCs and HUVECs, and their FBS contents. Media mixtures were prepared in 1:1 volumetric ratio.	31
Table 2.2: Sequences used for real-time PCR analysis were GAPDH (glyceraldehyde-3-phosphate dehydrogenase) as housekeeping gene; neural progenitor marker; nestin; neuronal marker beta-tubulin3; neuronal marker ENO2 (enolase 2, gamma, neuronal); myogenic marker MYOG (myogenin); precursor neuroprogenitor cell markers NEFH (neurofilament) and NEFL (neurofilament).	33



LIST OF FIGURES

	<u>Page</u>
Figure 1.1: A muscle cell, also called muscle fiber consists of many myofibrils which consist of two filaments called actin and myosin. A muscle fiber contains many nuclei because of embryonic fusion of smaller cells. Muscle cells have a modified endoplasmic reticulum called the sarcoplasmic reticulum.....	7
Figure 1.2: The skeletal muscle is organized into numerous fascicles, also referred to a bundle of muscle cells or fibers. A single fiber consists of numerous myofibrils, which are then made up of myofilaments.....	8
Figure 1.3: When observed under an electron microscope, the Z lines act as border lines of sarcomeres and are clearly observed within each myofibril. The thick filaments comprise the A bands; the thin filaments are within the I bands and stick partway into the A bands, overlapping with the thick filaments. There is no overlap of thick and thin filaments at the central region of an A band, which is therefore lighter in appearance. This is the H band.	8
Figure 1.4: Electron micrograph (a) and diagram (b) of the sliding filament mechanism of contraction. As the thin filaments slide deeper into the centers of the sarcomeres, the Z lines are brought closer together. (1) Relaxed muscle; (2) Partially contracted muscle.	9
Figure 1.5: Thick filaments are composed of myosin. (a) Each myosin molecule consists of two polypeptide chains wrapped around each other; at the end of each chain is a globular region referred as the “head” (b) Thick filaments consist of myosin molecules combined into bundles from which the heads protrude at regular intervals.....	10
Figure 1.6: Thin filaments are composed of globular actin proteins. Two rows of actin proteins are twisted together in a helix to produce the thin filaments	10
Figure 1.7: Thin and thick filament interaction: In striated muscle sarcomeres, there is a thin and thick filament. The heads of the thick filaments face opposite directions. (a) This allows the cross bridges to pull the thin filaments and Z lines on the side of sarcomeres towards the center. (b) When this happens, there is a sliding of the filaments, which then produces a muscle contraction.	11
Figure 1.8: The cross-bridge cycle in muscle contraction. (a) With ADP and Pi attached to the myosin head. (b) The head is in a conformation that can bind to actin and form a crossbridge. (c) Binding causes the myosin head to assume a more bent conformation, moving the thin filament along the thick filament and releasing ADP and Pi. (d) Binding of ATP to the head detaches the cross-bridge; cleavage of ATP into ADP and Pi puts the head into its original conformation, allowing the cycle to begin again. .	11

Figure 1.9: Calcium controls striated muscle contraction. (a) A long filament of the protein tropomyosin, when the muscle is at rest, blocks the myosin-binding sites on the actin molecule. (b) When Ca ⁺⁺ binds to troponin, the Ca ⁺⁺ -troponin complex displaces tropomyosin and exposes the myosin-binding sites on actin, permitting cross-bridges to form and contraction to occur.	12
Figure 1.10: The relationship between the myofibrils, transverse tubules, and sarcoplasmic reticulum. Impulses travel down the axon of a motor neuron that synapses with a muscle fiber.....	13
Figure 1.11: A neuron has a very long projection called an axon.....	14
Figure 1.12: The number and size of motor units. (Left) Weak, precise muscle contractions use smaller and fewer motor units. (Righth) Larger and stronger movements require additional motor units that are larger.....	15
Figure 1.13: Muscle twitches summate to produce a sustained, tetanized contraction. This pattern is produced when the muscle is stimulated electrically or naturally by neurons. Tetanus, a smooth, sustained contraction, is the normal type of muscle contraction in the body (Raven and Johnson, 2002).....	16
Figure 1.14: The myotube fusion and maturation into myofibers (Rendl, 2004).	24
Figure 2.1: Live cell imaging system, Olympus IX81 Life Science Imaging System.	34
Figure 2.2: Schema of studies conducted.....	36
Figure 3.1: Phase contrast micrographs of human skeletal muscle derived cells after 4 days of incubation; A) cells at the preplate, B) skeletal muscle myoblast colonies in the flask. Arrows point the myoblast colonies. Scale bars represent ~ 100 μm.	37
Figure 3.2: Myotubes obtained by fusion of myoblasts in DMEM/F12 medium with 10% FBS. BF image of myotubes immunohistochemically stained for desmin after 7 days of culture. Scale bar represent ~ 100 μm.	38
Figure 3.3: Myotubes obtained by fusion of myoblasts in DMEM/F12 medium with 10% FBS. Phase contrast micrograph of myotubes obtained after 14 days of culture. Arrows point the multinucleated myotubes. Scale bars represent ~ 100 μm.	39
Figure 3.4: Flow cytometry histograms of human skeletal muscle stem cell surface antigens: CD44, CD90, CD45, CD34, CD105 and their isotype control.	39
Figure 3.5: Confocal micrographs of hSkMSCs subjected to neuronal differentiation and stained for beta-tubulin3: green, GFAP: red, nuclei (DAPI): blue...	41
Figure 3.6: Confocal micrograph of hSkMSCs subjected to neuronal differentiation and stained for beta-tubulin3: green, Nestin: red, nuclei (DAPI): blue. Cells were negative for GFAP which is an astrocyte marker and positive for nestin and beta-tubulin3.....	42
Figure 3.7: Human umbilical vein endothelial cells (HUVECs) in culture after 4 days of incubation. Phase contrast micrograph of HUVECs. Scale bar represents ~ 100 μm.	43
Figure 3.8: Human umbilical vein endothelial cells (HUVECs) in culture at passage 2. Fluorescence micrograph of HUVECs immunostained for their cell surface marker CD31 (green).	44

Figure 3.9: Confocal micrographs of hSkMSC-HUVECs co-cultured in DMEM/F12 medium supplemented with 5% FBS (D5), (A) 5X, (B) 10X. CD31: green, Desmin: red, nuclei (DAPI): blue.....	45
Figure 3.10: Confocal micrographs of hSkMSC-HUVECs co-cultured in DMEM/F12 medium supplemented with 10% FBS (D10), (A) 5X, (B) 20X. CD31: green, Desmin: red, nuclei (DAPI): blue.....	45
Figure 3.11: Confocal micrographs of hSkMSC-HUVECs co-cultured in DMEM/F12 medium supplemented with 20% FBS (D20), (A) 5X, (B) 10X. CD31: green, Desmin: red, nuclei (DAPI): blue.....	46
Figure 3.12: Confocal micrographs of hSkMSC-HUVEC co-cultured in DMEM/F12 10% FBS: EGM-2 (1:1) (D10-E2). (A) 5X, (B) 10X. CD31: green, desmin: red, cell nuclei (DAPI): blue.....	47
Figure 3.13: Confocal micrographs of hSkMSC-HUVEC co-cultured in DMEM/F12 5% FBS: EGM-2 (1:1) media (D5-E2). (A) 5X, (B) 10X. CD31: green, desmin: red, cell nuclei (DAPI): blue.....	47
Figure 3.14: Confocal micrographs of hSkMSC-HUVEC co-cultured in DMEM/F12 20% FBS: EGM-2 (1:1) media (D20-E2). (A) 5X, (B) 10X CD31: green, desmin: red, cell nuclei (DAPI): blue.....	48
Figure 3.15: Confocal micrographs of (A, B) neuron-like cells in association with myotubes in the human <i>in vitro</i> skeletal muscle model formed by co-culturing myotubes, capillary networks and the neuron-like cells for 24h. Beta-tubulin3: green, desmin: red, cell nuclei (DAPI): blue.....	49
Figure 3.16: Sequential confocal micrographs of a Z-stack of capillary network and myotubes in human <i>in vitro</i> skeletal muscle model formed by co-culturing myotubes, capillary networks and the neuron-like cells for 24h. CD31: green, desmin: red, cell nuclei (DAPI): blue. Scale bar: 50 μ m..	51
Figure 3.17: NEFH (396 bp) , 7 NEFL (283 bp), ENO2 (269 bp) PCR products. Marker: DNA Ladder 50-1000 bp.....	52
Figure 3.18: Nestin (302 bp) and MYG (279 BP) PCR products. Marker: DNA Ladder 50-1000 bp.	52
Figure 3.19: Beta-tubulin3 (175 bp) PCR products. Marker: DNA Ladder 100-1000 bp.....	53
Figure 3.20: hSkMSCs with complete neural differentiation medium at day 1 and examined for 3 hours with live cell imaging system (A,B) (10x).....	53
Figure 3.21: hSkMSCs with complete neural differentiation medium at day 1 and examined for 48 hours with live cell imaging system (A-D) (40x).	54
Figure 3.22: hSkMSCs incubated for 72 hours in complete neural differentiation medium and examined for 6 hours with live cell imaging system (A-D) (10x).	55
Figure 3.23: hSkMSCs stained with CellTracker™ CM-DiI (Orange) at day 3 (4x).	56
Figure 3.24: hSkMSCs and HUVECs stained with CellTracker™ CM-DiI (Orange) and CFSE (Green), respectively, at day 1.	57
Figure 3.25: hSkMSCs and HUVECs stained with CellTracker™ CM-DiI (Orange) and CFSE (Green), respectively, at day 1 and examined for 6 hours. HUVECs were found with nuclear fragmentation which is the indication of apoptosis (A-D).....	58
Figure 3.26: hSkMSCs and HUVECs stained with CellTracker™ CM-DiI (Orange) and CFSE (Green), respectively. Samples incubated for 2 days after live cell imaging (A, B).....	58

Figure 3.27: Electrophysiological muscle contraction study with the myotubes obtained by fusion of myoblasts. Arrows point the contraction side of the cells (10x).....**59**



***IN VITRO* SKELETAL MUSCLE MODEL DEVELOPMENT THROUGH CO-CULTURE OF CELLS**

SUMMARY

Skeletal muscle defects occur because of several reasons and as a promising interdisciplinary approach, skeletal muscle tissue engineering aims the reconstruction of this loss. Transfer of an adjacent muscle tissue in a pediculated form or a distant one as a free flap is a method often applied in treatment of muscular defects and losses but there are limitations for autologous grafting because of the difficulty in procuring donor tissue. Generating new muscle tissue from autologous precursor cells (stem cells) attempts to address this problem via skeletal muscle tissue engineering.

The most preferred source of cells for skeletal muscle tissue engineering applications is either a myoblast cell line or the primary satellite cells that can easily be obtained by muscle biopsies and cultured *in vitro*. Transplanted satellite cells can take part in muscle regeneration and contribute to the satellite cell population in host animals. This makes satellite cells perfect candidates for cell based transplantation therapy for muscle degeneration. Incapability of self-renewal, defective migration of donor cells after transplantation, host immune defense and poor survival are the factors that have affected therapeutic use of satellite cells in clinics. Satellite cells are characterized as a heterogeneous population of progenitors and stem cells. More comprehensive understanding on satellite cell hierarchy is needed at single cell level and their performance should be followed over time.

Skeletal muscle that contains *in vivo* functionality requires the induction of main types of tissues such as vascular, nervous, muscle and connective tissues. Henceforth, numerous connective tissues cover the different muscle bundle, the muscle fibers and the whole muscle, while a skeletal muscle is instilled by capillaries and joined to the nerve branches. Vascularization is an important concern in capacious tissues having high oxygen demand such as the skeletal muscle. It is responsible for the storage and breakdown of glucose and fat since it is a highly metabolic organ. On top of that, skeletal muscle is the primary tissue accountable for the augmented glucose metabolism during exercise and hyperinsulinemia. It is a challenge to mimic this complex system *in vitro* conditions.

Myofiber is large single cell which is formed by fusion of many cells during development. Bundling of these muscle fibers leads to muscle formation. Skeletal muscle cells are innervated by motor neurons. Each neuron can control a small number of myofibers and fires a contraction. There is a need for neuronal stimulation

during myogenesis. With the help of tissue engineering principles, differentiated skeletal muscle tissue can be restored by utilizing multiple stem or progenitor cells from different sources. Self regeneration of mature muscle fibers that are vascularized and multinucleated is not possible because of terminal differentiation. Satellite cells or myoblasts are capable of maintaining the regenerative potential of injured muscle tissue.

As it is common in other tissues, the vascular network in skeletal muscle contains arteries splitting into increasingly smaller vessels. In skeletal muscle, a terminal arteriole gives rise to collections of capillaries that run parallel to muscle fibers, and each muscle fiber can be supplied by numerous unlike groups of capillaries from independent terminal arterioles.

As the other invaluable component of the muscle tissue, *in vitro* establishment of innervation by the motor neurons would better mimic the native tissue and provide an opportunity to test the effect of drugs targeting the neuromuscular junctions. Both innervated and vascularized human muscle tissue construct is expected to have a reduced time for functional integration in the body and eliminate the species-related variability associated with animal-based systems when used in drug discovery and toxicology studies.

This study presents a report on the generation of a novel human muscle tissue model using skeletal muscle derived stem cells and human umbilical vein endothelial cells (HUVECs).

In this study, isolation of skeletal muscle stem cells was carried out by pre-plate method. They were differentiated into neuron-like cells that were negative for the astrocyte marker glial fibrillary acidic protein (GFAP) and positive for neuronal beta-tubulin III and nestin.

Satellite cells matured *in vitro* into myoblasts and fused with each other and create the myotubes. Capillary network and multinucleated myotube formation were provided by the co-culture of skeletal muscle stem cells with the HUVECs under optimized fetal bovine serum and media conditions. Cells were immunostained for the myogenic marker desmin and the endothelial marker CD31. It was observed that HUVECs did not survive in a DMEM/F12 medium, supplemented with 5%, 10% and 20% FBS. When EGM-2 medium was mixed with DMEM/F12, however, the HUVECs survived and proliferated. The best media combination for the formation of both myotubes and capillary networks was found as DMEM/F12 (10% FBS):EGM-2 (2% FBS) (1:1) mixture.

The seeding of the neuron-like cells derived from the human skeletal muscle stem cells was performed on the vascularized myotubes to form neuromuscular junctions. It was found that the neuron-like cells were in contact with the myotubes after 24 hours of co-culture. Real time observation with time lapse imaging used in order to investigate neural differentiation of human skeletal muscle derived stem cells (hSkMSCs) and the behavior of cells in co-culture conditions. Finally, electrophysiological study was carried out and contraction of the multinucleated cells was observed under the phase contrast microscope.

This study presents a novel *in vitro* human skeletal muscle model with advanced capillary networks with an interaction of myotubes and neurons, and it can be utilized in the *in vitro* testing of drugs and also used for the regeneration of skeletal

muscles by means of cellular therapy or cell-laden tissue engineered muscle constructs.





IN VITRO İSKELET KAS MODELİNİN ORTAK-KÜLTÜR ARACILIĞIYLA GELİŞTİRİLMESİ

ÖZET

İskelet kası kusurları çeşitli sebeplerden oluşabilir ve iskelet kas doku mühendisliği bu kaybın yeniden inşasını amaçlayan umut verici bir disiplinler arası yaklaşımdır. Kas dokusunun pedikül halinde yandaki ya da serbest halde uzaktaki kas dokusuna aktarılması, kas kusurlarının ve kayıplarının tedavisinde sıklıkla uygulanan bir yöntemdir, ancak, donör dokunun temin edilmesinin zor olması nedeniyle otolog greftleme için sınırlamalar vardır. İskelet kas dokusu mühendisliği, otolog öncü hücrelerden (kök hücreler) yeni kas dokusu üretimi sağlayarak bu sorunu çözmeye çalışır.

İskelet kası dokusu mühendisliği uygulamaları için en çok tercih edilen hücre kaynakları, miyoblast hücre hattı ya da kas biyopsileri ile kolayca elde edilebilen ve *in vitro* kültürlenmiş uydu (satellit) hücreleridir. Nakledilen uydu hücreleri kas rejenerasyonuna katılabilir ve konakçı hayvanlarda uydu hücre popülasyonuna katkıda bulunurlar. Bu, uydu hücrelerini, kas dejenerasyonunda hücre bazlı transplantasyon tedavisi için mükemmel bir aday haline getirir. Kendi kendini yenilemenin yetersizliği, nakilden sonra donör hücrelerin kusurlu göçü, konakçının immün savunması ve hayatta kalma olasılığının azlığı, uydu hücrelerinin kliniklerdeki terapötik kullanımını etkileyen faktörlerdir. Uydu hücreleri, öncül hücre ve kök hücrelerden oluşan heterojen bir popülasyon olarak karakterize edilmiştir. Uydu hücresi hiyerarşisi hakkında tek hücre seviyesinde yapılacak daha kapsamlı bir araştırma gereklidir ve bunların performansı zamanla takip edilmelidir.

In vivo işlevsellik içeren iskelet kası, vasküler, sinir, kas ve bağ dokuları gibi ana doku türlerinin indüksiyonunu gerektirir. Bundan böyle çeşitli kas dokuları; kas lifleri ve kasın tamamını kaplarken, iskelet kası kılcal damarlarla sarılır ve sinir dallarına bağlanır. Damarlanma, iskelet kası gibi yüksek oksijen ihtiyacı olan geniş dokularda önemli bir sorundur. Kas, oldukça metabolik bir organ olduğu için glikoz ve yağın depolanması ve parçalanmasından sorumludur. Ayrıca iskelet kası, egzersiz ve hiperinsülinemi sırasında artmış glukoz metabolizmasının sorumlu olduğu birincil dokudur. Bu kompleks sistemi *in vitro* koşullarda taklit etmek bir zorlu görevdir.

Miyofiber, gelişme süresince birçok hücrenin birleşmesi ile oluşan geniş tek bir hücredir. Bu kas liflerinin bir araya toplanması kas oluşumuna neden olur. İskelet kası hücreleri motor nöronlar tarafından innerve edilir. Her nöron, az sayıda miyofiberi kontrol edebilir ve kasılmasına yardımcı olur. Miyogenez sırasında nöronal stimülasyona ihtiyaç vardır. Doku mühendisliği prensipleri yardımıyla, farklı

kaynaklardan çok sayıda kök veya öncü hücreler kullanılarak farklılaştırılmış iskelet kası dokusu restore edilebilir. Vaskülarize edilmiş ve çok çekirdekli olgun kas liflerinin kendiliğinden rejenerasyonu, özelleşmenin sonlanması nedeniyle mümkün değildir. Uydu hücreleri veya miyoblastlar, yaralı kas dokusunun rejeneratif potansiyelini koruyabilir.

Diğer dokularda da olduğu gibi, iskelet kasındaki damar ağı, giderek artan daha küçülerek dallanır. İskelet kasında, özelleşmiş arteriyol kas liflerine paralel çalışan kılcal damarlar oluşumlarına neden olur ve her kas lifi, bağımsız özelleşmiş arteriyollerin oluşturduğu kılcal gruplar tarafından beslenebilir.

Kas dokusunun diğer paha biçilemez bileşeni olarak, motor nöronlar tarafından *in vitro* innervasyonun kurulması doğal dokuyu taklit ederek nöromüsküler kavşakları hedef alan ilaçların etkisini test etme fırsatı sağlar. Hem innerve hem de vaskülarize olan insan kas dokusu vücutta fonksiyonel dokuların oluşturulması için bize zaman kazandırırken, ilaç keşfi ve toksikoloji çalışmalarında kullanıldığında hayvan temelli sistemler arasındaki değişkenleri de ortadan kaldırır.

Bu çalışma, iskelet kası kökenli kök hücreler ve insan umbilikal damar endotel hücreleri (HUVEC) kullanılarak yeni bir insan kas dokusu modeli oluşturulması üzerine bir araştırma sunmaktadır.

Bu çalışmada, İskelet kası kök hücrelerinin izolasyonu pre-plate yöntemi ile gerçekleştirilmiştir. Hücreler, astrosit belirteci glial fibriler asidik protein (GFAP) için negatif ve nöronal beta-tubulin III ve nestin için pozitif nöron-benzeri hücrelere farklılaştırılmıştır. Kılcal ağ ve çok çekirdekli miyotüp oluşumu, optimize konsantrasyonda fetal sığır serumu kullanımı ve uygun ortam koşulları altında iskelet kası kök hücrelerinin HUVEC'lerle birlikte ortak-kültürlenmesi ile sağlanmıştır.

In vitro koşullarda uydu hücreleri, miyoblastlara olgunlaştırılmış ve birleşmeleri sağlanarak miyotüpler oluşturulmuştur. Kılcal ağ ve çok çekirdekli miyotüp oluşumu, fetal sığır serumu ve ideal ortam koşulları altında iskelet kası kök hücrelerinin HUVEC'lerle birlikte kültürlenmesiyle sağlanmıştır. Hücreler, miyojenik belirteç desmin ve endotelial belirteç CD31 için immünolojik olarak boyanmıştır. HUVEC'lerin, % 5, % 10 ve % 20 FBS ile takviye edilmiş bir DMEM / F12 ortamında hayatta kalmadığı gözlenmiştir. Bununla birlikte, EGM-2 ortamı DMEM / F12 ile karıştırıldığında, HUVEC'ler hayatta kalmış ve çoğalmışlardır. Hem miyotüplerin hem de kılcal damar ağlarının oluşturulması için en iyi ortam kombinasyonu, DMEM / F12 (% 10 FBS): EGM-2 (% 2 FBS) (1: 1) karışımı olarak bulunmuştur.

İnsan iskelet kası kök hücrelerinden üretilen nöron benzeri hücrelerin vaskülarize miyotüpler üzerine ekilmesi ile nöromüsküler kavşaklar oluşturulmuştur. Nöron benzeri hücrelerin, ortak- kültürden 24 saat sonra miyotüplerle temas ettiği bulunmuştur. İnsan iskelet kası kaynaklı kök hücrelerin (hSkMSC) sinirsel farklılaşmasını ve ortak-kültür koşullarında hücrelerin davranışını araştırmak için, hızlandırılmış zaman görüntüleme tekniği ile gerçek zamanlı gözlem yapılmıştır. Son olarak elektrofizyolojik çalışma ile çok çekirdekli hücrelerin kasılması faz kontrast mikroskopu altında gözlenmiştir.

Bu çalışma, miyotüplerin ve nöronların etkileşimiyle geliştirilmiş kılcal ağlarla yeni bir *in vitro* insan iskelet kası modeli sunmaktadır. Bu model, ilaçların *in vitro* testinde ve ayrıca hücresel terapi yoluyla iskelet kaslarının yenilenmesi çalışmasında

ya da hücre içeren doku mühendisliği biyomalzemeleri kullanılarak oluşturulacak kas yapılarının elde edilmesinde kullanılabilir.



1. INTRODUCTION

Traumatic injury, congenital defects or tumor ablations cause skeletal muscle defects and as a promising interdisciplinary approach, skeletal muscle tissue engineering aims the reconstruction of this loss. Transfer of an adjacent muscle tissue in a pediculated form or a distant one as a free flap is a method often applied in treatment of muscular defects and losses but there are limitations for autologous grafting because of the difficulty in procuring donor tissue. The goal here is sometimes just to cover the defect but this approach may also be used to restore the functionality of a contractile muscle. However, long and difficult surgical procedures are required and donor site morbidity often causes an additional burden for the patient. In some cases, the muscles that are used for coverage does not have the neural transmission, therefore, secondary surgeries are carried out to provide neurotization and innervation. Generating new muscle tissue from autologous precursor cells (stem cells) attempts to address this problem via skeletal muscle tissue engineering (Guettier-Sigrist et al., 1998).

Skeletal muscle contains basically three major cell types: myofibers, neurons, and endothelial cells, that are actively involved in the muscle contraction phenomenon. Myofibers are large single cells which are formed by fusion of many cells during development. Bundling of these muscle fibers leads to muscle formation (Sjøgaard et al., 2014). Skeletal muscle cells are innervated by motor neurons. Each neuron can control a small number of myofibers and fires a contraction. There is a need for neuronal stimulation during myogenesis (Pette et al., 2002). With the help of tissue engineering principles, differentiated skeletal muscle tissue can be restored by utilizing multiple stem or progenitor cells from different sources.

Self regeneration of mature muscle fibers that are vascularized and multinucleated is not possible because of terminal differentiation. Satellite cells or myoblasts, first described by Mauro in 1961, are the cells that give the muscle tissue the ability to regenerate itself. Muscle injury causes myoblast activation by external stimuli.

They reenter the mitotic cell cycle and form new myofibers or fuse with damaged myofibers (Laumonier and Menetrey, 2016). Some of the cells reenter the G0 state and therefore, are capable of maintaining the regenerative potential of injured muscle tissue (Dhawan and Rondo, 2005; Sinanan et al., 2006; Dumont et al., 2015; Snijders et al., 2015).

The most preferred source of cells for skeletal muscle tissue engineering applications is either a myoblast cell line (Caridade et al., 2015) or the primary satellite cells that can easily be obtained by muscle biopsies and cultured *in vitro* (Powell et al., 1999). Transplanted satellite cells can take part in muscle regeneration and contribute to the satellite cell population in host mice. This makes satellite cells perfect candidates for cell based transplantation therapy for muscle degeneration (Partridge et al., 1989). Incapability of self-renewal, defective migration of donor cells after transplantation, host immune defense and poor survival are the factors that have affected therapeutic use of satellite cells in clinics. Satellite cells are characterized as a heterogeneous population of progenitors and stem cells. More comprehensive understanding on satellite cell hierarchy is needed at single cell level and their performance should be followed over time (Rendl, 2014).

Skeletal muscle that contains *in vivo* functionality requires the induction of main types of tissues such as vascular, nervous, muscle and connective tissues. Henceforth, numerous connective tissues cover the different muscle bundle, the muscle fibers and the whole muscle, while a skeletal muscle is instilled by capillaries and joined to the nerve branches (Ostrovidov et al., 2014). Vascularization is an important concern in capacious tissues having high oxygen demand such as the skeletal muscle (Levenberg et al, 2005). It is responsible for the storage and breakdown of glucose and fat since it is a highly metabolic organ. On top of that, skeletal muscle is the primary tissue accountable for the augmented glucose metabolism during exercise and hyperinsulinemia (DeFronzo et al., 1985). As it is common in other tissues, the vascular network in skeletal muscle contains arteries splitting into increasingly smaller vessels. In skeletal muscle, a terminal arteriole gives rise to collections of capillaries that run parallel to muscle fibers, and each muscle fiber can be supplied by numerous unlike groups of capillaries from independent terminal arterioles (Emerson et al., 1985). It was shown that the

muscle capillaries of rat were lengthy and twisted (Newman et al., 1996), and hence had several interactions with myocytes. Initial approaches to evaluate the structure and location of the microcirculatory system in skeletal muscle make use of microscopy to obtain 2D images from frozen or fixed tissues. Nevertheless, the skeletal muscle is predominantly sensitive to certain artefacts when freezing (Meng et al., 2014), and disadvantages with 2D microscopy include lack of estimation of capillary length, tortuosity or fiber size (Janacek et al., 2009).

As pioneers in this field, several research groups have focused on engineering skeletal muscle tissue that harbored only the myoblasts in their structure (Moon et al., 2008, Choi et al., 2008, Eberli et al., 2009, Hosseini et al., 2012). The major goal of these studies was to obtain the contracting myotubes in anisotropic arrangement to mimic the native skeletal muscle physiology. These were closely followed by other reports introducing methods for vascularization of engineered constructs (Levenberg et al., 2005, De Coppi et al., 2005, Delo et al., 2008, Klumpp et al., 2012, Shandalov et al., 2014, 2015). Most approaches were dependent on the host for generation of a blood vessel system that could provide enough oxygen and nutrients for survival (De Coppi et al., 2005, Delo et al., 2008, Klumpp et al., 2012, Juhas et al., 2014). However, in expanded tissues with high oxygen demand like skeletal muscle, vascularization is a fundamental concern and its prior *in vitro* establishment would better help to *in vivo* survival and integration of the three dimensional (3D) implant. Introduction of capillary network to *in vitro* tissue engineered muscle was a good strategy (Levenberg et al., 2005, Shandalov et al., 2014, 2015, Gholobova et al., 2015), and *in vivo* integration of such a construct was found to be more successful (Levenberg et al., 2005, Shandalov et al., 2014). As the other invaluable component of the muscle tissue, *in vitro* establishment of innervation by the motor neurons would better mimic the native tissue and provide an opportunity to test the effect of drugs targeting the neuromuscular junctions (Uzel et al., 2016). It was shown in a study by Guo et al. (2011) that *in vitro* functional human neuromuscular junction can be established by co-culture of motoneurons derived from human fetal spinal cord stem cells and myotubes derived from human skeletal muscle stem cells in a defined serum-free system. Larkin et al. (2007) were successful in obtaining a functional neuromuscular junction *in vitro* when they used a model where 3D skeletal muscle constructs were co-cultured with

fetal nerve explants. On the other hand, both innervated and vascularized human muscle tissue construct is expected to have a reduced time for functional integration in the body and eliminate the species-related variability associated with animal-based systems when used in drug discovery and toxicology studies.

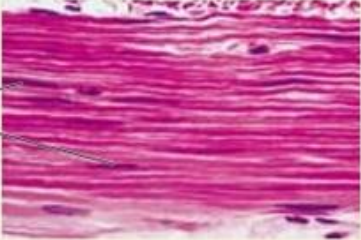
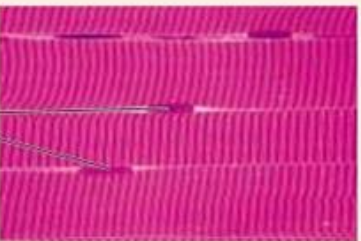
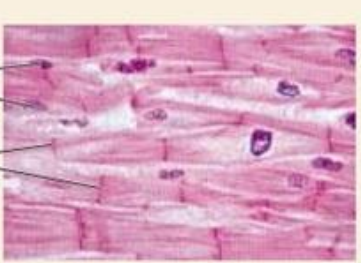
1.1 Muscle Tissue

The evolution of muscles was driven by the necessity for a variety of functions which require large differences in performance. Sudden instances of activity or extended contractions may require skeletal muscle. Continuous activity is the most typical feature of cardiac muscle which can function for many decades without interruption. A midge can beat its wings 1,000 times a second by contracting its flight muscles. One square centimeter of the adductor muscle of mollusks can lift a 10 kg weight (Bagshaw, 2012).

Muscle cells are the motors of the vertebrate body. They are unique due to the relative abundance and organization of actin and myosin filaments within them. While these filaments form a fine network in all eukaryotic cells contributing to cellular movements, they are far more abundant in muscle cells specialized for contraction. The vertebrate body possesses three different kinds of muscle cells: smooth muscle, skeletal muscle, and cardiac muscle (Table 1.1).

Skeletal and cardiac muscles are also known as striated muscles because their cells appear to have transverse stripes when viewed under high magnification. Skeletal muscle contractions are voluntary movements, whereas the contractions of cardiac and smooth muscles are generally involuntary.

Table 1.1: Muscle tissues localization, function, characteristic cell types (Raven and Johnson, 2002).

 <p>Nuclei</p>	<p>SMOOTH MUSCLE <i>Typical Location</i> Walls of blood vessels, stomach, and intestines <i>Function</i> Powers rhythmic, involuntary contractions commanded by the central nervous system <i>Characteristic Cell Types</i> Smooth muscle cells</p>
 <p>Nuclei</p>	<p>SKELETAL MUSCLE <i>Typical Location</i> Voluntary muscles <i>Function</i> Powers walking, lifting, talking, and all other voluntary movement <i>Characteristic Cell Types</i> Skeletal muscle cells</p>
 <p>Nuclei</p> <p>Intercalated discs</p>	<p>CARDIAC <i>Typical Location</i> Walls of heart <i>Function</i> Highly interconnected cells; promotes rapid spread of signal initiating contraction <i>Characteristic Cell Types</i> Cardiac muscle cells</p>

1.1.1 Smooth Muscle

Smooth muscle, the earliest form of muscle to evolve, is found throughout the animal kingdom. In vertebrates, smooth muscle is found in the organs of the internal environment, or viscera, and it is also known as visceral muscle. Elongated spindle-shaped cells with a single nucleus are arranged into sheets to form smooth muscle tissue. When the cells are stimulated by a nerve, they contract and in some tissues, all cells in the sheet contract. Many blood vessel walls and the iris of the eye are examples of this type of tissues in vertebrates. In other smooth muscle tissues, nerves regulate the activity. A good example is the ones in the wall of the gut in which the individual cells contract spontaneously, causing slow, steady contraction of the tissue.

1.1.2 Cardiac Muscle

The vertebrate heart is composed of striated cardiac muscle in which the fibers are arranged very differently from the fibers of skeletal muscle. Cardiac muscle differs from multinucleated skeletal cells running the length of the muscle. Cardiac cells are smaller and interconnected to each other, and therefore, contain only one nucleus. Under microscope, two cells appears to be connected using dark lines referred to the intercalated discs. However, in reality, the dark lines are regions in which adjacent cells are joined to another one using a gap junction. These junctions possess openings that facilitate the movement of a substance between adjacent cells. Apart from substances, these openings also permit the movement of electric charges from one cell to another. Interconnections enable the cardiac muscle to form one functional unit referred to as myocardium. The cardiac muscle also contains specialized cells that spontaneously generate impulses. Due to interconnections, the impulse is spread from one cell to another, thus causing the entire muscle to contract.

1.1.3 Skeletal Muscle horizontally

Skeletal muscles are usually attached to bones by tendons, so contraction of the muscles causes bones to move at their joints. A skeletal muscle is made up of numerous, very long muscle cells, called muscle fibers, which lie parallel to each other within the muscle and tendons are located at the ends of the muscle. Skeletal muscle fibers are connected to the nerve fibers that stimulate them to contract; therefore, a stronger muscle contraction will result when more fibers are stimulated. Thus, the nervous system can regulate the strength of skeletal muscle contraction. Muscle fibers contract with the help of substructures named as myofibrils (Figure 1.1).

Myofibrils consist of highly ordered actin and myosin filaments, thus giving the muscle the striated appearance. A skeletal muscle is developed by joining of cells end to end.

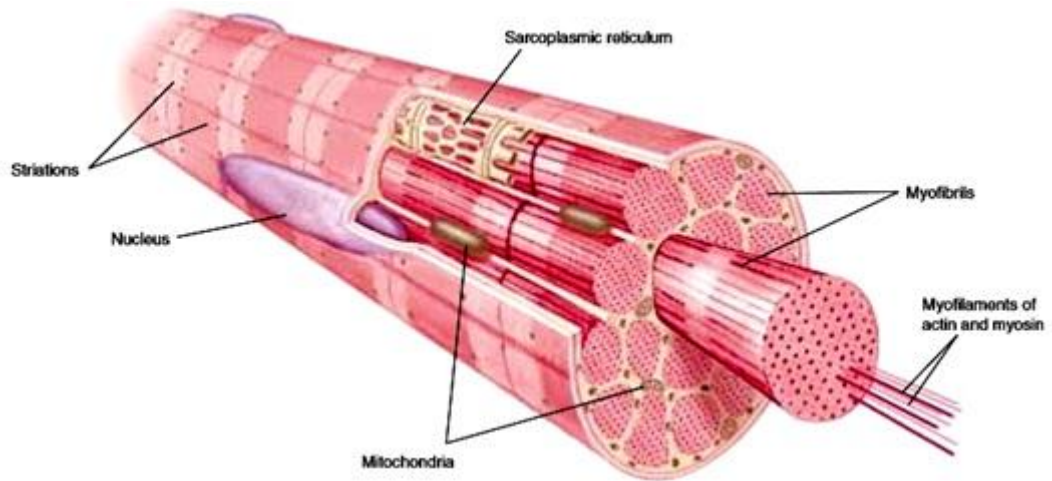


Figure 1.1: A muscle cell, also called muscle fiber consists of many myofibrils which consist of two filaments called actin and myosin. A muscle fiber contains many nuclei because of embryonic fusion of smaller cells. Muscle cells have a modified endoplasmic reticulum called the sarcoplasmic reticulum (Raven and Johnson, 2002).

1.2 Muscle Contraction

Numerous muscle fibers are found in each skeletal muscle. Each muscle fiber is bounded by myofibrils which contain a package of 4 to 20 elongated structures. Each myofibril, on the other hand, is composed of thick and thin myofilaments (Figure 1.2). The striated appearance of skeletal muscle fiber is due to its myofibrils that are striated with dark and light bands.

The organization of the myofilaments within the myofibril causes a banding pattern. The thin filaments are found in I band which is also known as the light band; A bands, dark bands, are also produced when thick myofilaments are stacked together. Due to the appearance of each I band in electron micrographs, it is split into two by a disc protein called Z line which is formed by the thin filaments anchored to the disc proteins (Figure 1.3).

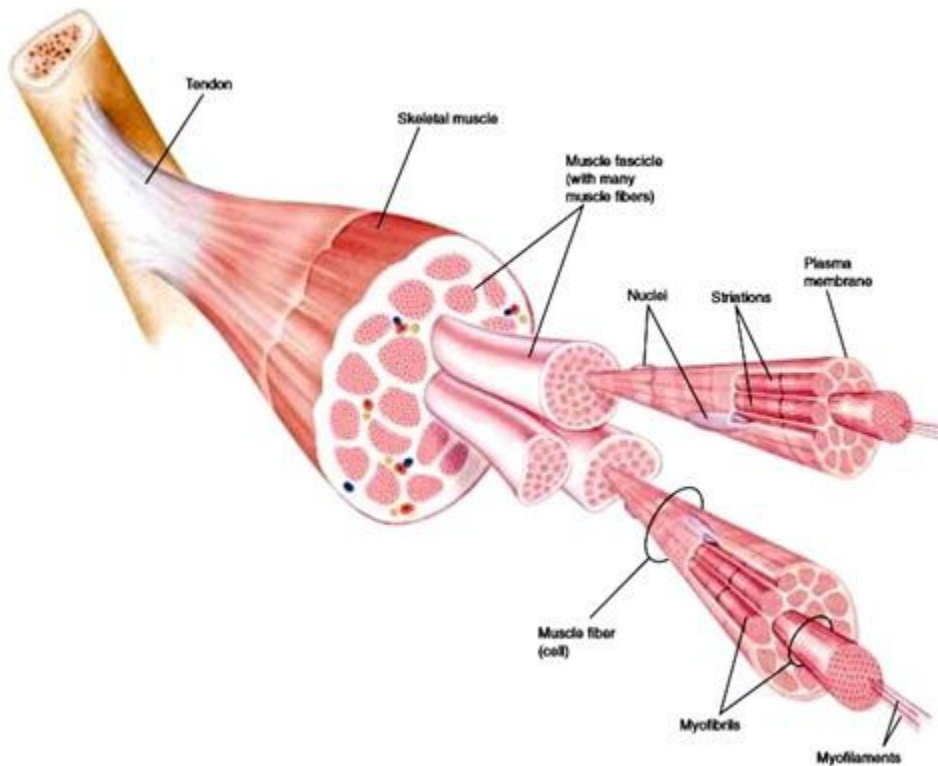


Figure 1.2: The skeletal muscle is organized into numerous fascicles, also referred to a bundle of muscle cells or fibers. A single fiber consists of numerous myofibrils, which are then made up of myofilaments (Raven and Johnson, 2002).

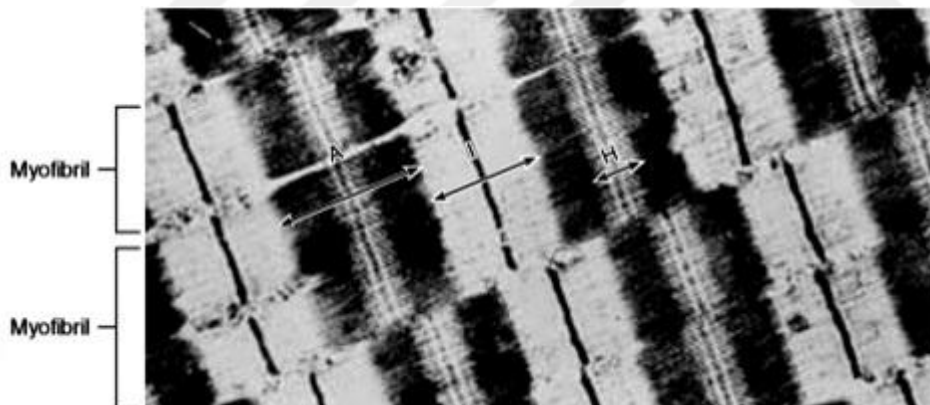


Figure 1.3: When observed under an electron microscope, the Z lines act as border lines of sarcomeres and are clearly observed within each myofibril. The thick filaments comprise the A bands; the thin filaments are within the I bands and stick partway into the A bands, overlapping with the thick filaments. There is no overlap of thick and thin filaments at the central region of an A band, which is therefore lighter in appearance. This is the H band (Raven and Johnson, 2002).

The smallest subunit of muscle contraction is sarcomere which is a repeating structure. In resting muscle, the thin filaments are developed all the way to the

middle of the center band, however, they stick partially into the stack of thick filaments on each side of an A band. Due to this property, the center of A band, also known as H band, is lighter than each side and has thin filaments. When the muscle contracts the morphology of the sarcomeres alters. Once the myofibril shortens and contracts, the muscle also does the same. Instead of myofibril shortening the thin filaments slide deeper into the A band when this occurs (Figure 1.4).

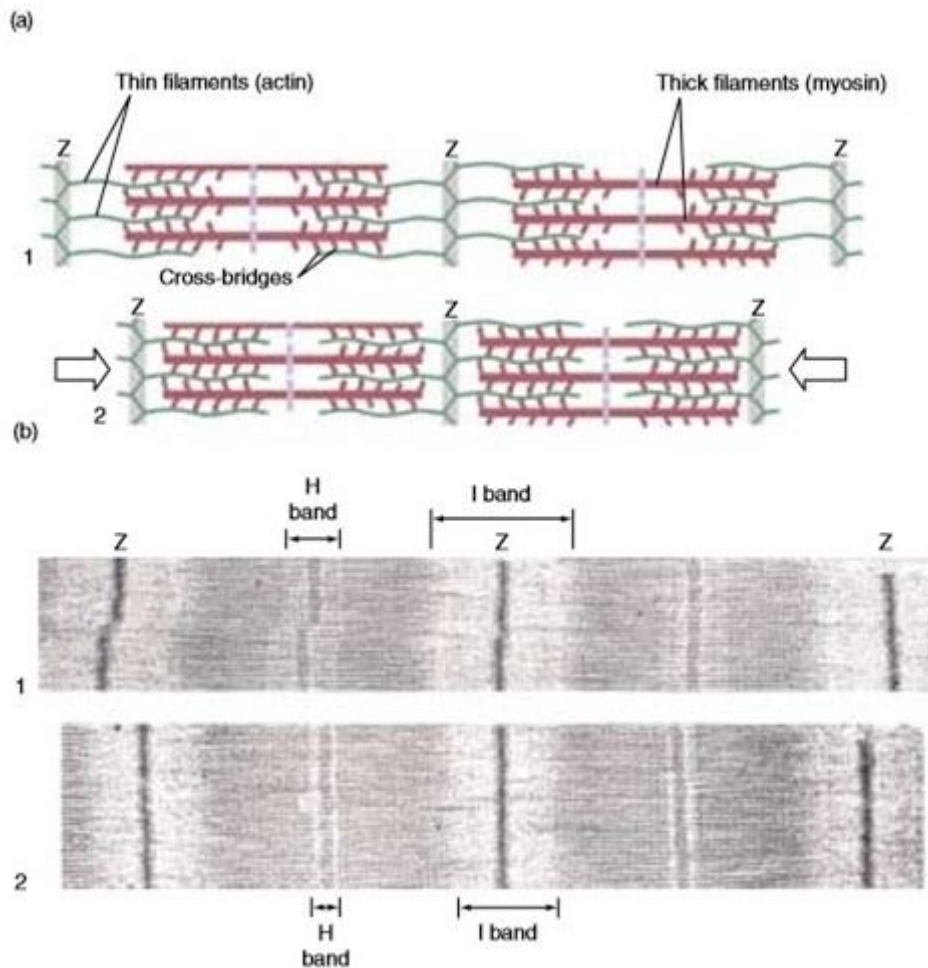


Figure 1.4: Electron micrograph (a) and diagram (b) of the sliding filament mechanism of contraction. As the thin filaments slide deeper into the centers of the sarcomeres, the Z lines are brought closer together. (1) Relaxed muscle; (2) Partially contracted muscle (Raven and Johnson, 2002).

This makes H bands, at maximal shortening, to disappear completely after narrowing. It also makes I bands narrower, since the dark A bands are brought nearer. Thick filaments are formed from packed myosin proteins having a “head” region that projects from the thick filament (Figure 1.5). The cross-bridges seen in

electron microscopy are formed by these myosin heads. Every thin filament mainly contains numerous globular actin proteins twisted into a double helix (Figure 1.6).

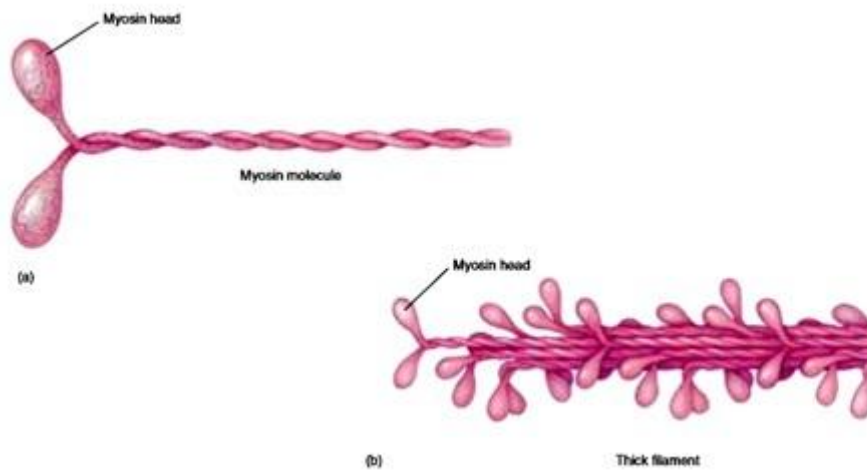


Figure 1.5: Thick filaments are composed of myosin. (a) Each myosin molecule consists of two polypeptide chains wrapped around each other; at the end of each chain is a globular region referred as the “head” (b) Thick filaments consist of myosin molecules combined into bundles from which the heads protrude at regular intervals (Raven and Johnson, 2002).

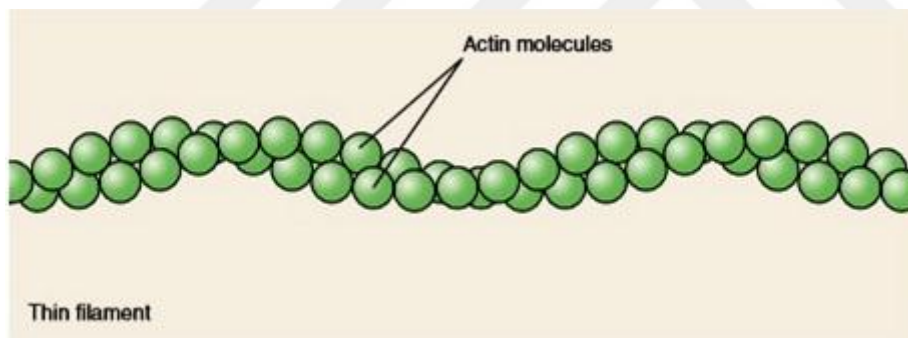


Figure 1.6: Thin filaments are composed of globular actin proteins. Two rows of actin proteins are twisted together in a helix to produce the thin filaments (Raven and Johnson, 2002).

The myosin heads act as adenosin trifosfatase (ATPase) enzymes, splitting adenosin trifosfat (ATP) into inorganic phosphate (Pi) and adenosin difosfat (ADP), before binding to the actin of the filaments. This triggers the heads, raising them so that they can join to actin and form cross-bridges. The myosin head undergoes a conformational change in shape, bringing the thin filament toward the center of the sarcomere in a power stroke, once it binds to actin (Figure 1.7). The myosin head binds to a new molecule of ATP at the conclusion of the power stroke. This offers the head to move on the cross-bridge cycle and separates itself from

actin (Figure 1.8). The cell can no longer give out ATP when it has died and, henceforth, causes rigor mortis because the cross-bridges cannot be broken.

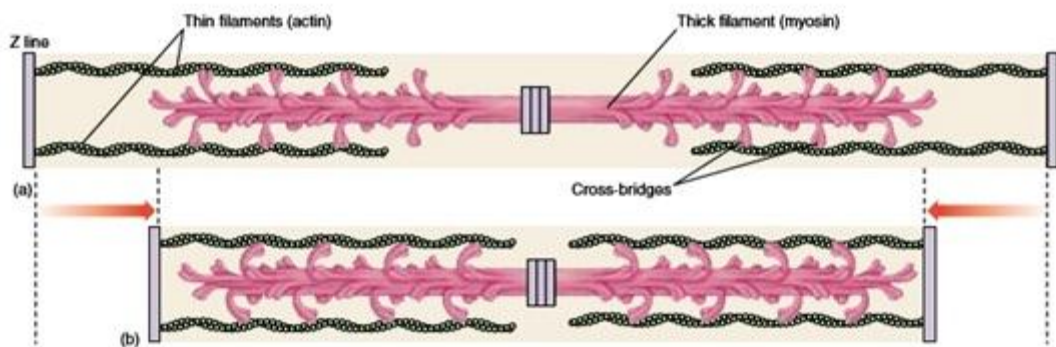


Figure 1.7: Thin and thick filament interaction: In striated muscle sarcomeres, there is a thin and thick filament. The heads of the thick filaments face opposite directions. (a) This allows the cross bridges to pull the thin filaments and Z lines on the side of sarcomeres towards the center. (b) When this happens, there is a sliding of the filaments, which then produces a muscle contraction (Raven and Johnson, 2002).

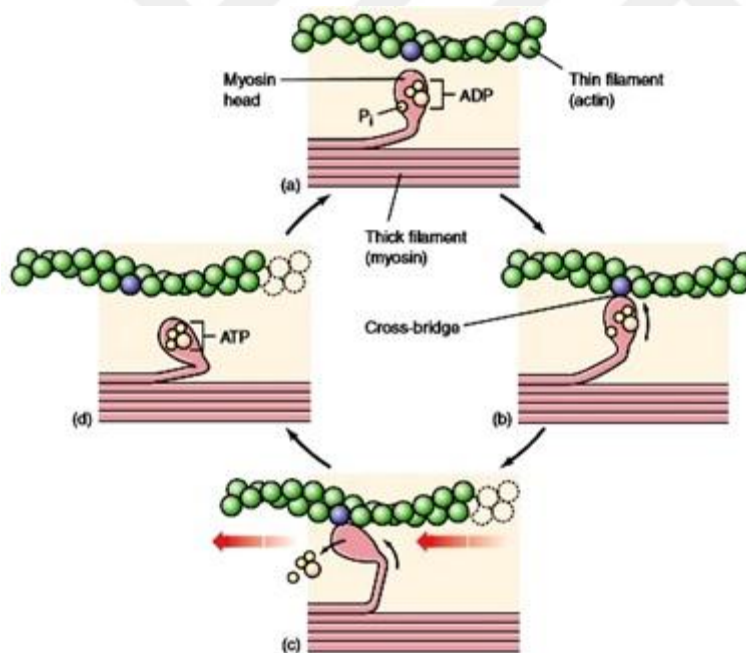


Figure 1.8: The cross-bridge cycle in muscle contraction. (a) With ADP and P_i attached to the myosin head. (b) The head is in a conformation that can bind to actin and form a crossbridge. (c) Binding causes the myosin head to assume a more bent conformation, moving the thin filament along the thick filament and releasing ADP and P_i . (d) Binding of ATP to the head detaches the cross-bridge; cleavage of ATP into ADP and P_i puts the head into its original conformation, allowing the cycle to begin again (Raven and Johnson, 2002).

1.3 The Control of Muscle Contraction

1.3.1 The Role of Ca^{++} in Contraction

The myosin heads are incapable of binding to actin due to the fact that tropomyosin in the thin filaments, which is another protein, physically blocks the attachment sites for the myosin heads on the actin. Therefore, neither the filaments slide nor the cross-bridges are formed in the relaxed muscle. The tropomyosin should be moved out of the way so that the myosin heads can bind to actin which is followed by muscle contraction. This requires the function of a regulatory protein, known as troponin, to bind the tropomyosin. The calcium ion (Ca^{++}) concentration of the muscle cell cytoplasm regulates the interaction of tropomyosin and troponin. The muscle is relaxed and tropomyosin inhibits cross-bridge formation when there is a low concentration of calcium in the muscle cell cytoplasm (Figure 1.9).

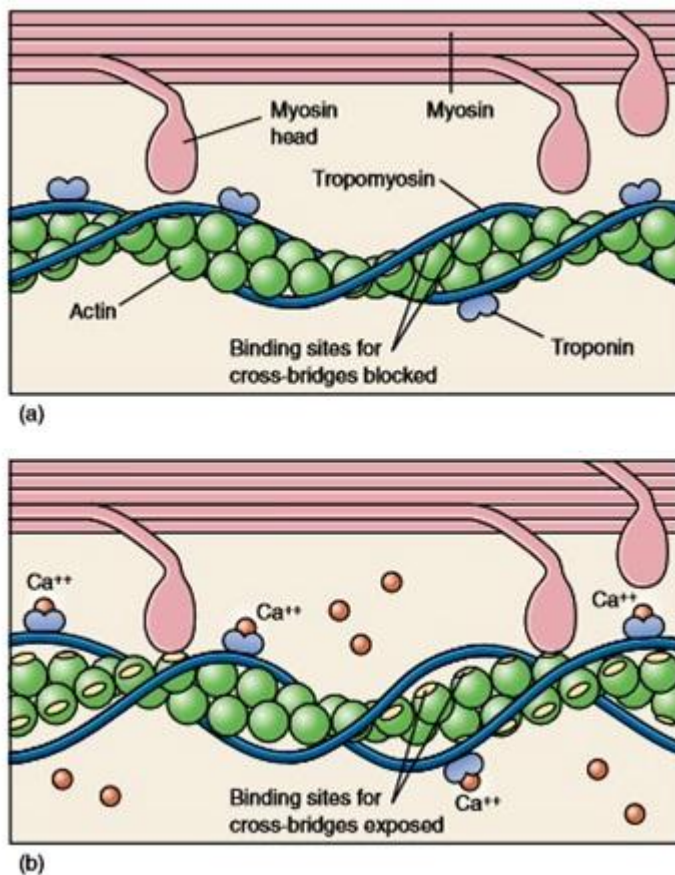


Figure 1.9: Calcium controls striated muscle contraction. (a) A long filament of the protein tropomyosin, when the muscle is at rest, blocks the myosin-binding sites on the actin molecule. (b) When Ca^{++} binds to troponin, the Ca^{++} -troponin complex displaces tropomyosin and exposes the myosin-binding sites on actin, permitting cross-bridges to form and contraction to occur (Raven and Johnson, 2002).

Ca⁺⁺ binds to troponin when there is an increase in Ca⁺⁺ concentration. This makes the tropomyosin-troponin complex to move away from the attachment sites for the myosin heads on the actin. Henceforth, production of muscle contraction and power strokes can be achieved by cross-bridges. To regulate this event, muscle cells have sarcoplasmic reticulum (SR), an improved endoplasmic reticulum, where Ca⁺⁺ is stored by muscles fibers (Figure 1.10).

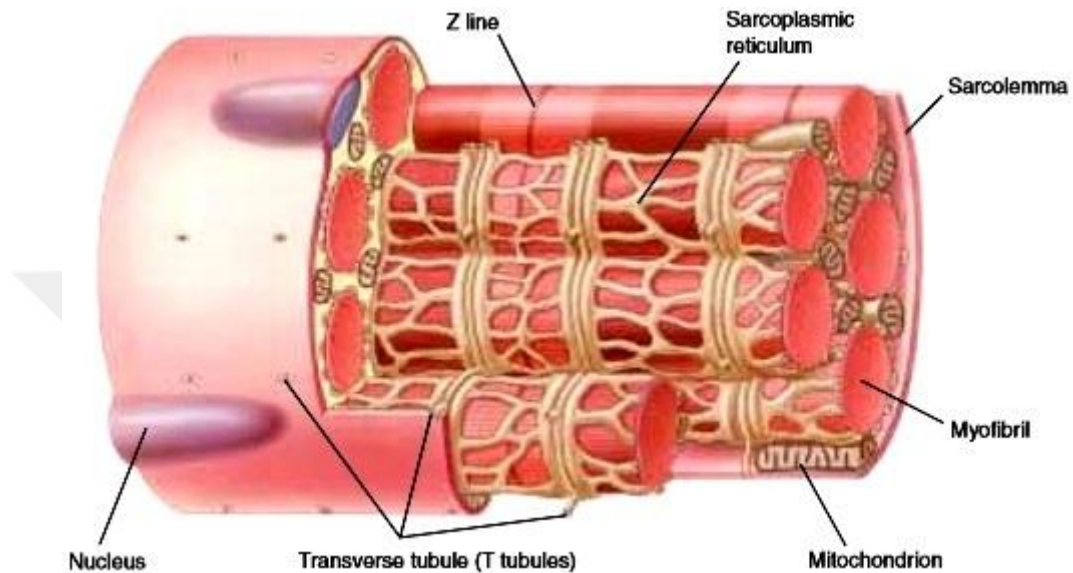


Figure 1.10: The relationship between the myofibrils, transverse tubules, and sarcoplasmic reticulum. Impulses travel down the axon of a motor neuron that synapses with a muscle fiber. (Raven and Johnson, 2002).

An electrical impulse goes into muscle fibers through routings called the transverse tubules, T tubules, when there is a stimulation to contract in a muscle fiber. This activates SR to release the Ca⁺⁺ followed by muscle contraction.

1.3.2 Nerves Stimulate Contraction

Somatic motor neurons are particular motor neurons that innervate skeletal muscles, as opposed to cardiac and smooth muscles. The axon (Figure 1.11) of a somatic motor neuron with a certain amount of muscle fibers prolongs from the neuron cell body and branches to cause functional synapses or connections.

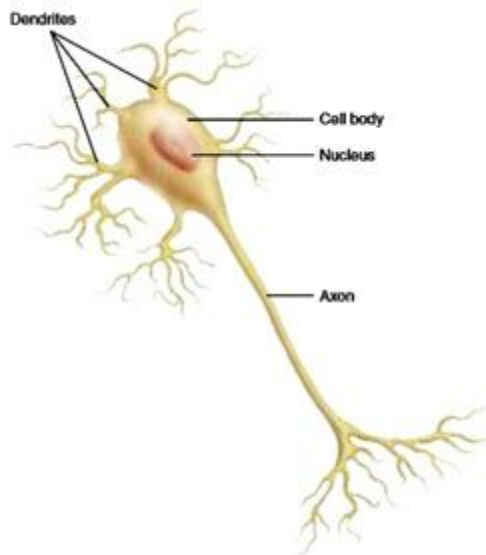


Figure 1.11: A neuron has a very long projection called an axon (Raven and Johnson, 2002).

Muscle fiber in particular animals might be innervated by more than one motor neuron and one axon can also stimulate numerous muscle fibers. Nevertheless, every muscle fiber in human beings has only one synapse with a single branch of axon. The contraction of muscle fibers is motivated with electrochemical impulses brought by a somatic motor neuron. Acetylcholine (ACh) which performs on the muscle fiber membrane to arouse the muscle fiber to give out its own electrochemical impulses, is the specific neurotransmitter that is released by the somatic motor neurons. The impulses towards SR are carried by the T tubules which release Ca^{++} . Then, cross-bridging sites are exposed on the actin myofilaments and Ca^{++} binds to troponin, encouraging muscle contraction. The end of impulse production in the muscle fiber is caused upon the cease of the impulses from the nerve causing it to stop ACh release. Ca^{++} is transferred into the SR through active transport and the muscle is permitted to relax.

1.3.3 Motor Units and Recruitment

Stimulation causes single muscle fiber to respond in all-or-none fashion. Motor unit is defined as the combination of muscle fibers innervated by the entire axonal branches of a certain motor neuron (Figure 1.12).

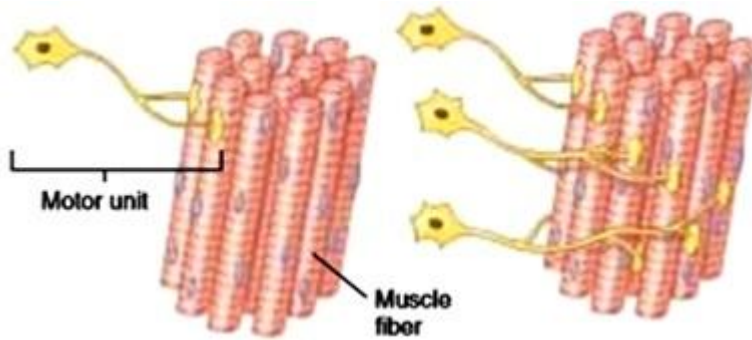


Figure 1.12: The number and size of motor units. (Left) Weak, precise muscle contractions use smaller and fewer motor units. (Right) Larger and stronger movements require additional motor units that are larger (Raven and Johnson, 2002).

Every muscle fiber in the motor unit contracts altogether when impulses are given out by the motor neuron. The splitting of the muscle into motor units finely adjusts gradation of the muscle's strength, which is a necessity for the skeleton to move in a coordinated manner. Muscles that need low precise control but producing more force such as large muscles of the leg has numerous motor units, while a few muscle fibers per motor neuron are present in the muscles that require a finer degree of control, like the ones responsible for eye movement. Motor units of almost all muscles can be selectively activated by the nervous system in a multiple of different magnitudes. Limited small motor units can be activated for the weakest contractions. Further smaller motor units are activated, if a slightly more contraction is necessary. The force increments become larger as more and bigger motor units are called into action by nervous system when greater forces are needed.

1.4 Types of Muscle Fibers

Stimulating isolated skeletal muscles can be studied by using electrical shocks. When muscle is stimulated with only one electric shock, it will rapidly contract in and relax in a response known as twitch. The addition of the stimulus voltage increases the strength of the twitch till a maximum level is reached. A second twitch will be produced that may partly be "ride piggyback" on the first, if only a second electric shock is given out instantaneously after the first one, summation, the cumulative response, is observed (Figure 1.13).

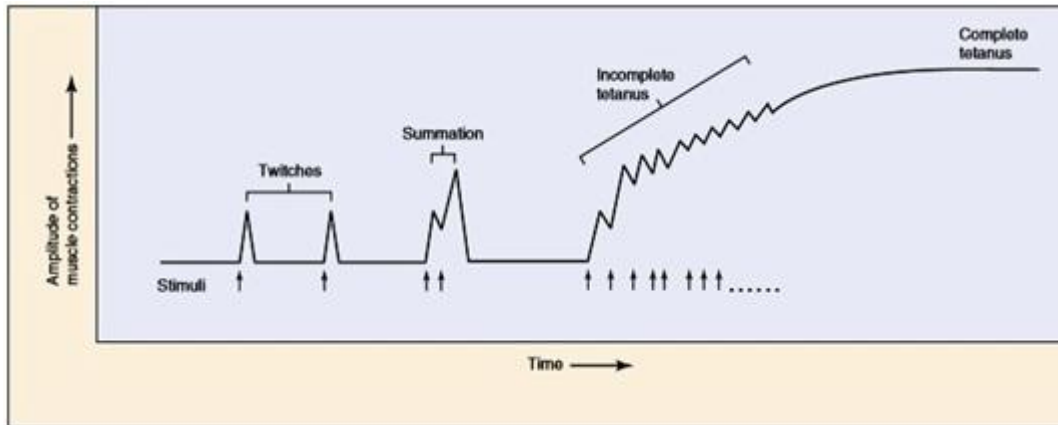


Figure 1.13: Muscle twitches summate to produce a sustained, tetanized contraction. This pattern is produced when the muscle is stimulated electrically or naturally by neurons. Tetanus, a smooth, sustained contraction, is the normal type of muscle contraction in the body (Raven and Johnson, 2002).

The strength of contraction increases as the relaxation time between consecutive twitches getting shorter, if the stimulator is set to give an increasing frequency of electric shock automatically. In conclusion, there is no relaxation between continuous twitches at stimulations in a particular frequency. During normal muscle contraction of the body, a contraction is persistent and smooth and called as tetanus. Skeletal muscle fibers can be separated on the base of their contraction speed into slow-twitch, or type I, fibers, and fast-twitch, or type II, fibers.

1.5 Muscle Metabolism during Rest and Exercise

The aerobic respirations of fatty acids provide the energy to the skeletal muscles when at rest. Blood glucose and muscle glycogen are used as energy sources while exercising. ATP is made by energy attained from the aerobic respiration, and is required for (1) pumping of Ca^{++} into the SR in order for the muscle to relax and (2) movement of the cross-bridges in the course of muscle contraction. Skeletal muscle obtains ATP quickly by combining ADP with phosphate from creatine phosphate that is developed by resting muscle from ATP generated by cell respiration. During the first 45 to 90 second of moderate to heavy exercise, the skeletal muscle respire anaerobically to offer adequate time to the cardiopulmonary system to increase oxygen supply. During moderate exercise, anaerobic respiration is the major contributor of energy in the first two minutes. The difference between light, moderate and heavy exercise in a person depends on

the maximal capacity for aerobic respiration. The maximum rate of oxygen uptake in the body during aerobic respiration refers to the maximal rate of oxygen uptake or in another word aerobic capacity. The lactate threshold which defines the intensity of an exercise, refers to the maximal oxygen at which there is a significant rise in lactate in the blood as a result of anaerobic respiration. While using an average healthy person, a significant blood lactate only appear when the person is at 50% to 70% of the maximal oxygen uptake (Raven and Johnson, 2002).

1.6 Stem Cells

1.6.1 Embryonic Stem Cells

After totipotent embryo, the zygote, is formed, the first fate determination occurs when morula stage starts after subsequent rounds of cell division. Not all blastomeres differentiate into trophoblast cells and only a few stay with pluripotent capacity, i.e. can develop into more than one mature cell type, and these form inner cell mass (ICM) at the blastocyst phase. The trophoblast cells will grow into placenta after imbedding and ICM will mature into epiblast, then into fully grown body. The embryonic stem cell (ESC) lines could be obtained from ICM, and ESC lines sustain a higher percentage, if not all, given the proper culture conditions are used (Kang et al., 2010). Therefore, the embryonic stem cells are known as cultured cell lines resulting from the blastocyst's ICM and two remarkable features, self-renewal and pluripotency, describe them. The ability to go through several cycles of cell division while retaining the undifferentiated state is known as self-renewal. In practice, it implies that they can be propagated in the culture for a long period of time without losing their characteristics and potential. Pluripotency, on the other hand, means that the embryonic stem cells can differentiate into almost all cell types and this differentiates ESC from multipotent adult stem cells that have limited capacity.

It was shown before that pluripotency is germline characteristic for mouse cells that exhibits the capability to make all cell types (Bradley et al., 1984). The generation of teratoma in immunodeficient mice that received stem cells also showed the pluripotent nature of these cells (Damjanov et al., 2005). The teratoma assay is considered as the most severe assay to show the pluripotency of human stem cells due to the rich diversity of developed histologically different tissues types (Mueller

et al., 2010). Adult stem cells have never been revealed to taking part in germline transmission, hence they are still capable of differentiating into a wide variety of cell types but they are restricted in lineages. The study of the early embryogenesis shows that the embryonic stems are the exceptional model. They are instrumental in early stages of organisms in which tissue differentiation and cell signaling are not available. But we still have to remember that ESCs do not exist in the body and are actually an artificial system. ESCs are obtained from blastocyst in middle stage during gastrulation in which the cells would be in pluripotent state for a few hours. This stage is unbalanced and causes a problem regarding with long-term upkeep of ESCs in culture.

1.6.2 iPSCs

Several vastly expressed genes in ESCs have been recognized through investigating the gene expression profiles. Based on these outcomes, Shinya Yamanaka and his partners did a landmark experiment in 2006, whereby they applied the retroviral infection methodology and effectively introduced 24 transcription aspects that were highly expressed in ESCs into the mice fibroblast cells (Takahashi and Yamanaka, 2006). A few ES-like colonies appeared in the culture dish in the two weeks post retroviral infection. Furthermore, the cells morphologically show a resemblance to the ES-like cells once propagated *in vitro*. After characterization of the pluripotency of the induced pluripotent stem cells (iPSCs), it was deduced that the teratoma in the immune deficient mice could be formed by the iPSCs. More significantly, they found that four transcription factors, octamer-binding transcription factor 4 (Oct4), (sex determining region Y)-box 2 (Sox2), Kruppel-like factor 4 (Klf4) and cellular Myc (c-Myc), were crucial for altering the fibroblast cells into iPSCs. Yamanaka's method used for mouse iPSCs, has also been used in the restructuring of the human somatic cells (Takahashi et al., 2007).

1.6.3 Adult Stem Cells

Multipotent stem cells are found in almost all adult tissues and can lead to organ or tissue specific lineages, comprising of the heart, brain, muscle, adipose, intestine, teeth, skin and lung. Their ability of self-renewal and differentiation into more specialized cell types are two major features of these stem cells. Adult stem cells have important potential for applications in regenerative medicine. The mesenchymal and hematopoietic stem cells are clinically well-known and best characterized ones.

1.6.3.1 Hematopoietic Stem Cells

In 1959, hematopoietic stem cell (HSC) transplant was the first effective transplant executed, when a patient anguishing from acute leukemia was being transplanted with the bone marrow cells from the identical twin (Damjanov et al., 2005). The HSC donation has turned out to be a less hurtful procedure and henceforth has helped in the growth of bone marrow registries, due to the discovery that granulocyte colony-stimulating factor (GCSF) can be resourcefully activate HSC from the bone marrow to the peripheral blood (Molineux et al., 1990). Nevertheless, keeping collected HSC remains inadequate due to the cryopreservation with reduced cell viability (El Beshlawy et al., 2009). Technologies to expand HSC culture before transplantation have been discovered in the laboratories but they have not reached the clinics. The hematopoietic system regenerates faster compared to transplanted bone marrow when an HSC transplant is done from the peripheral blood (Bensinger et al., 2001). Nevertheless, bone marrow-derived cells are not in a risk of causing the chronic GvHD (graft-versus-host disease) compared to peripheral blood stem cells (Cutler et al., 2001). It also appears that different stem cell sources perform in a different way in distinct patient populations making the prediction of the response to the therapy difficult. Due to their simplicity of harvest, a large number of adult HSC transplantations are done using peripheral blood stem cells mobilized with GCSF (Jenq and van den Brink, 2010). In clinical practices, HSC transplantation is the only stem cell therapy broadly used, regardless of widespread research to improve other stem cell populations into the clinic.

1.6.3.2 Fetal Stem Cells

Fetal stem cells (FSC) are self-renewing cells situated in the amniotic membrane, umbilical cord blood, fetal blood and umbilical cord matrix, which are different kinds of fetal tissue (Reinisch et al., 2009; Jaeger et al., 2009; Zeddou et al., 2010; Magatti et al., 2008; Chong et al., 2010). Two of the more reachable stem cell populations among them are the HSCs and mesenchymal stem cells (MSC). In the liver of the first trimester fetus, peripheral blood and bone marrow are the places where fetal MSC can be found. The adult stem cells have a bit longer doubling times than fetal stem cells. The adult cells possess less telomere lengths and low plasticity compared to that of the FSC. Henceforth, FSC have superior expansion and growth potential without becoming senescent, and their self-renewal ability might be more than that of the adult stem cells (Chong et al., 2010). Fetal stem cells seem immunologically more inexperienced compared to adult stems cells thus enabling enhanced transplantation efficiency (Jaeger et al., 2009; Eapen et al., 2007; Reimann et al., 2009). The adult stem cells are not tolerated well in host tissue because of low levels of major histocompatibility complex (MHC) class I and class II expressed in them (Reimann et al., 2009; Gotherstrom et al., 2004). FSC may also have some immunogenic potential which could cause graft rejection, regardless to the potent immunosuppressive properties of some fetal stem cell types (Rameshwar et al., 2009; Campeau et al., 2009; Neri et al., 2010). The use of FSC for transplants has several shortcomings. First, they are hard to find in large numbers. Also, their use for therapeutic and research purposes carries a lot of ethical quizzes, as they are often obtained from terminated pregnancies. The technical challenges also limit their usage. After freezing and cryopreservation, the non-hematopoietic stem cells cannot be detected to an adequate degree and are also limited in fresh blood (Koegler et al., 2009). Nevertheless, the umbilical cord stored in cryopreservation banks offers an important reserve for fetal stem cells. An excess of 300,000 cryopreserved allogenic transplants are present worldwide (Barker et al., 2009), and can be requested from stem cell donor registries through the central cord blood banks (Reimann et al., 2009). However, technical difficulties have arisen due to inadequate number of cells that can be removed from the umbilical cord (Zeddou et al., 2010). After BM HSC, fetal stem cells are the best clinically progressive stem cell population and more than 30,000 patients have been given umbilical cord

blood transplant until 1988 (Gluckman et al., 1989). Although cord bloods have been stored in private banks for more than 10 years, there is still no clinical application of autologous hematopoietic stem cells from that source. Privately run cord blood banks keep donors' cord blood for their own use for a certain period of time, and paid by the parents who consider this provision as "biological life insurance policy" for their children. Nonetheless, up to now usefulness of such services and scientific rationale are missing. The probability that a child's life will rely on his/her own cord blood is tremendously low. Including allogeneic transplants for siblings, a maximum of 100 people have been transplanted so far over a 2.5 million autologous donations stored worldwide (Moldenhauer et al., 2007; Reimann et al., 2009). Stem cells have been used for a long time to treat blood disorders and cancers. However, there is a risk of reverse transmission in autologous transplantation together with cord autologous blood transmission in the case of leukemia in the childhood period due to genetic origin of a patient (somatic mutation) (Mullighan et al., 2005; 2009).

1.6.3.3 Mesenchymal Stem Cells

Mesenchymal stem cells (MSC) are the most studied stem cell population for analysis and transplantation because they can be easily secluded from the adult tissue. Together with HSC, MSCs are part of the bone marrow. In 1974, they were first secluded from the bone marrow and termed as multi-potential stromal precursor cells (Friedenstein et al., 1974). MSC in the adult have then been also isolated from other sources such as placenta, dental pulp and lung tissue (Zuk et al., 2001; Phinney and Prockop, 2007; Gronthos et al., 2000). They are well recognized as multipotent cells that are readily differentiated into cells of osteoblasts, adipocytes and chondrocytes (Pittenger et al., 1999). Scientists have been able to induce MSC differentiation into cells from other embryonic heredities such as hepatocyte-like cells, astrocytes and neurons showing that these cells have transdifferentiation ability (Cho et al., 2005; Kopen et al., 1999; Petersen et al., 1999). The Mesenchymal and Tissue Committee of the International Society for Cellular Therapy embraced a set of standards regarding marker expression, *in vitro* capacity and differential capability (Dominici et al., 2006). Procedures exist for the isolation of MSC populations from both the adipose and bone marrow aspirates, but the low MSC yields from the bone marrow necessitate *in vitro* expansion for

therapeutic use (Kern et al., 2006). Expanding MSC in culture needs to be done in caution since substantial variances in gene expression have been detected between early and late passages (Guenter et al., 2008). Polyploidy, up regulation of miRNAs, genetic and epigenetic anomalies have been seen in the cultured MSCs (Izadpanah et al., 2008; Wagner et al., 2008). Disparities also exist in the differentiation potential of cells obtained from distinct sources (Alviano et al., 2007). MSC from different origin has largely the same cytokine profile but the profile could vary by cellular morphology (Helmy et al., 2010). Another source of variability arises from the donor age which is also evident in the HSC (Stolzing et al., 2008). Its weak immunogenicity, on the other hand, is ideal for transplantation. The forbearance for non-HLA accorded MSC transfusion has been proven in the both human and animal studies (Bartholomew et al., 2002; Le Blanc et al., 2004). This feature of MSC can be described in part by their cytokine synthesis. Hepatocyte growth factor, IL-6, tumor necrosis factor alpha (TNF- α), IL-8, macrophage colony stimulating factor (M-CSF), and immunosuppressive cytokines IL-10 and TGF- β are the repertoire of cytokines produced by MSC (Nauta et al., 2007; Rossignol et al., 2009). MSC have been largely explored for applications in regenerative medicine and only a narrow translation to the clinic has been explored for its regenerative potential. There is a clear ambiguity that cells will differentiate correctly once they have been implanted to the target location. The threat of instigating a tumor from the transplanted stem cells is the most worrying concern. The duration and efficiency of engraftment is also not known (Helmy et al., 2010) despite the proof of successful preclinical and clinical engraftment of transplanted MSC (Pereira et al., 1995; Horwitz et al., 1999). The effects of *in vitro* culture situations and storage should be thoroughly assessed. Once transplanted, the culture time and cell culture conditions have been proven to influence MSC tropism. For instance, in adherent culture conditions, human MSCs require little efficiency for the places of injury due to the loss of C-X-C chemokine receptor type (CXCR4) (Potapova et al., 2008). One should also consider the likelihood of graft rejection when non-autologous cells are used as transplants. MSCs seem to be a good stem cell source for off-the-shelf therapy due to their weak immunogenicity but *in vitro* studies showed that re-expression of MHCII could be observed (Castillo et al., 2008 ; Behr et al., 2009). The possibility of re-expression of MHC-II after implantation and rejection of the implanted cells by the host immune system should

be addressed in forthcoming therapies, hence making this finding highly significant. A lot of discussion concerning tumor growth by MSC transplant has been done. It has been advocated that the mouse MSC could impulsively be transformed into a tumor while human MSC could not (Guenter et al., 2008). Although the results of similar studies were questioned (de la Fuente et al., 2010), they depict that post-senescent human MSCs are regularly transformed (Rubio et al., 2005). Transformational prospective might have been influenced by the tissue source of MSC. It has been shown that bone marrow-derived MSCs are not readily transformed compared to adipose tissue-derived ones (Bernardo et al., 2007). However, other groups have discovered that there is a significant transformation threat in bone marrow-derived MSC (Sawada et al., 2006). In more than 100 clinical trials, MSC transplants have been shown to be harmless with no menace risk (Helmy et al., 2010).

1.6.3.4 Satellite Cells

One of the three main germ layers is the mesoderm where all skeletal muscle in vertebrates comes from. Muscles of the limb and trunk, and almost all skeleton, originate from the somites, which are segmented structures removed from paraxial mesoderm that form pair-wise along the posterior/anterior axis of the embryo (Christ and Ordahl, 1995). Upon stimulus from exercise or following muscle injury, the myotubes fuse and eventually matures into myofibers (Figure 1.14), hence the satellites enter mitosis after they become activated, undergo cellular division and form myogenic progenitor, called myoblast which is an exceedingly proliferative transient cell population.

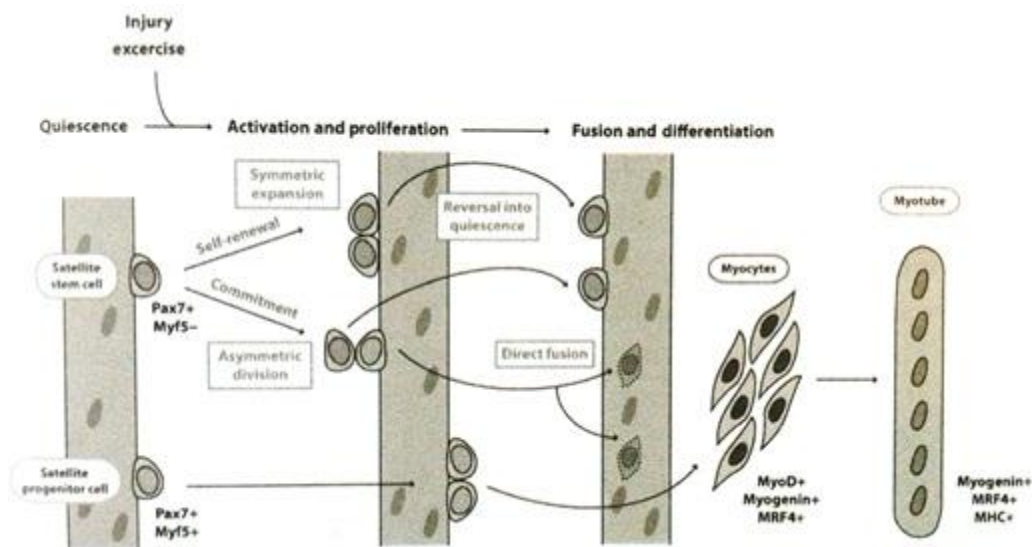


Figure 1.14: The myotube fusion and maturation into myofibers (Rendl, 2004).

Pax3 and Pax7 are both repressing genes that prompt the terminal myogenic differentiation and the target genes that promote commitment and proliferation to the myogenic lineage (Kassar-Duchossoy et al., 2005; Soleimani et al., 2012). There is a diverse population of satellite progenitor cells (Pax7+/Myf5+) and satellite stem cells (Pax7+/Myf5-). The satellite cells exit quiescence and become activated during exercise and muscle injury. The satellite stem cells can go through either planar symmetric cell division or asymmetrical cell division alongside the apical-basal axis and also self-renew. Myf5 is expressed in the occasion of myogenic commitment and these progenitor cells may help in muscle redevelopment either by direct fusion into the redeveloping myofibers or through the creation of new myotubes. They are categorized by the up regulation of genes that encrypt myosin heavy chain, an example of sarcomeric protein (Rendl, 2004). Both MyoD and MtF5 are induced and regulated by Pax3 and Pax7, through openly binding to distal enhancer components and the proximal promoter of these MRF genes, respectively (Bajard, et al., 2006; Hu, et al., 2008; McKinnell et al., 2008). Pax7 is down regulated before terminal differentiation, following adequate development of myogenic progenitor cells (Olguin and Olwin, 2004).

1.7 Aim of the Thesis

The induction of main types of tissues such as vascular, nervous, muscle and connective tissues is required for *in vivo* functionality of skeletal muscle. Vascularization is an important concern in capacious tissues having high oxygen demand such as the skeletal muscle. It is responsible for the storage and breakdown of glucose and fat since it is a highly metabolic organ. As the other invaluable component of the muscle tissue, *in vitro* establishment of innervation by the motor neurons would better mimic the native tissue and provide an opportunity to test the effect of drugs targeting the neuromuscular junctions. Both innervated and vascularized human muscle tissue construct is expected to have a reduced time for functional integration in the body and eliminate the species-related variability associated with animal-based systems when used in drug discovery and toxicology studies.

In this thesis, it was aimed to develop a new *in vitro* skeletal muscle model by co-culturing endothelial cells, myotubes and human neuron-like cells. To achieve that purpose, three different cell types were used to form muscle model. First, capillary network and multinucleated myotube formation were provided by the co-culture of skeletal muscle stem cells with the HUVECs under optimized fetal bovine serum and media conditions. Also as a third cell type, human skeletal muscle stem cells were differentiated into neuron-like cells that were negative for the astrocyte marker and positive for neuronal markers.

This is the first study presents a novel *in vitro* human skeletal muscle model with advanced capillary networks with an interaction of myotubes and neurons, and it can be utilized in the *in vitro* testing of drugs and also used for the regeneration of skeletal muscles by means of cellular therapy or cell-laden tissue engineered muscle constructs.



2. MATERIALS AND METHODS

2.1 Human Skeletal Muscle Stem Cell Isolation

Under the guidelines of the Yeditepe University Hospital Human Ethics Committee, human skeletal muscle stem cells (hSkMSCs) were isolated with enzymatic digestion of muscle tissue acquired from hamstring grafts for anterior cruciate ligament surgery. First, the non-pathological human skeletal muscle tissue was put into HBSS (Hank's Buffered Salt Solution) with 5% penicillin-streptomycin-amphotericin (PSA) and divided into small pieces with the help of a scalpel. Then, an enzyme cocktail containing 0.1% collagenase I and 1.38 mg/mL dispase was prepared in HBSS and the muscle pieces were incubated in this solution in a shaking water bath for 2h at 37°C. The final slurry was filtered through a 100 µm pore size filter and the filtrate was centrifuged at 1,500 rpm for 5 min. The cells in the pellet were resuspended in media and centrifuged again under the same conditions to remove the debris. The pellet was resuspended in DMEM/F12 (Dulbecco's Modified Eagle's Medium/Nutrient F-12) (1:1) medium supplemented with 20% fetal bovine serum (FBS), 100 u/mL PSA, 20 µg/L human recombinant epidermal growth factor (EGF) and 10 µg/L basic fibroblast growth factor (bFGF) and pre-cultured on gelatin coated flasks, named as pre-plates, for 3h to reduce the number of fibroblasts. Unattached cells in the medium were transferred to an uncoated T25 flask and cultured at 37°C in 5% CO₂ incubator. The media in the flasks was refreshed every third day and when 70% confluency was reached, the cells were trypsinized with 0.25% Trypsin-EDTA for 5 min at 37°C and subcultured. Phase contrast microscope images were taken at day 4 of the primary culture.

2.2 Human Skeletal Muscle Stem Cell Characterization by Flow Cytometry

Two types of cells were differentiated from hSkMSCs; neuron-like cells and skeletal muscle cells. Flow cytometry was performed to characterize the hSkMSCs. Immunophenotyping of hSkMSCs was performed with antibodies against the following cell surface antigens: CD44 (Hyaluronate/lymphocyte homing associated cell adhesion molecule-HCAM), CD34 (hematopoietic progenitor cell antigen), CD45 (Protein tyrosine phosphatase, receptor type, C/PTPRC/leukocyte common antigen/cell marker of hematopoietic origin), CD90 (Thy-1/Thy-1.1) and CD105 (Endoglin). Cells (1×10^4) were immunostained for each antibody and analyzed by BD FACSCalibur™ flow cytometer (BD biosciences, USA). Samples were normalized to isotype control.

2.3 Myotube formation

A hemocytometer was used to count hSkMSCs and calculate the cell concentration. The cells were plated on a tissue culture dish approximately at 3×10^3 cells/cm² using DMEM/F12 medium supplemented with 20% FBS, 20 µg/L EGF and 10 µg/L bFGF for cell proliferation. Following 24 hours of incubation, the FBS percentage was lowered to 10%. At the end of 7 and 14 days of incubation, the multinucleated myotubes were observed under the light microscope. Immunocytochemical staining was carried out using the streptavidin–peroxidase method (UltraVision Plus Large Volume Detection System Anti-Polyvalent, HRP immunostaining Kit; Thermo Scientific, UK) to reveal the desmin positive myotubes. Briefly, cultured cells were fixed in ice-cold methanol with 0.3% hydrogen peroxide for 15 min and allowed to dry. After washing with phosphate buffer saline (PBS), the cells were incubated first with Ultra V Block for 5 min at room temperature, then with the primary antibody for desmin overnight at 4°C. The following day, biotinylated secondary antibody was added and cells were incubated for 15 min at room temperature. Streptavidin peroxidase treatment was then carried out for 15 min at room temperature and signal was detected with the AEC kit (Zymed Laboratories/Invitrogen, Carlsbad, CA). After counter-stained with hematoxylin (Santa Cruz Biotechnology), cells were examined under the light microscope.

2.4 Neuron-like Cell Differentiation

hSkMSCs were counted with hemocytometer and plated on a tissue culture dish (approximately 2.5×10^3 cells/cm²) using DMEM/F12 medium supplemented with 20% FBS, 20 µg/L EGF and 10 µg/L bFGF. Cell morphology was observed after 24 hours of incubation to ensure cell attachment to the surface. The cells were rinsed twice with DPBS and complete neural differentiation media (AdvanceSTEM Neural Differentiation Medium and AdvanceSTEM Stem Cell Growth Supplement (Thermo) mixed in 9:1 ratio according to manufacturer's recommendation) was added. The cells were incubated at 37°C in a 5% CO₂ incubator and the neural differentiation medium was refreshed every 48 hours. The morphology of neuron-like cells was observed after 72 hours of incubation. In order to maintain cells in their differentiated state, additional neural differentiation medium was supplied in every 48 hours.

2.5 Neuron-like Cell Characterization by Immunostaining

The cells were incubated for 3 days in complete neural differentiation media and finally fixed and immunostained the mouse anti-beta3-tubulin (Santa Cruz, sc-69966), the goat anti-nestin (Santa Cruz, sc-21248) and the goat anti-GFAP (Santa Cruz, sc-6171). Briefly, the cells on the slides were rinsed with PBS, fixed in cold 3.7% formaldehyde for 10 min at RT. After a subsequent wash in PBS, the slides were incubated with 1.5% blocking serum of the species used to raise the secondary antibodies (Santa Cruz Biotechnology, Heidelberg, Germany) for 20 min at 37°C to suppress nonspecific binding of IgGs. After washing three times with PBS for 5 min each, the cells were incubated overnight at 4°C with the primary antibodies specific for the mouse anti-beta3-tubulin and goat anti-GFAP. After washing 3-times, the slides were incubated with the secondary anti-mouse and anti-goat antibodies, respectively, for 45 min in dark. Finally, the samples were counterstained with DAPI (Sigma-Aldrich, USA) for 15 min, washed three times again, mounted and observed under the confocal microscope (Zeiss, LSM).

2.6 Isolation of HUVECs

Umbilical cords were obtained from full-term births with well-versed (informed consent) approval of the mothers who experienced a caesarean section or normal delivery. They were aseptically stored at 4°C in HBSS with 2% Pen/Strep until processing. The cords were washed extensively with PBS to remove the blood clots. Culture medium was flushed through the vein to blow out the coagulated blood. One end of the vein was closed with a clamp and after air removal, it was filled with 0.1% collagenase I (from *Clostridium histolyticum*, Gibco) prepared in HBSS, and the open end was closed with another clamp to retain the enzyme solution in the vein. The umbilical cord was placed into a 50 mL Falcon tube containing warm PBS and incubated in a shaking water bath at 37°C for 25 min. One end of the vein was cut and the enzyme solution containing the endothelial cells was taken into a 15 mL Falcon tube and lumen of the vein washed with the medium to retrieve all detached endothelial cells. After centrifugation, the cell pellet was resuspended in endothelial cell growth medium-2 (EGM-2; Lonza) completed with 2% FBS and transferred into a gelatin-coated T25 flask. Human umbilical vein endothelial cells (HUVECs) were cultured in CO₂ incubator (5%) at 37°C until 70% confluent monolayer was reached. Then, they were trypsinized and cryopreserved. HUVECs' endothelial cell surface marker, CD31 expression was determined by immunostaining with the primary antibody according to the procedure mentioned in Section 2.5.

2.7 Co-Culture of hSkMSCs and HUVECs

HUVECs were co-cultured with hSkMSCs to check whether they form a capillary network that is specifically significant in growth of tissue engineered skeletal muscle constructs. In order to optimize hSkMSC and HUVEC co-culture, different media compositions were investigated. Growth medium (GM) of hSkMSCs (DMEM/F12 medium supplemented with 20% FBS) was tested at different FBS concentrations either alone or in 1:1 mixture with the growth medium of HUVECs (EGM-2 medium supplemented with 2% FBS). Six types of media were tested in the co-culture: DMEM/F12 medium with (1) 5% FBS, (2) 10% FBS, (3) 20% FBS, (4) 5% FBS: EGM-2 medium with 2% FBS (1:1), (5) 10% FBS: EGM-2 medium

with 2% FBS (1:1), and (6) 20% FBS: EGM-2 medium with 2% FBS (1:1) (Table 2.1).

Table 2.1: Media types tested in the co-culture of hSkMSCs and HUVECs, and their FBS contents. Media mixtures were prepared in 1:1 volumetric ratio.

Medium Type/Code	D5	D10	D20	D5-E2	D10-E2	D20-E2
DMEM/F12 (D)	5% FBS	10% FBS	20% FBS	5% FBS	10% FBS	20% FBS
EGM-2 (E)	-	-	-	2% FBS	2% FBS	2% FBS

hSkMSCs and HUVECs were mixed in 1:1 ratio and seeded (7×10^3 cells/well) on untreated coverslips in 24 well plates. The cells were incubated for 13 days in optimization media, then fixed and immunostained. The same procedure in Section 2.5 was carried out. This time primary antibodies were changed to myogenic marker rabbit anti-desmin and endothelial marker Mouse anti-CD31.

2.8 *In vitro* human skeletal muscle model: co-culture of myotubes, neuron-like cells and the capillary network

Co-culture of hSkMSCs and HUVECs was maintained for 13 days to obtain *in vitro* model of the human skeletal muscle. First, cells were mixed in 1:1 ratio and seeded (7×10^3 cells/well) on untreated coverslips in a 24-well plate. On day 14, the neuron-like cells obtained by differentiating hSkMSC in a separate culture were trypsinized and added on top of the co-cultured cells with a density of 4×10^3 cells per well. The co-culture containing three different cell types was continued for 24h in the neural differentiation medium (AdvanceSTEM Neural Differentiation Medium and AdvanceSTEM Stem Cell Growth Supplement (Thermo) mixed in 9:1 ratio according to manufacturer's recommendation) and the cells were then fixed and immunostained. The procedure mentioned in Section 2.5 was carried out, but

the primary antibodies were changed to myogenic marker rabbit anti-desmin, endothelial marker Mouse anti-CD31, and neuronal marker mouse anti-beta3-tubulin.

2.9 Real-Time PCR

Total RNA was isolated from the wells on days 1, 7 and 14, by using an RNeasy Mini Kit (Qiagen, Germany). A Sensiscript Reverse Transcriptase was used to perform first-strand cDNA synthesis. Primer sequences used for real-time PCR were; GAPDH (glyceraldehyde-3-phosphate dehydrogenase), the neural progenitor marker; nestin, neuronal marker beta-tubulin3, neuronal marker ENO2 (enolase 2, gamma, neuronal), myogenic marker MYOG (myogenin), precursor neuroprogenitor cell markers NEFH (neurofilament, heavy polypeptide 200 kDa) and NEFL (neurofilament, light polypeptide 68 kDa). All primer sequences were designed for homo sapiens based on a study by Karaöz et al. (2010) (Table 2.2) and purchased from Metabion (Germany). hSkMSCs were differentiated into neuron-like cells on T75 flasks to obtain positive control. All of the co-culture experiments were carried out in 24 well plates. Following RNA isolation, RT-PCR was run to obtain first-strand cDNA. Then, temperature optimization was carried out for each primer with PCR machine (Bio-Rad, MyCycler) and agarose gel (1.5%) analysis were done. Then, for each sample, 12.5 µL Maxima SYBR Green qPCR Master Mix (x2; Fermentas, Vilnius, Lithuania), 0.5 µL forward and reverse primer for each (from 10 µM), a 2 µL template and 9 µL distilled water were used in an iCycler™ real-time system (BIO-RAD, CA, USA).

Table 2.2: Sequences used for real-time PCR analysis were GAPDH (glyceraldehyde-3-phosphate dehydrogenase) as housekeeping gene; neural progenitor marker; nestin; neuronal marker beta-tubulin3; neuronal marker ENO2 (enolase 2, gamma, neuronal); myogenic marker MYOG (myogenin); precursor neuroprogenitor cell markers NEFH (neurofilament) and NEFL (neurofilament).

Gene (Product Size)	Forward primer (F) (5'→3') Reverse primer (R) (5'→3')	GeneBank accession no.	AT (°C)
GAPDH (211 bp)	F: TCCTCAGGGGAGATGATGGT R: TTCTCGATGTAGCTGGCAAAG	NM_001131019	56°C
Nestin (302 bp)	F: CTCTGACCTGTCAGAAGAAT R: GACGCTGACACTTACAGAAT	NM_006617	54°C
Beta- tubulin3 (175 bp)	F: CATGGACAGTGTCCGCTCAG R: CAGGCAGTCGCAGTTTTCAC	NM_006086	58°C
ENO2 (269 bp)	F: TTATTGGCATGGATGTTGCTGC R: CCCGCTCAATACGTTTTGGG	NM_001975	55°C
NEFH (396 bp)	F: TTATTGGCATGGATGTTGCTGC R: CCCGCTCAATACGTTTTGGG	NM_021076	54°C
NEFL (283 bp)	F: GAACACAGACGCTATGCGCTCAG R: CACCTTTATGTGAGTGGACACAGAG	NM_006158	54°C
MYOG (279 bp)	F: TATGAGACATCCCCCTACTTCTACC R: CTTCTTGAGCCTGCGCTTCT	NM_002479	54°C

2.10 Live cell imaging

Time lapse imaging of hSkMSCs in complete neural differentiation media was carried out first. Then, the same procedure was applied to HUVECs and hSkMSCs in the co-culture by labeling the cells using fluorescent dyes in order to investigate the behavior of cells under the co-culture conditions.

hSkMSCs were seeded on untreated coverslips in a 24-well plate with complete neural differentiation media and investigated for different time points and periods.

In the second part of live cell imaging, fluorescent dyes Chloromethylbenzamido (CellTracker™ CM-DiI) and 5(6)-Carboxyfluorescein diacetate N-succinimidyl ester (CFSE) were used to label hSkMSCs and HUVECs, respectively. The CFSE dye is purchased as carboxyfluorescein diacetate succinimidyl ester (CFDA, SE) and stock solutions (10 mM) were prepared in DMSO (Dimethylsulfoxide). The dilutions of the stock solution were prepared with PBS. Concentrations and incubation times were optimized. Cells were detached and incubated for 5 min at 37 °C and an additional 15 min at 4°C with CellTracker™ CM-DiI (3 μM) and 15 min at 37°C with CFSE (5 μM).

After labeling, cells were washed with PBS and resuspended in fresh medium. The cells in 6-well plate were maintained in DMEM/F12 (10% FBS): EGM-2 (2% FBS) (1:1) mixture at 37°C, in 5% CO₂ and imaged. The videos were recorded at a frame frequency of 2 frames/hour. The Olympus IX81 life science imaging system (Figure 2.1) was used to follow cell movement, differentiation, and interaction.

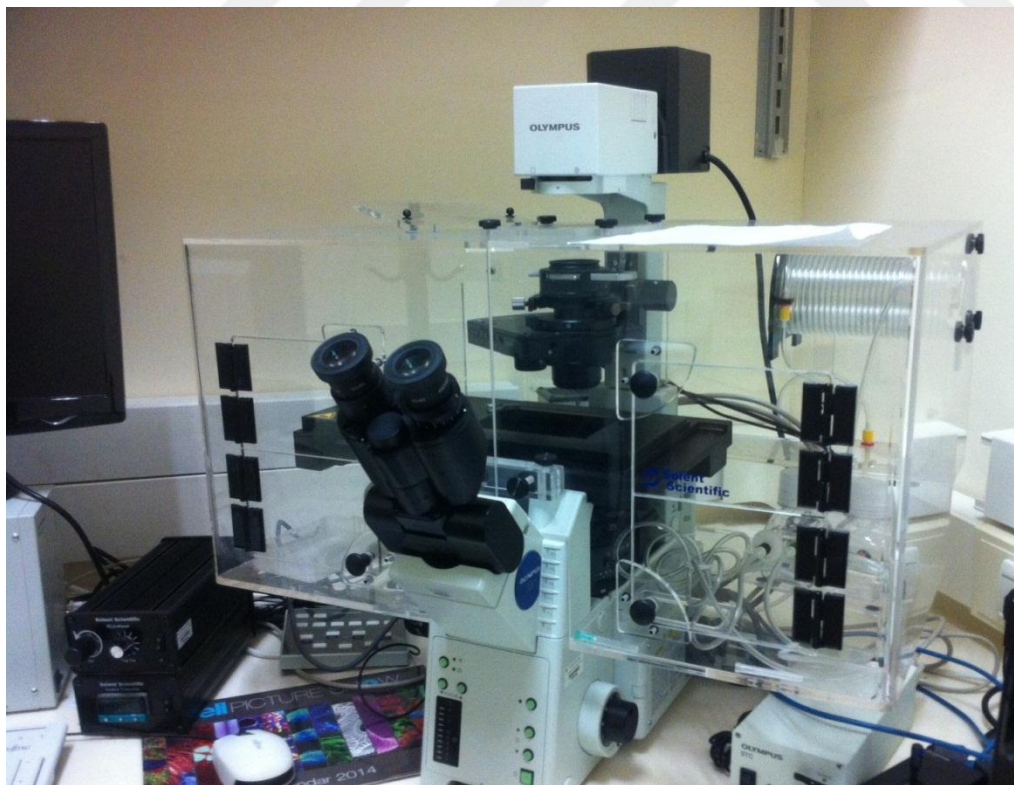


Figure 2.1: Live cell imaging system, Olympus IX81 Life Science Imaging System.

2.11 Electrophysiological Study

The electrophysiological contraction study was conducted at Yeditepe University Mechanical Engineering laboratory using Bi-phasic 1Hz square wave that has 5V amplitude with a 20 ms pulse width. After the application of this method, muscle contraction was observed. The study of Electrophysiology was carried out through the attachment of a computer utilizing MATLAB program in the form of a pulse generator. This system includes computer with oscilloscope and two sterilized probes which were placed into the wells without disturbing the cells and interacting with the media called NBActiv 4. The probes were placed on opposite sides in 24 well plates. The electrophysiological data were processed with MATLAB program. Myotubes and human neuron-like cells were observed under the phase-contrast microscope throughout the entire procedure.

2.12 Study Summary Schema

Studies conducted during thesis was summarized in a schema in (Figure 2.2)

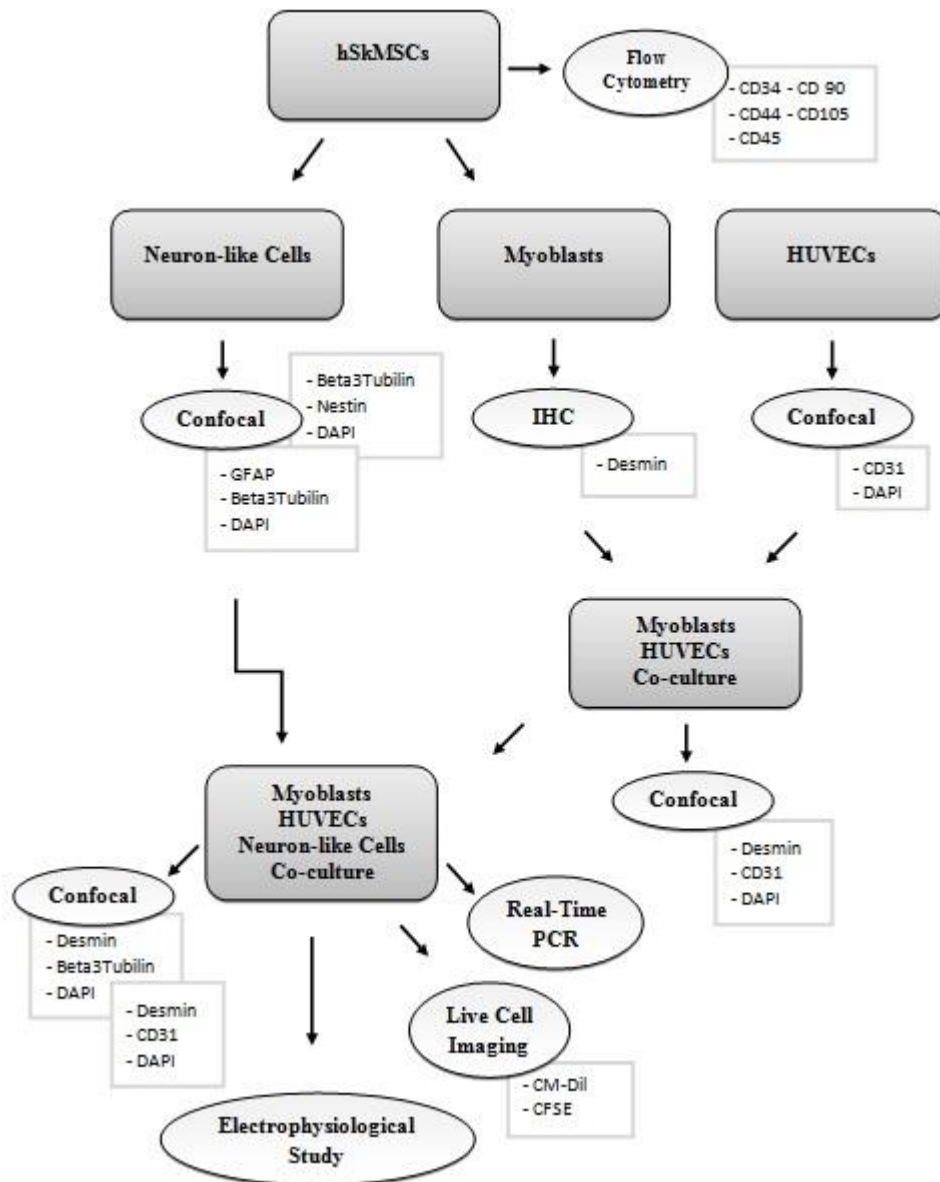


Figure 2.2: Schema of studies conducted.

3. RESULTS AND DISCUSSION

3.1 Human Skeletal Muscle Stem Cell Characterization

This study aimed to develop a novel human *in vitro* skeletal muscle model by co-culture of human neuron-like cells and myotubes obtained from human skeletal muscle derived stem cells and a capillary network obtained from human umbilical vein endothelial cells.

Under the phase contrast microscope, isolated human skeletal muscle stem cells were checked and cell morphology was assessed. The preplate had mainly the cells of fibroblastic morphology (Figure 3.1A), whereas the cells seeded in flasks and produced from the cells floating in the media of preplate were mostly the myoblasts that created colonies (Figure 3.1B).

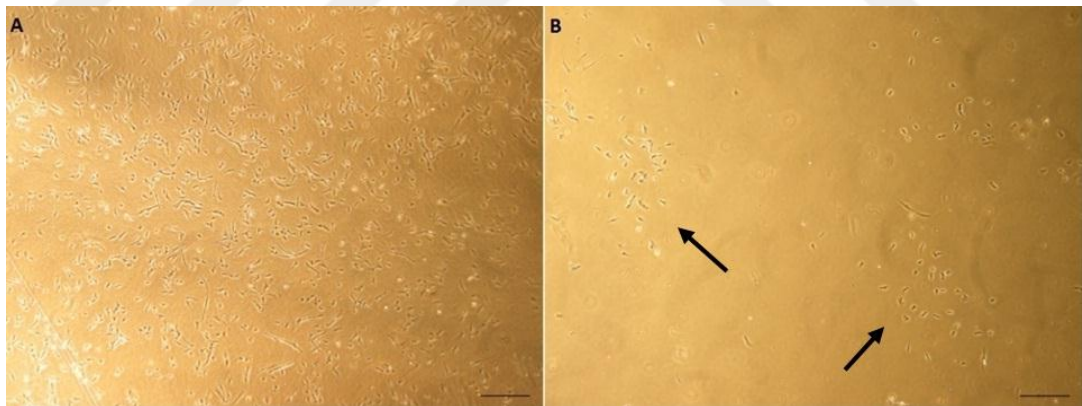


Figure 3.1: Phase contrast micrographs of human skeletal muscle derived cells after 4 days of incubation; A) cells at the preplate, B) skeletal muscle myoblast colonies in the flask. Arrows point the myoblast colonies. Scale bars represent ~ 100 μm .

In this research, the muscle stem cells were isolated through whole tissue digestion. The pre-plating technique (Qu-Petersen et al., 2002) was adapted to eliminate the fast-adhering fibroblasts in the pre-plate and the tests were conducted using the enriched muscle stem cells.

In order to validate the ability of myoblasts to form multinucleated myotubes, they were incubated in DMEM/F12 medium having 10% FBS for 14 days and the myotubes were inspected underneath the brightfield microscope for 7 days (Figure 3.2) and also the phase contrast microscope after 14 days of incubation (Figure 3.3). From day 7 to day 14, nuclei amount of myotubes increased (Figure 3.2 and 3.3).

Flow cytometry results of isolated human skeletal muscle stem cells showed that they expressed the typical mesenchymal stem cells' surface markers- CD44 (95.30% positive), CD90 (96.83% positive), CD105 (85.58% positive) - and they were negative for hematopoietic cell surface markers - CD45 (1.27% positive), CD34 (0.78% positive) (Figure 3.4).

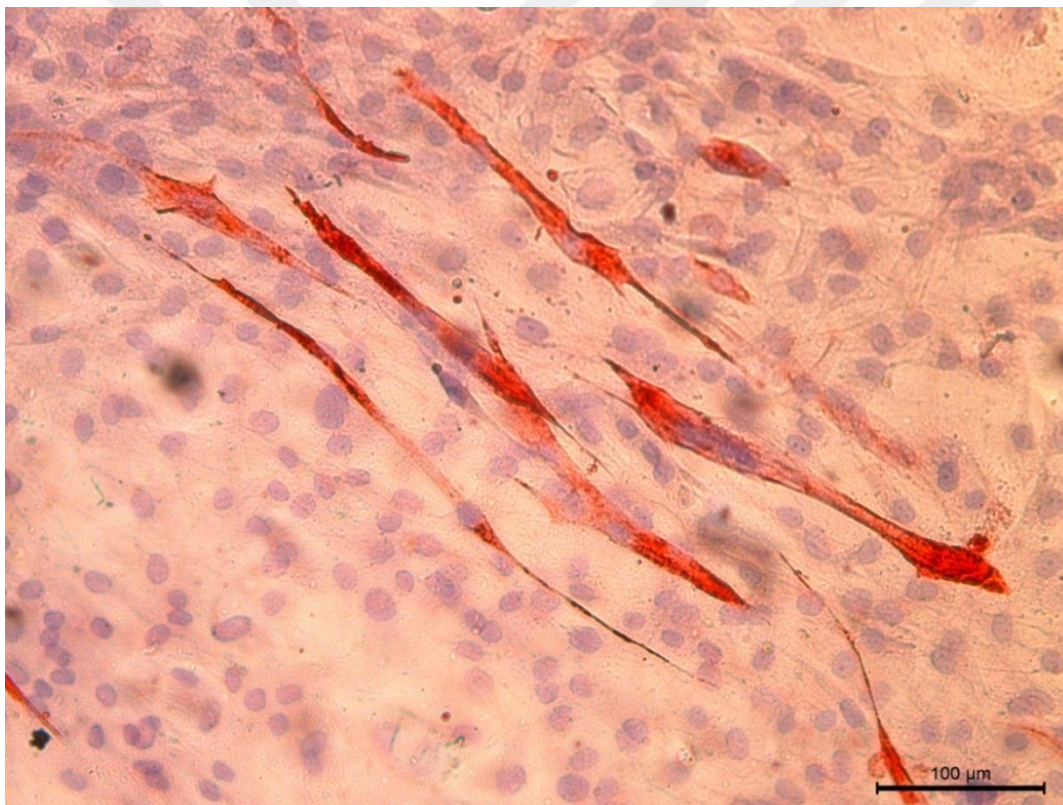


Figure 3.2: Myotubes obtained by fusion of myoblasts in DMEM/F12 medium with 10% FBS. BF image of myotubes immunohistochemically stained for desmin after 7 days of culture. Scale bar represent ~ 100 μm.

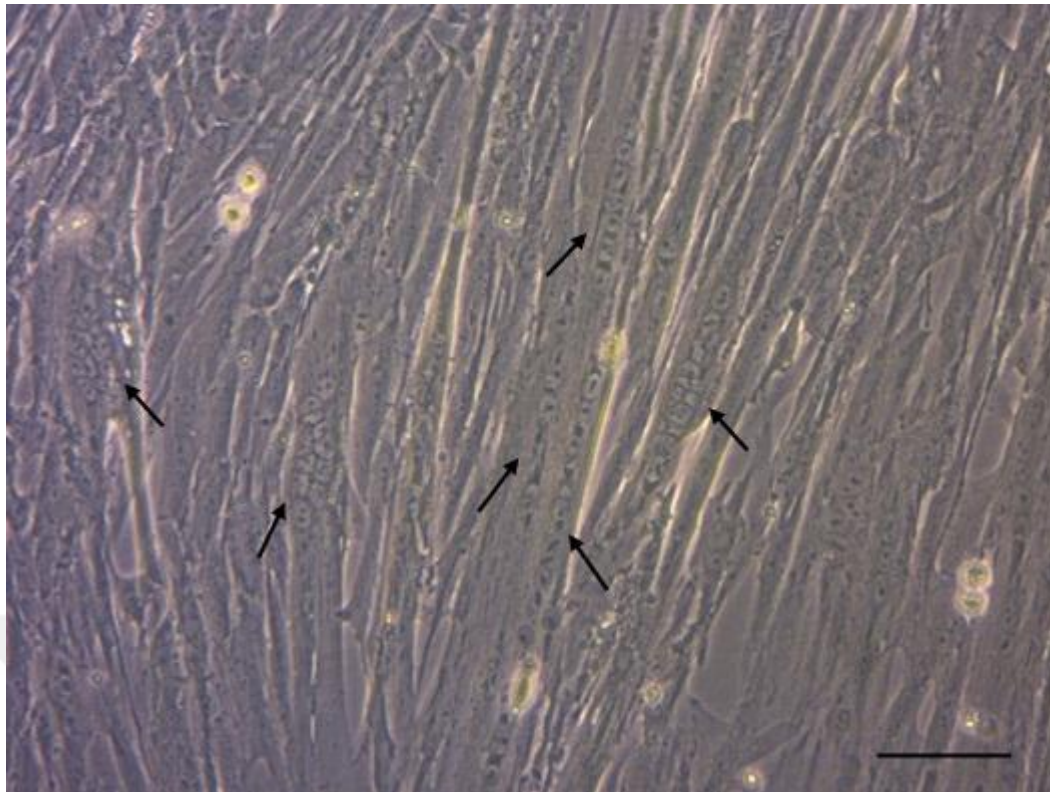


Figure 3.3: Myotubes obtained by fusion of myoblasts in DMEM/F12 medium with 10% FBS. Phase contrast micrograph of myotubes obtained after 14 days of culture. Arrows point the multinucleated myotubes. Scale bars represent $\sim 100 \mu\text{m}$.

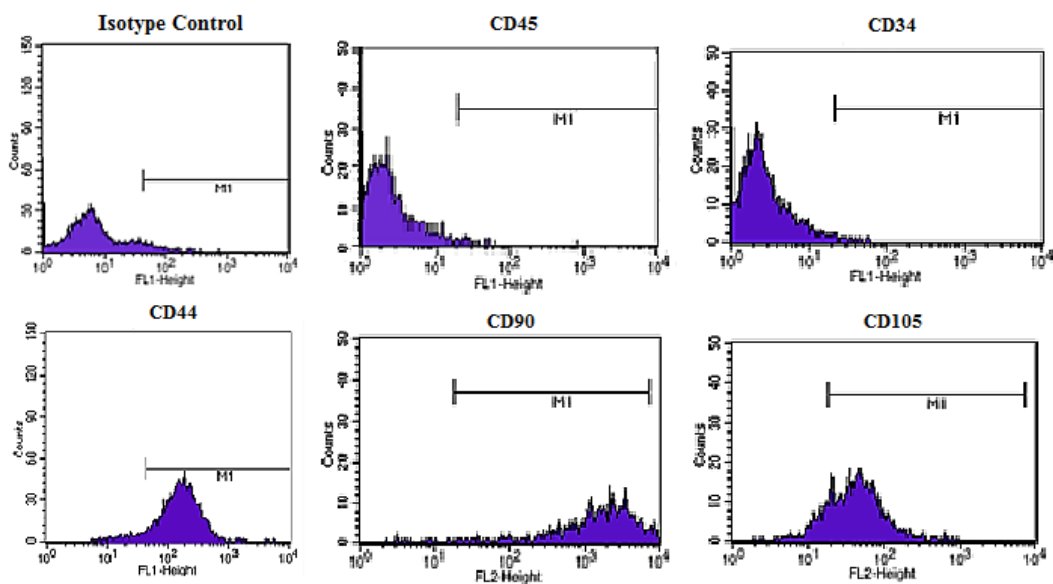


Figure 3.4: Flow cytometry histograms of human skeletal muscle stem cell surface antigens: CD44, CD90, CD45, CD34, CD105 and their isotype control.

The muscle stem cells, cultured in a media of high FBS percentage to prevent myoblast maturation, were characterized by flow cytometry for their cell surface

markers. Passage 2 cells were found to be positive for the mesenchymal stem cell markers CD90, CD44, and CD105 and negative for the hematopoietic lineage markers CD45 and CD34. Chirieleison et al. (2012) used the pre-plate method to establish the phenotypic characteristics of the human skeletal muscle stem cells that attached differentially to the surface in a time based mode. The skeletal muscle cells used by this group adhered to the tissue culture plate surface after 30 to 60 min (PP2) and expressed the same surface markers with the one used in our research.

3.2 Neuron-like Cell Differentiation and Characterization

Neuron-like cell differentiation was established with confocal microscopy followed by staining the cells for beta-tubulin 3 (a neuronal marker), nestin (an early neuronal marker), and GFAP (an astrocyte marker). Astrocyte and neuron cells can be distinguished with this staining; the cells subjected to neuronal differentiation were found negative for GFAP (Figure 3.5), whereas they stained positive for nestin and beta-tubulin 3 (Figure 3.6). Nestin is an intermediate filament protein and neural stem/progenitor cell marker. It is also essential for the neural stem cells' survival and self-renewal. Throughout neuro- and gliogenesis, nestin is substituted by cell type-specific intermediate filaments like neurofilaments and GFAP (Michalczyk and Ziman, 2005).

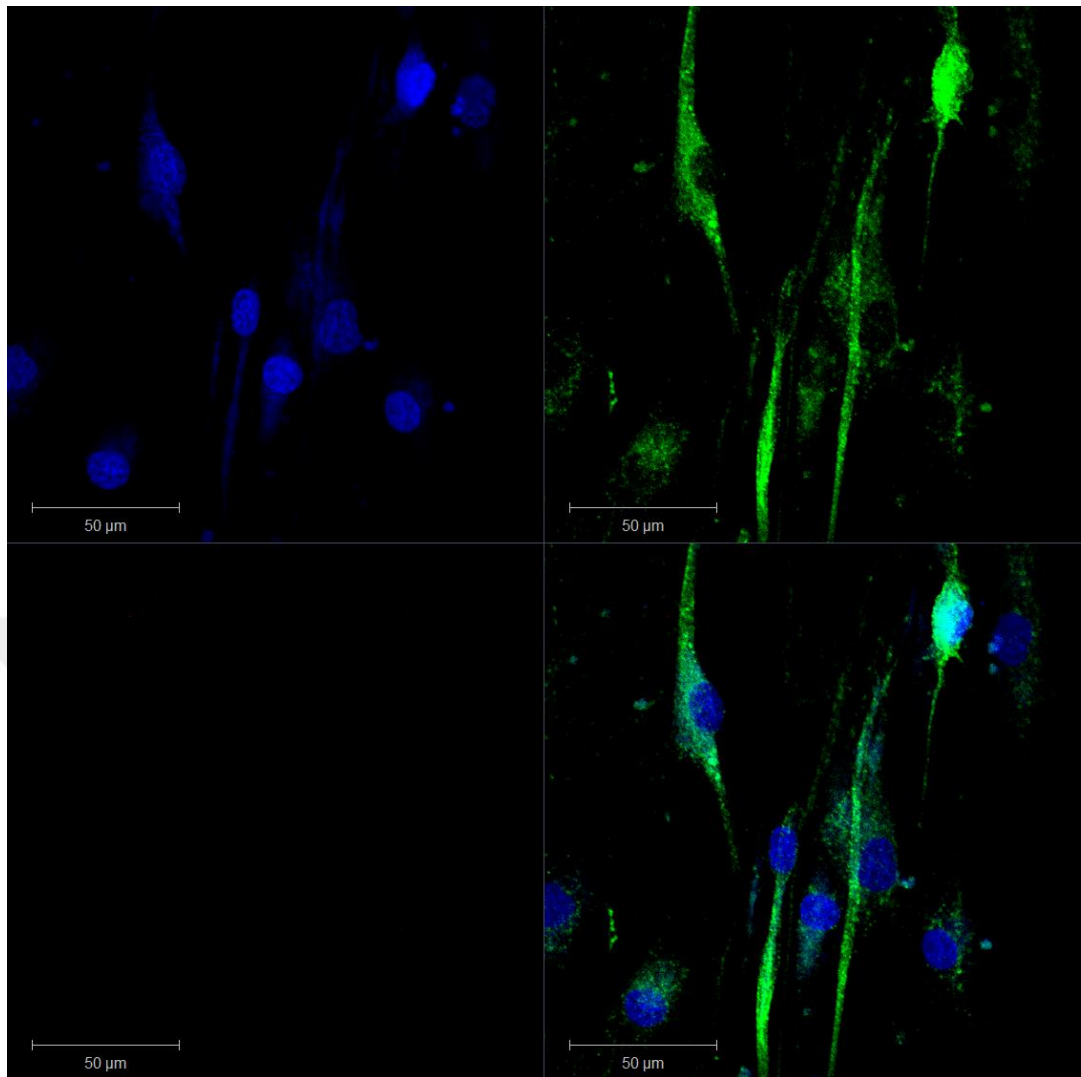


Figure 3.5: Confocal micrographs of hSkMSCs subjected to neuronal differentiation and stained for beta-tubulin3: green, GFAP: red, nuclei (DAPI): blue.

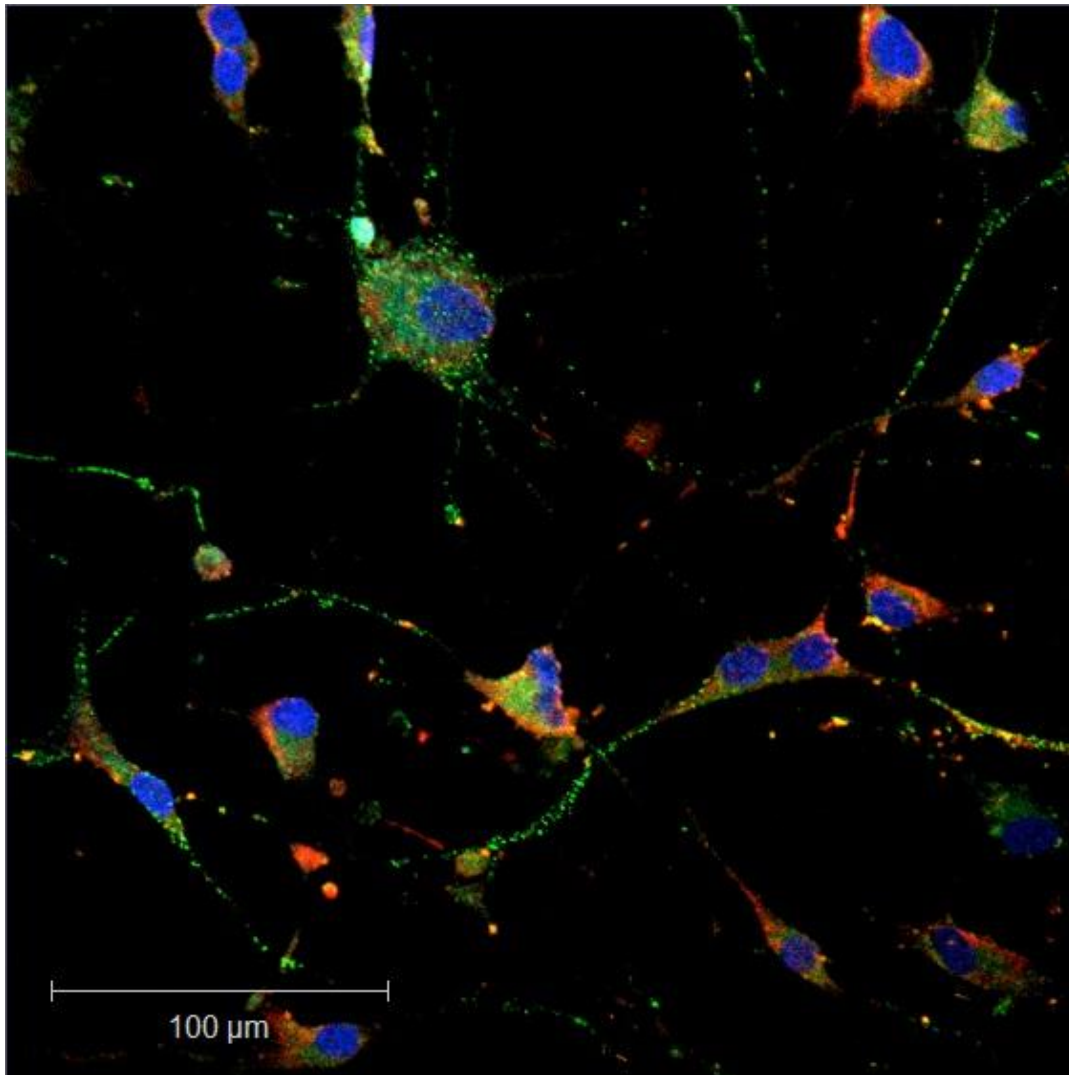


Figure 3.6: Confocal micrograph of hSkMSCs subjected to neuronal differentiation and stained for beta-tubulin3: green, Nestin: red, nuclei (DAPI): blue. Cells were negative for GFAP which is an astrocyte marker and positive for nestin and beta-tubulin3.

Human skeletal muscle contains not only the satellite cells that mature *in vitro* into myoblasts and fused with each other to create the myotubes, but also a group of multipotent stem cells that are capable of differentiation into adipocytes, osteoblasts, and neurons. Lately, Tamaki et al. (2015) were able to demonstrate that CD34⁻/CD45⁻/CD29⁺ cells from human skeletal muscle actively contributed to muscle fiber regeneration *in vivo*, whereas CD34⁺/CD45⁻ cells actively engrafted to the interstitium linked with differentiation into Schwann cells, perineurial/endoneurial cells alongside pericytes and vascular endothelial cells. At least two groups reported differentiation of human skeletal muscle originated stem cells into neurons *in vitro*: Alessandri et al. (2004) isolated the skeletal muscle stem cells within a serum free medium and demonstrated their ability to differentiate into

both astrocytes and neurons. Schultz and Lucas (2006) revealed the capability of skeletal muscle stem cells to differentiate more into neurons and less into astrocytes once cultured within a neurococktail. A commercially accessible neuronal differentiation medium was used in our research and the resultant neuron-like cells were found to be positive for neuronal markers, beta-tubulin 3 and nestin and negative for the astrocyte marker, GFAP.

3.3 Characterization of HUVECs by Immunocytochemistry

Phase contrast micrographs of the primary culture of HUVECs at day 4 (Figure 3.7) were obtained and passage 2 cells were immunostained for endothelial cell surface marker CD31 (Figure 3.8). The HUVECs showed the characteristic cobblestone morphology and stained positive for CD31.

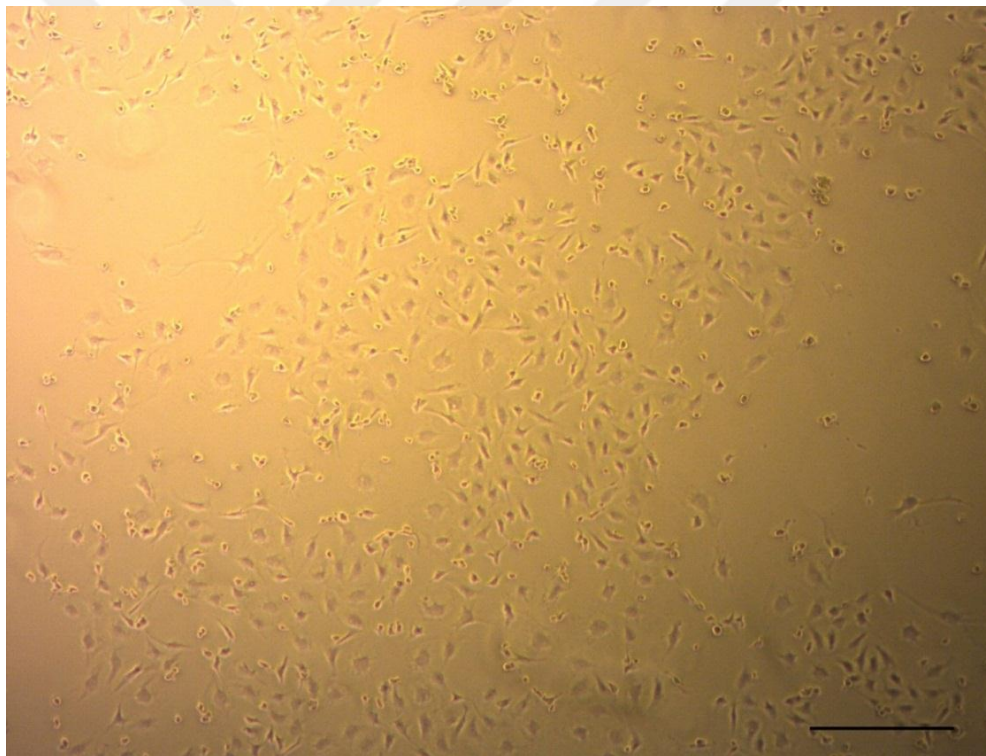


Figure 3.7: Human umbilical vein endothelial cells (HUVECs) in culture after 4 days of incubation. Phase contrast micrograph of HUVECs. Scale bar represents $\sim 100 \mu\text{m}$.

The endothelial cell surface marker CD31 protein, which is also found on the surface of monocytes, neutrophils, platelets, and some forms of T-cell, comprises a big proportion of endothelial cell intercellular junctions. The encoded protein is a member of the immunoglobulin super-family.

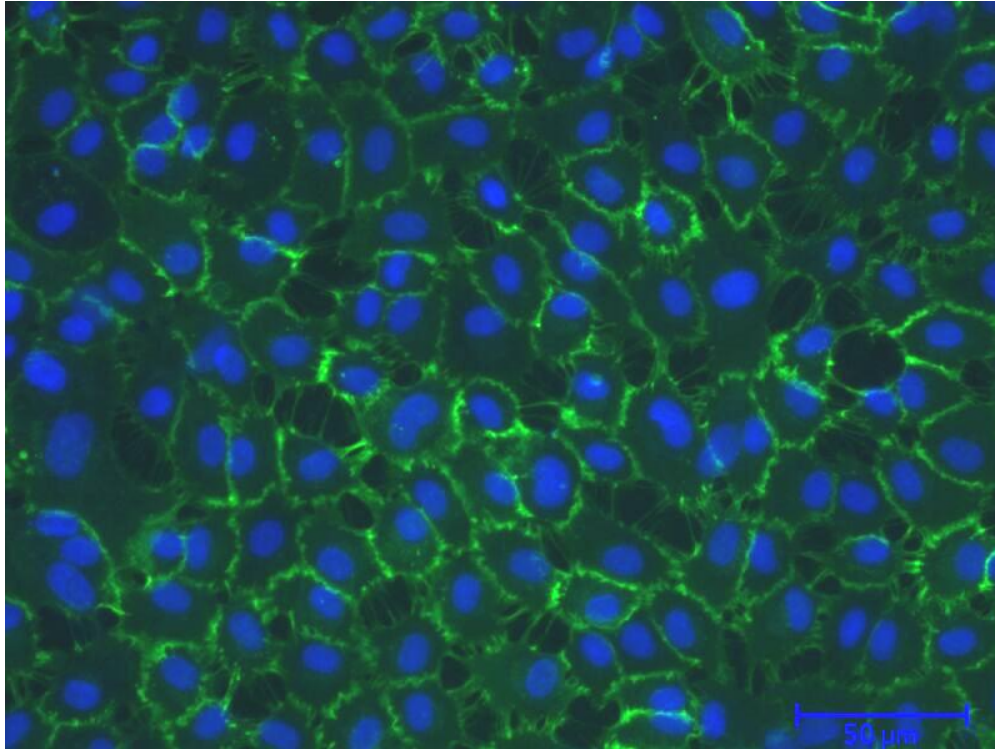


Figure 3.8: Human umbilical vein endothelial cells (HUVECs) in culture at passage 2. Fluorescence micrograph of HUVECs immunostained for their cell surface marker CD31 (green).

Recently, researchers have attempted to produce vascularized muscle flaps by co-culturing myoblasts with HUVECs, to obtain better *in vivo* integration and assist the cells within the thick 3D transplant. HUVECs need a growth factor (GF) cocktail to survive and proliferate at *in vitro* conditions.

3.4 Co-Culture of hSkMSCs and HUVECs

HUVECs and hSkMSCs were incubated in an incubator for 10 days, which is the minimum time necessary for capillary network formation in an optimized medium. After fixation, the cells were immunostained for the myogenic marker desmin and the endothelial marker CD31.

It was observed that HUVECs did not survive in a DMEM/F12 medium, supplemented with 5%, 10% and 20% FBS (Figure 3.9, 3.10, 3.11). When EGM-2 medium was mixed with DMEM/F12, however, the HUVECs survived and proliferated (Figure 3.12, 3.13, 3.14).

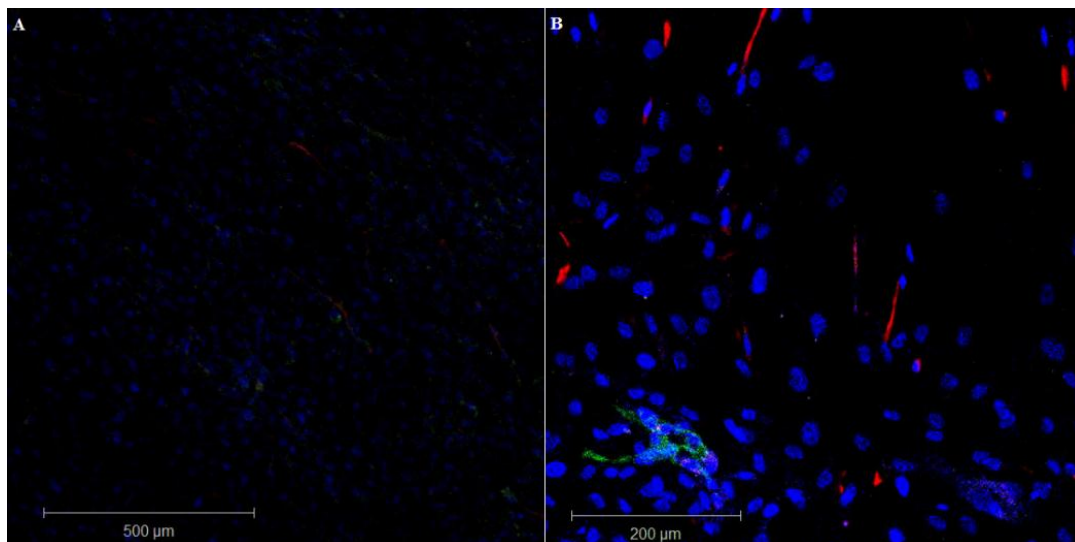


Figure 3.9: Confocal micrographs of hSkMSC-HUVECs co-cultured in DMEM/F12 medium supplemented with 5% FBS (D5), (A) 5X, (B) 10X. CD31: green, Desmin: red, nuclei (DAPI): blue.

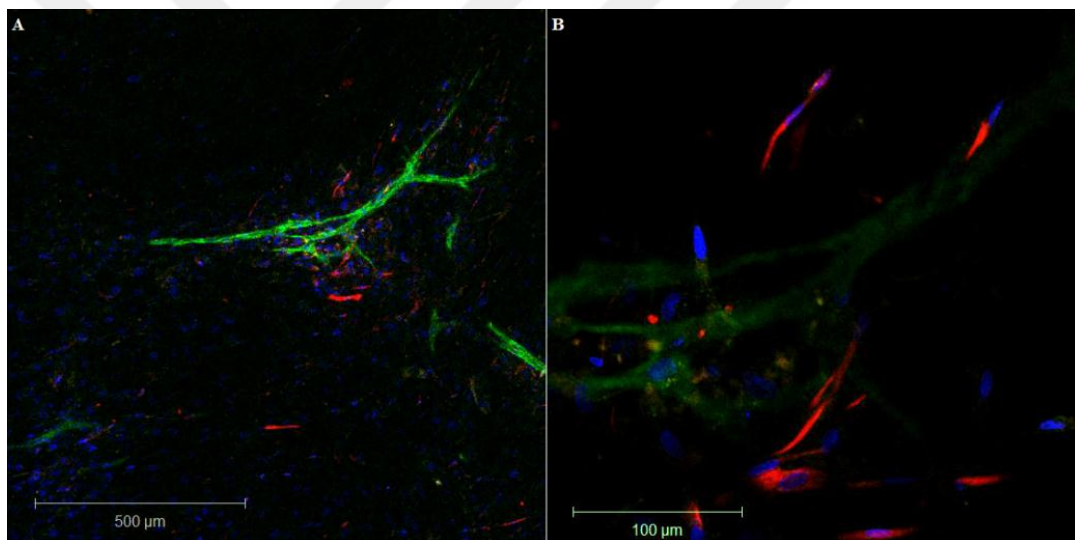


Figure 3.10: Confocal micrographs of hSkMSC-HUVECs co-cultured in DMEM/F12 medium supplemented with 10% FBS (D10), (A) 5X, (B) 20X. CD31: green, Desmin: red, nuclei (DAPI): blue.

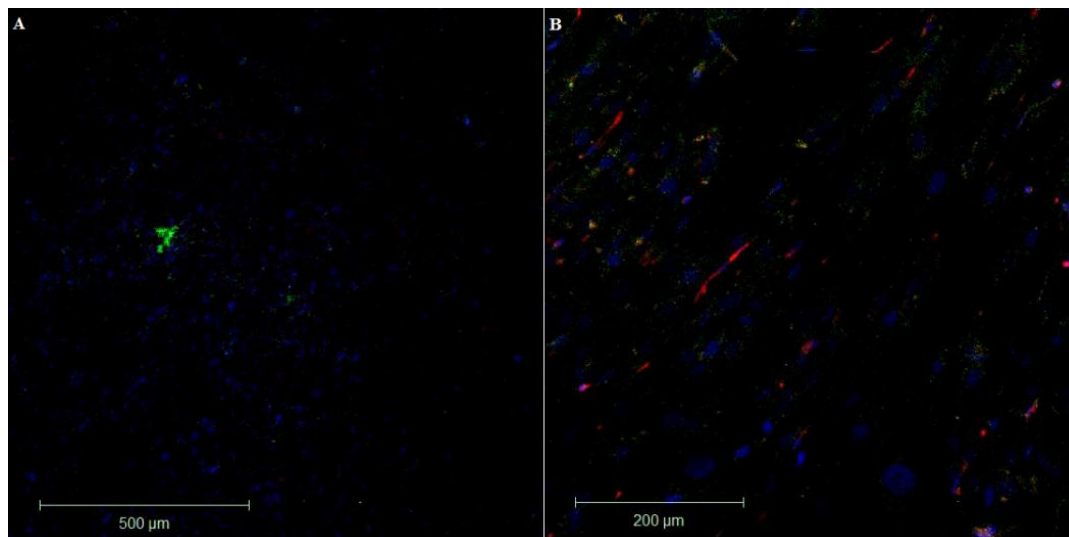


Figure 3.11: Confocal micrographs of hSkMSC-HUVECs co-cultured in DMEM/F12 medium supplemented with 20% FBS (D20), (A) 5X, (B) 10X. CD31: green, Desmin: red, nuclei (DAPI): blue.

It is known that in addition to FBS that contains GFs, mesenchymal stem cells also secrete some GFs, like VEGF, that might assist HUVECs to survive. Nagamori et al. (2013) studied HUVEC migration through human skeletal muscle myoblast sheets and they reported the formation of capillary networks within the myoblast sheets. This was believed to be caused by the local release of cytokines, such as FGF, VEGF, and HGF from the myoblasts. The HUVECs did not grow outside the sheets in DMEM containing 10% FBS. In contrast to our expectations, neither increasing the FBS concentration in DMEM/F12 medium, nor the skeletal muscle mesenchymal stem cell support improved the HUVECs survival or the formation of capillary networks without the endothelial cell growth medium. FBS concentration was critical for myotube formation and must be considered in a co-culture but it supports proliferation rather than fusion of myoblasts when used at a concentration of 20%. As a result, neither myotubes nor a capillary network could be formed in HUVEC and myoblast co-culture at that concentration in DMEM/F12 medium.

The capillary network formation was more robust in DMEM/F12 (5% FBS): (Figure 3.9) mixture, but no myotube formation could be detected.

The best results for the formation of multinucleated myotubes and capillary networks was obtained in the co-culture of HUVECs and hSkMSCs in the DMEM/F12 (10% FBS):EGM-2 (2% FBS) (1:1) mixture (Figure 3.12).

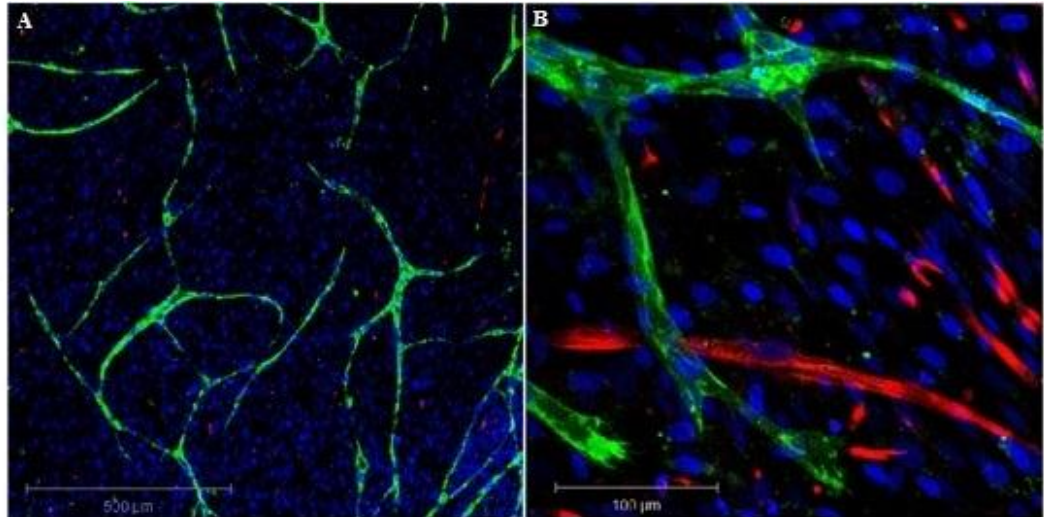


Figure 3.12: Confocal micrographs of hSkMSC-HUVEC co-cultured in DMEM/F12 10% FBS: EGM-2 (1:1) (D10-E2). (A) 5X, (B) 10X. CD31: green, desmin: red, cell nuclei (DAPI): blue.

Although the capillary network formation was more robust in DMEM/F12 (5% FBS):EGM-2 (2% FBS) (1:1) (Figure 3.13) mixture, the myoblasts formed aggregates just beneath the capillary network center and no myotube formation could be detected.

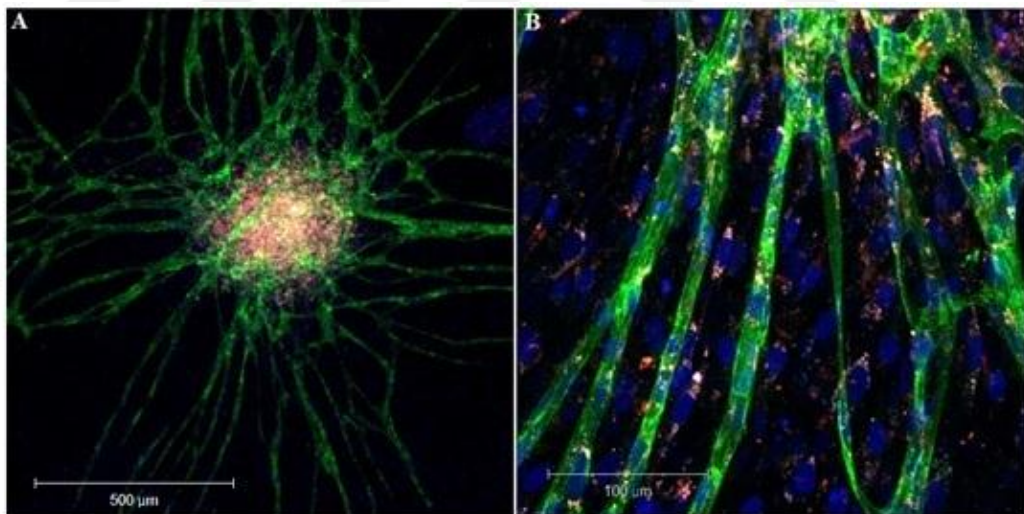


Figure 3.13: Confocal micrographs of hSkMSC-HUVEC co-cultured in DMEM/F12 5% FBS: EGM-2 (1:1) media (D5-E2). (A) 5X, (B) 10X. CD31: green, desmin: red, cell nuclei (DAPI): blue.

On the other hand, when the media mixture with the highest FBS concentration was used (DMEM/F12 (20% FBS):EGM-2 (2% FBS) (1:1) mixture) (Figure 3.14), the capillaries were found to be more stunted and myotube formation could not take place.

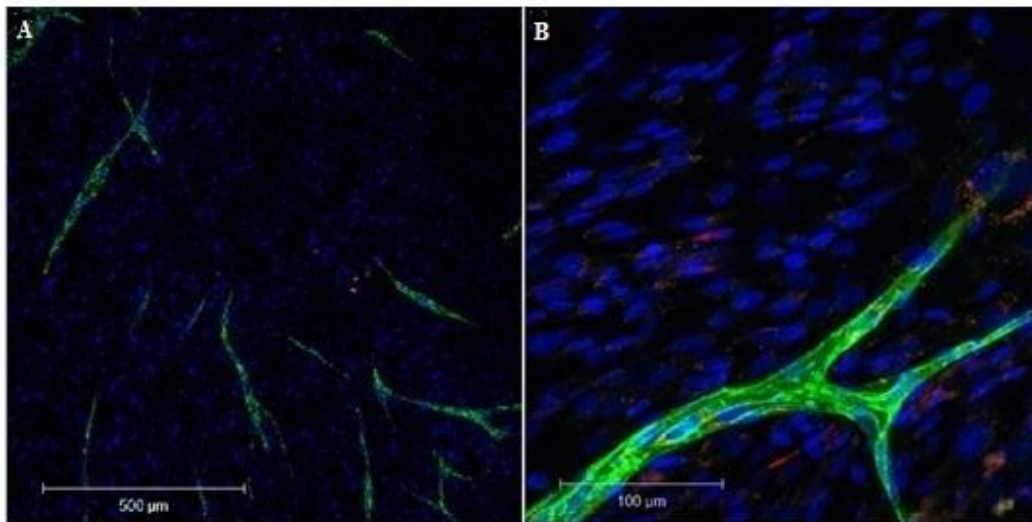


Figure 3.14: Confocal micrographs of hSkMSC-HUVEC co-cultured in DMEM/F12 20% FBS: EGM-2 (1:1) media (D20-E2). (A) 5X, (B) 10X CD31: green, desmin: red, cell nuclei (DAPI): blue.

A 1:1 volumetric mixture of EGM-2 and DMEM/F12 assisted HUVEC survival and capillary network formation in the co-culture. On the other hand, a final concentration of 3.5% FBS (D5:E2 medium) led to the formation of myoblast aggregates. The best media combination for the formation of both myotubes and capillary networks was found to be DMEM/F12:EGM-2 with a final FBS concentration of 6% (D10-E2). Increasing the FBS concentration to 11% (D20-E2) did not lead to any improvement; indeed it produced lower capillary network and myotube formation.

When the immortalized mouse myoblast cell line C2C12 was used in a similar co-culture, fibroblasts were also needed to induce physiological capillary network formation by the HUVECs (Levenberg et al., 2005; Shandalov et al., 2014). On the other hand, when primary human myoblasts were used in a co-culture with HUVECs, capillary networks were formed without any need to fibroblasts (Gholobova et al., 2015). This result can be attributed to the presence of mesenchymal stem cells or pericytes, among the primary cells derived from human skeletal muscle. Our research showed that co-culture of primary human myoblasts with HUVECs led to the formation of capillary networks within 10 days and, as mentioned above, this process strongly depended on amount of FBS used in the culture.

3.5 *In vitro* human skeletal muscle model: co-culture of myotubes, neuron-like cells and the capillary network

In order to have three types of cells, i.e. myotubes formed by satellite cells, capillaries formed by endothelial cells, and neuron-like cells from hSkMSCs, in co-culture in their functional differentiated states, separate precultures were performed before the final combination step. A co-culture of HUVECs and hSkMSCs in the DMEM/F12 (10% FBS):EGM-2 (2% FBS) (1:1) (D10-E2) mixture for 13 days led to the formation of a capillary network and myotubes. The neuron-like cells were obtained by differentiating the hSkMSCs in a separate culture and finally transferred on top of the co-cultured capillaries and myotubes. Confocal micrographs showed that the neuron-like cells were in association with the myotubes in the co-culture of these three different cell types after 24 hours of incubation (Figure 3.15).

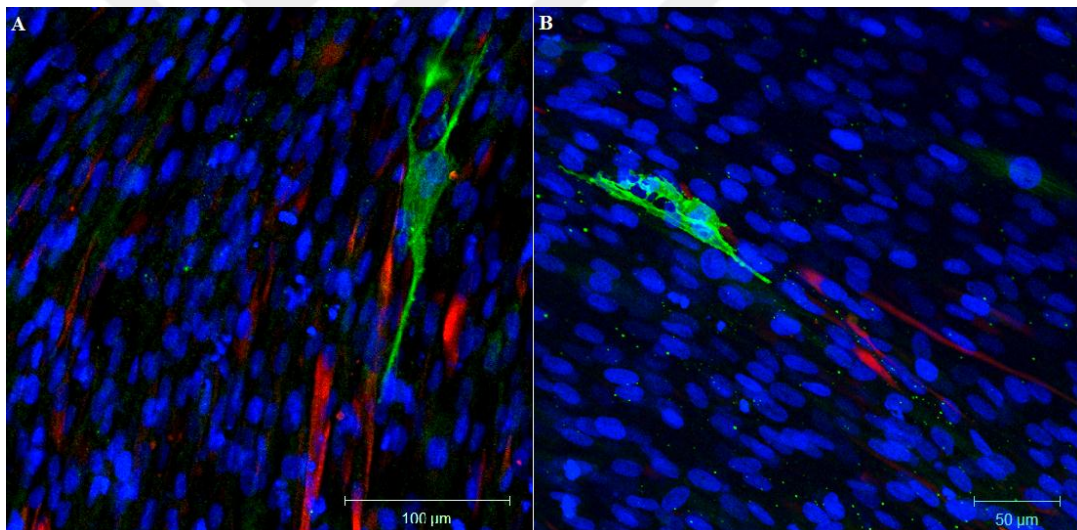


Figure 3.15: Confocal micrographs of (A, B) neuron-like cells in association with myotubes in the human *in vitro* skeletal muscle model formed by co-culturing myotubes, capillary networks and the neuron-like cells for 24h. Beta-tubulin3: green, desmin: red, cell nuclei (DAPI): blue.

For a better model of human skeletal muscle, that closely mimics the native tissue's structure and function, it is necessary to incorporate the motor neurons into the vascularized structure so that neuromuscular synapses are formed. Neuron-like cells derived from primary human skeletal muscle stem cells were seeded on the vascularized myotubes in our study to obtain the neuromuscular junctions at the co-culture. Given that each cell type has its own requirements for particular growth

factors and/or hormones, selecting and optimizing the culture medium is a crucial challenge when the co-culture of three different cells is needed *in vitro*. It is essential to determine how different media or their combination affect cell morphology and culture consistency, since each cell type utilizes medium of different composition and their viability and cell specific activities are crucially affected from the culture conditions.

The Z-stack projection of myotubes and the capillary network maintained in three-cell co-culture is presented in Figure 3.16, which reveals that myotubes were distributed near the bottom and mid sections while capillary network resided on top of them.

Taking into account our experience with HUVEC and hSkMSC co-culture as well as the literature on human endothelial cell line and human neural stem cell line co-culture (Chou et al., 2014), it is possible to say that a 50:50 combination of two particular media promotes cell morphology in a two cell co-culture. Concerning the co-culture of motoneurons with functional myotubes, Guo et al. (2011) revealed that *in vitro* functional human neuromuscular junction can be developed by a co-culture of motoneurons obtained from human fetal spinal cord stem cells and myotubes obtained from human skeletal muscle stem cells in a defined serum-free system, comprising sequential use of different media: first usage of co-culture media rich in neurotrophic factors for 4 days, and then addition of NBActiv 4 medium. After 24h-culture of our human skeletal muscle model in the commercial neuronal differentiation medium, the neuron-like cells were found to be alive and in contact with the myotubes, and the capillary network was also maintained.

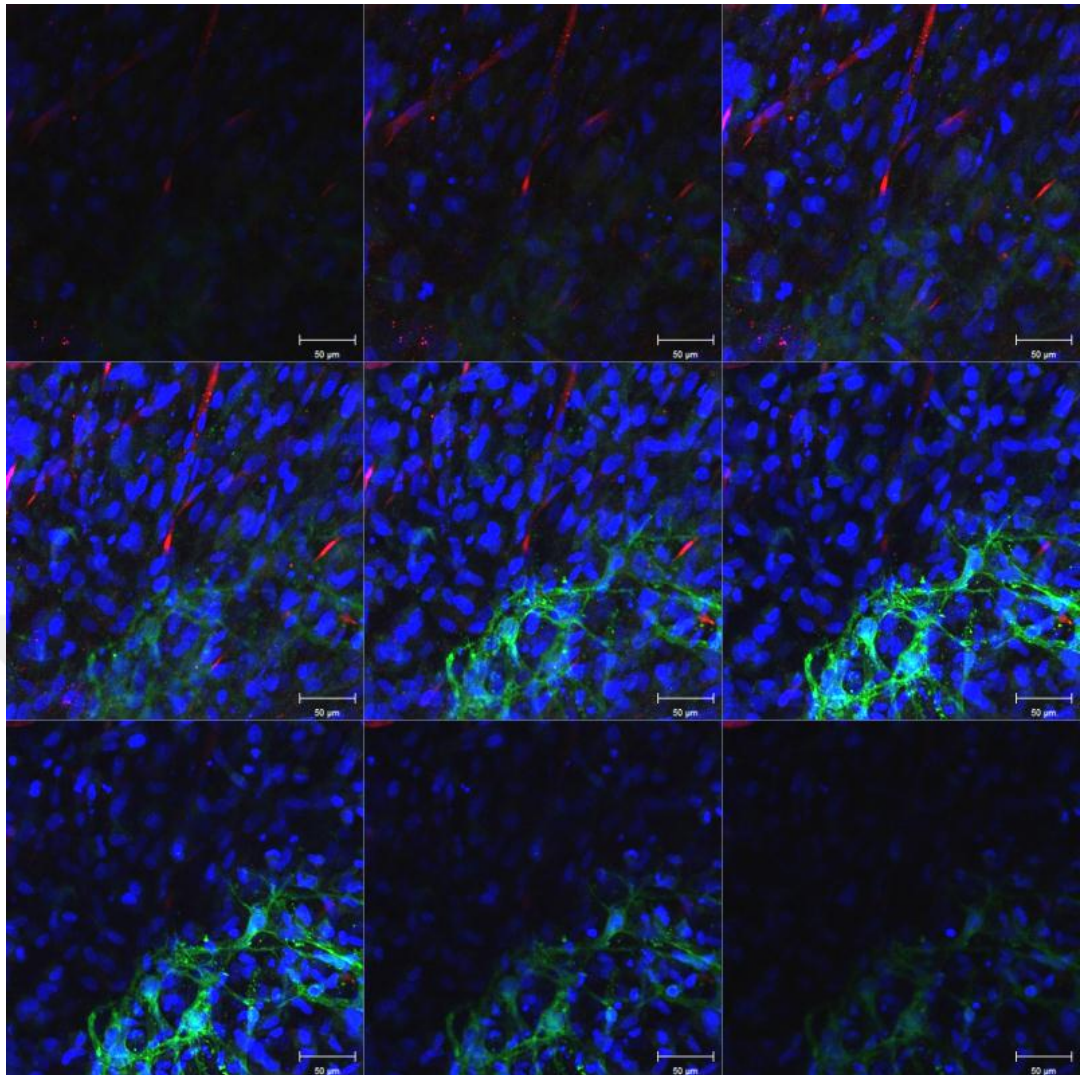


Figure 3.16: Sequential confocal micrographs of a Z-stack of capillary network and myotubes in human *in vitro* skeletal muscle model formed by co-culturing myotubes, capillary networks and the neuron-like cells for 24h. CD31: green, desmin: red, cell nuclei (DAPI): blue. Scale bar: 50 µm.

Our preliminary results with neuron-like cell and myotube co-culture suggest that the neuronal differentiation medium could not support the intact morphology of myotubes in the co-culture beyond 48 hours and, also, did not support the survival of endothelial cells. As in the research carried out by Guo et al. (2011), our three cell co-culture may require a change in media conditions after 24 hours of incubation and neuronal differentiation medium can either be replaced or combined with a medium such as NBActiv 4. The NBActiv 4 medium did not harm the endothelial cells in their monoculture for 4 days but, if the capillary network in three-cell co-culture is affected, the addition of EGM-2 to the co-culture should be considered.

3.6 Real-Time PCR

Optimal temperatures for the primers were determined by PCR. Product lengths were checked with markers. Negative and positive controls were used.

Best results for the genes NEFH, NEFL, ENO2 PCR products were obtained at 54 °C, 54 °C, 55 °C, respectively (Figure 3.17).

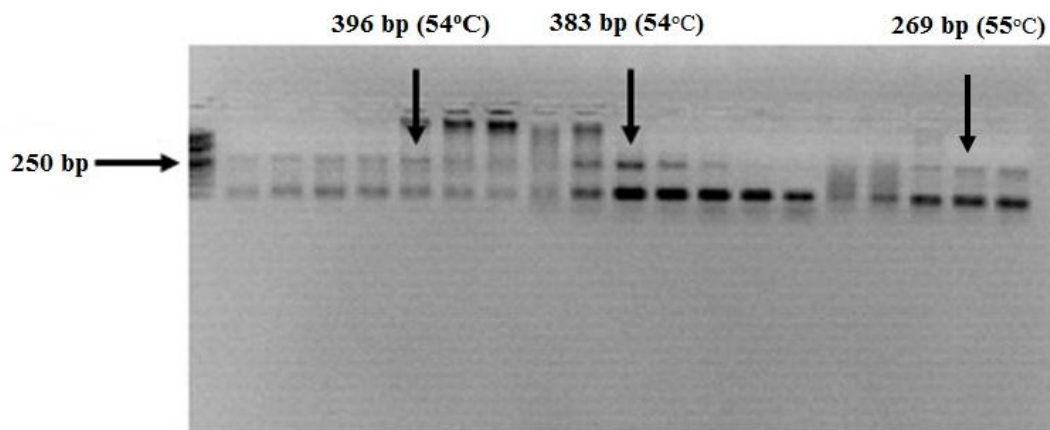


Figure 3.17: NEFH (396 bp) , 7 NEFL (283 bp), ENO2 (269 bp) PCR products. Marker: DNA Ladder 50-1000 bp.

Best results for the genes nestin and MYG PCR products were found at 54 °C (Figure 3.18).

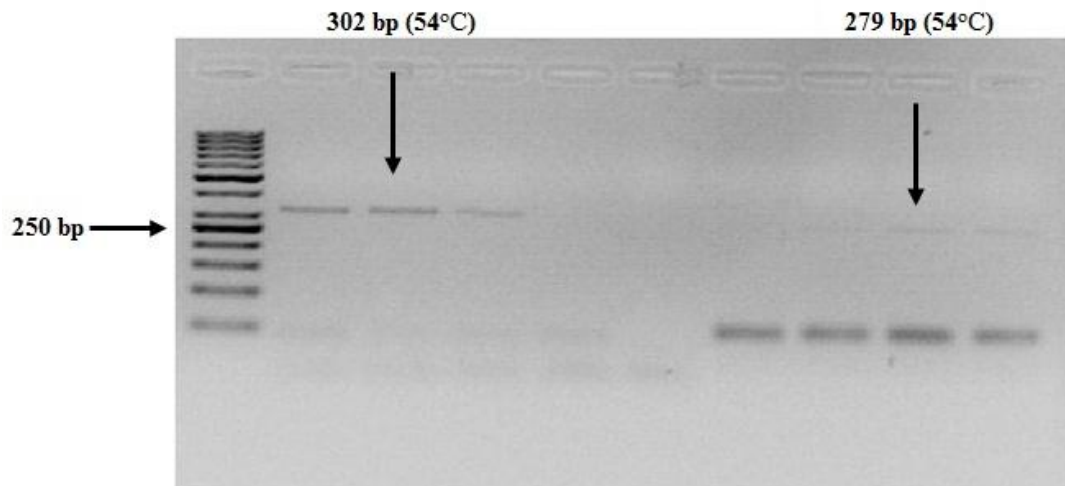


Figure 3.18: Nestin (302 bp) and MYG (279 BP) PCR products. Marker: DNA Ladder 50-1000 bp.

Best results for the gene beta-tubulin3 PCR products were found at 58 °C (Figure 3.19).

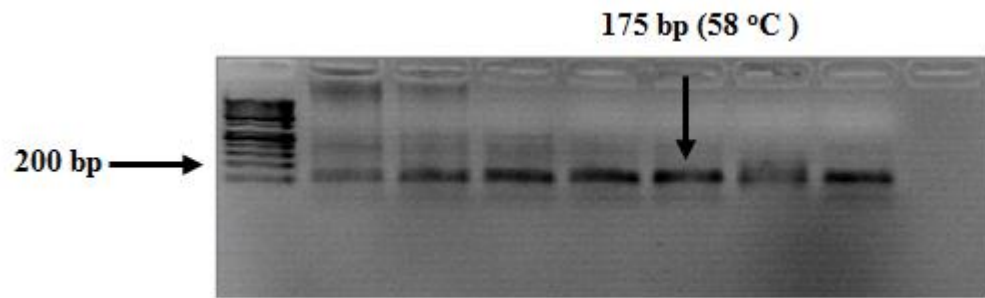


Figure 3.19: Beta-tubulin3 (175 bp) PCR products. Marker: DNA Ladder 100-1000 bp

Optimization studies were carried out by isolating RNA from the cells that were differentiated in T flasks, however, co-culture studies were carried out in 24 well plates. Therefore, especially the number of nerve cells in the co-culture conditions were too few to obtain enough RNA. Real-time SYBR Green's sensitivity was not enough to detect these products.

3.7 Live cell imaging

This study was conducted in two parts: without staining the cells and staining them with CellTracker™ CM-DiI and CFSE. In the first part, real time observation with time lapse imaging of hSkMSCs (2,500 cells/cm²) in complete neural differentiation media was carried out according to manufacturer's instructions to investigate their differentiation into neuron-like cells (Figure 3.20).

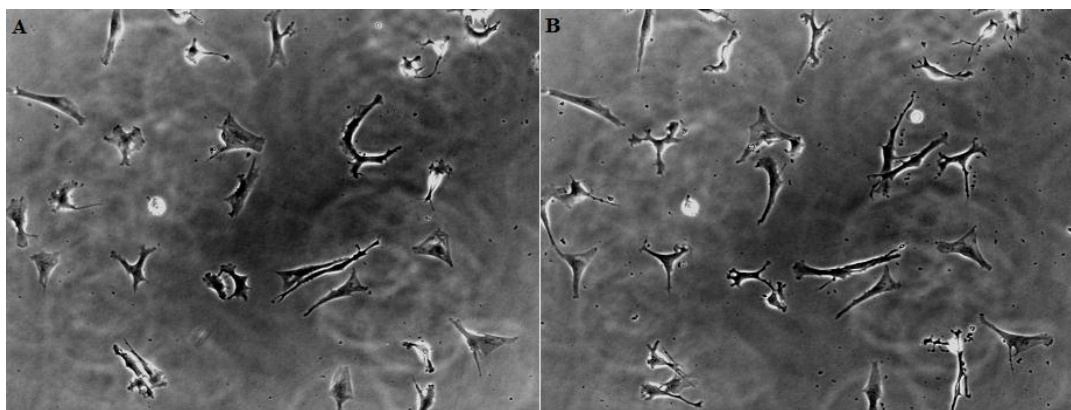


Figure 3.20: hSkMSCs with complete neural differentiation medium at day 1 and examined for 3 hours with live cell imaging system (A,B) (10x).

Since the amount of cells were not enough for cell to cell communication, more cells (5,000 cells/cm²) were used for the optimization. Then, differentiated hSkMSCs and neuron-like morphology changes were observed with time lapse

imaging at the end of 48 hours of incubation at 37°C in 5% CO₂ in live cell imaging incubator (Figure 3.21).

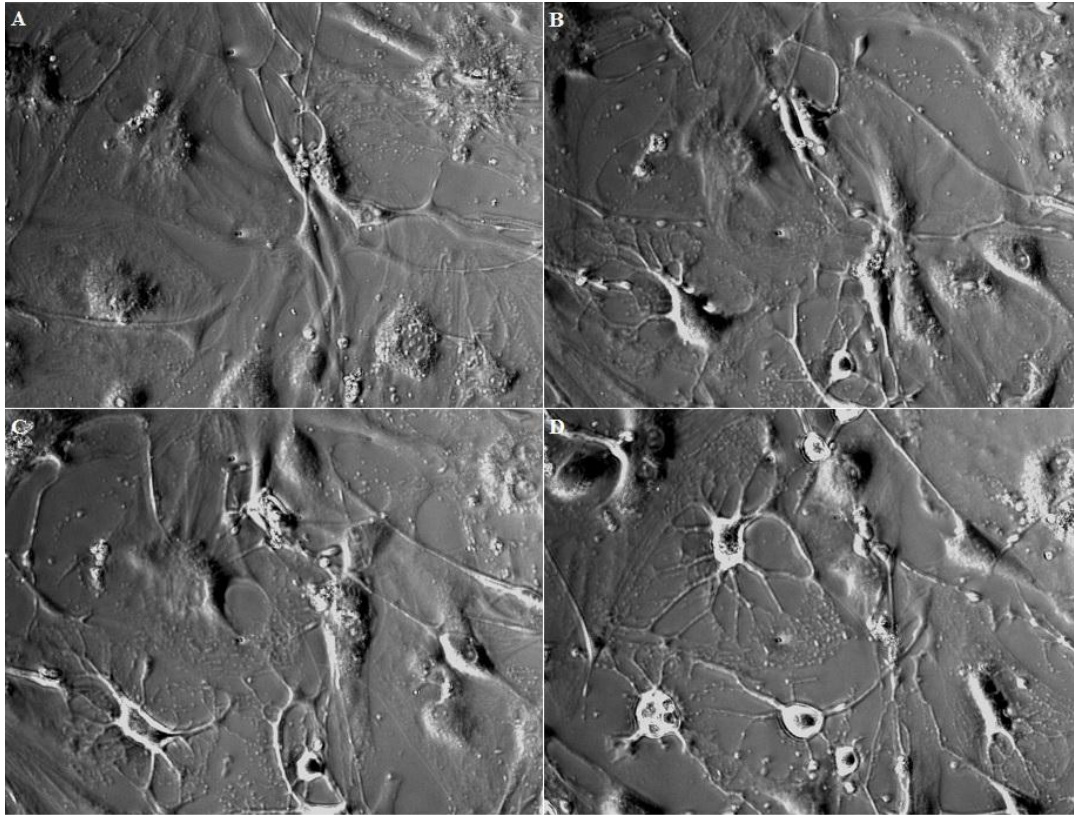


Figure 3.21: hSkMSCs with complete neural differentiation medium at day 1 and examined for 48 hours with live cell imaging system (A-D) (40x).

In order to further optimize the cell concentration, 3,000 cells/cm² were used and further examined for 72 hours. It was found that this cell concentration exhibited better results with respect to cell to cell communication (Figure 3.22).

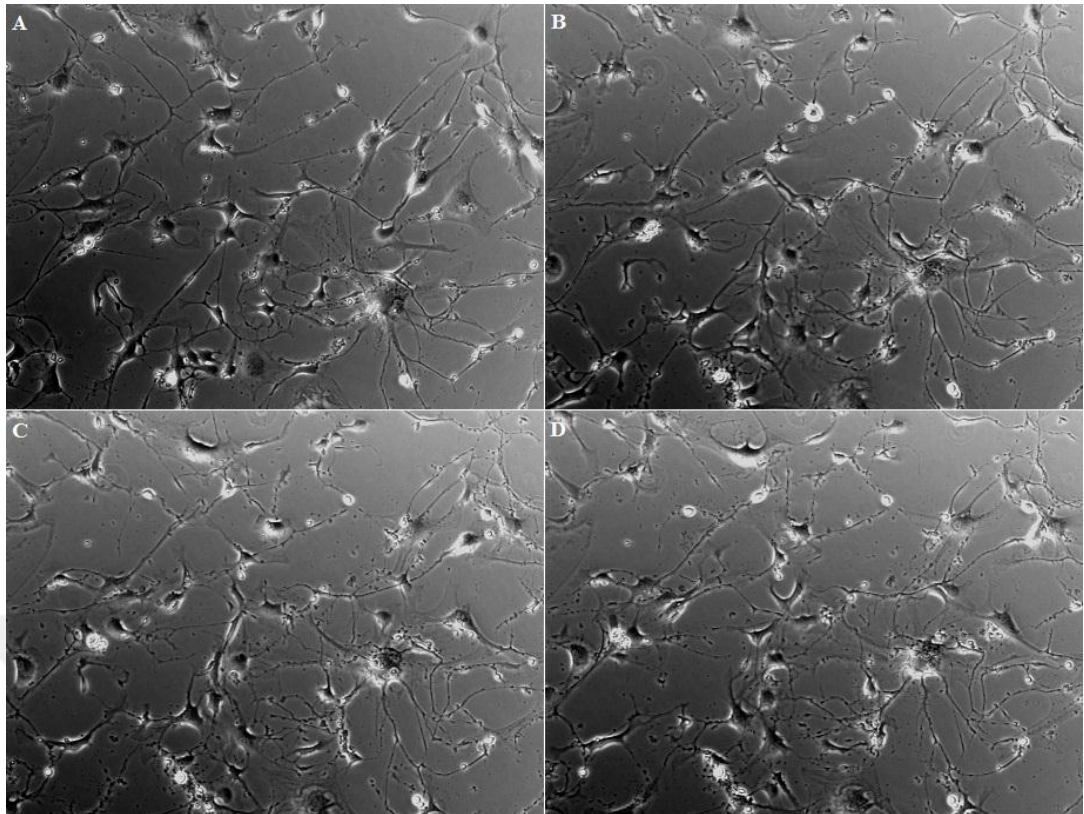


Figure 3.22: hSkMSCs incubated for 72 hours in complete neural differentiation medium and examined for 6 hours with live cell imaging system (A-D) (10x).

In the second part, in order to investigate co-culture behavior of cells, HUVECs and hSkMSCs were labeled by fluorescent dyes. The design of CellTracker™ CM-DiI fluorescent dye was made to freely move into cells through cell membrane where it undergoes transformation into cell membrane and becomes stable through several generations. Dye can only be transferred to the daughter cells but not to the adjacent cells in a population. CellTracker™ CM-DiI dye's fluorescence activity lasts for at least 72 hours and has ideal properties for longer tracking. For instance, it is nontoxic and stable at working concentrations, well retained in cells and brightly fluorescent at physiological pH. CM-DiI stains cell membrane, lipids and also some proteins (Andrade et al., 1996; Weir et al., 2008). In our study, CM-DiI was used to stain the hSkMSCs at day 3 (Figure 3.23) and cells were stained successfully.

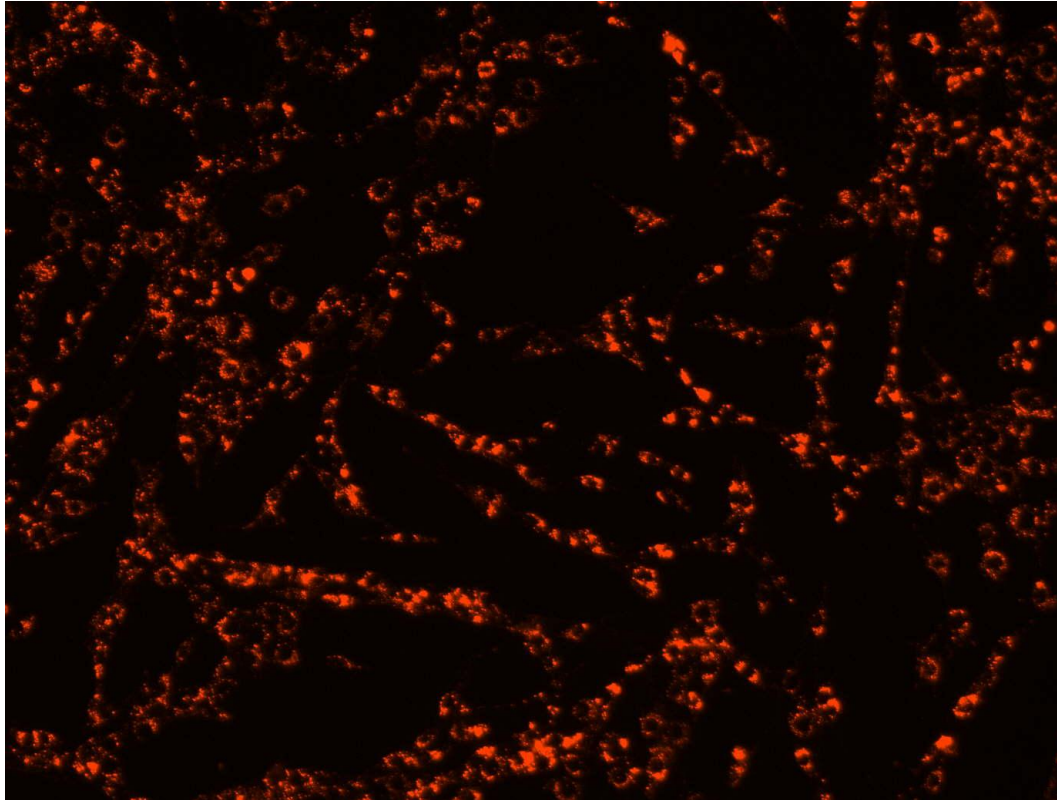


Figure 3.23: hSkMSCs stained with CellTracker™ CM-DiI (Orange) at day 3 (4x).

Second dye used in this study was CFSE. The diffusion of CFSE is provided passively into the cells. The colorless and non-fluorescent substance is altered into a highly fluorescent, amine-reactive carboxyfluorescein succinimidyl ester through its acetate groups cleaved by intracellular esterases. A reaction of ester group with intracellular amines results in well-retained fluorescent conjugates formation (Nose and Takeichi, 1986; Hemmrich et al, 2006). At the end of staining protocols, it was observed that both hSkMSCs and HUVECs were successfully stained with CM-DiI and CFSE (Figure 3.24).

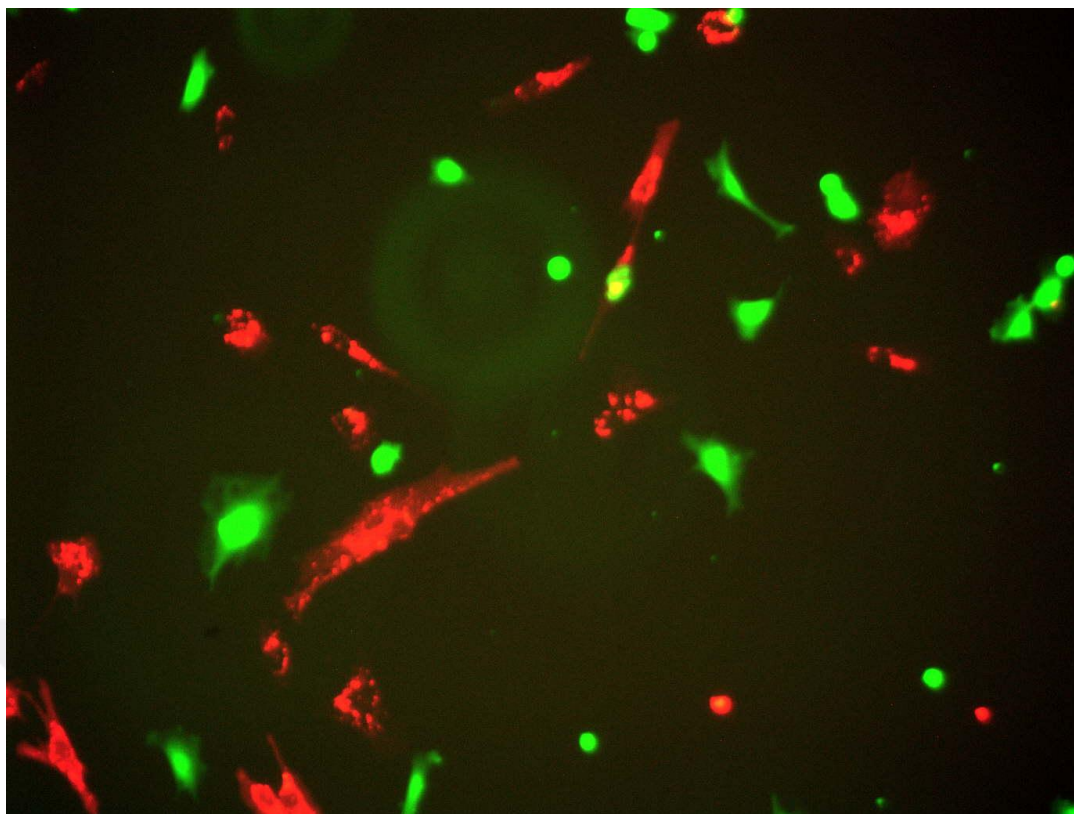


Figure 3.24: hSkMSCs and HUVECs stained with CellTracker™ CM-DiI (Orange) and CFSE (Green), respectively, at day 1.

Whenever co-culture was put into live cell imaging system, apoptosis/necrosis of the HUVECs was observed due to fluorescent light exposure throughout 6 hours of imaging (Figure 3.25 and 3.26).

Light, especially at short wavelengths, can induce phototoxic effects in cells (Hoebe et al., 2007; Jensen, 2012). CFSE stained HUVECs were exposed to 488 nm light source in our study. HUVECs which already become sensitive in co-culture conditions seemed to be affected most by the light exposure which was required for live cell imaging.

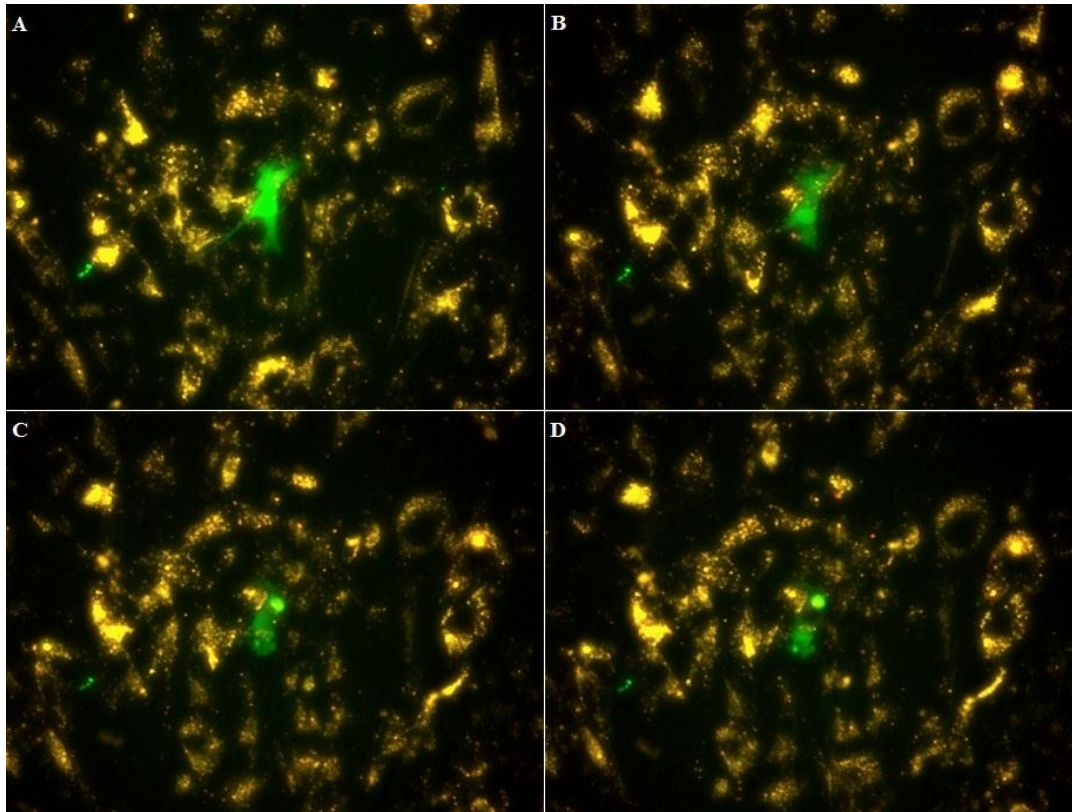


Figure 3.25: hSkMSCs and HUVECs stained with CellTracker™ CM-DiI (Orange) and CFSE (Green), respectively, at day 1 and examined for 6 hours. HUVECs were found with nuclear fragmentation which is the indication of apoptosis (A-D).

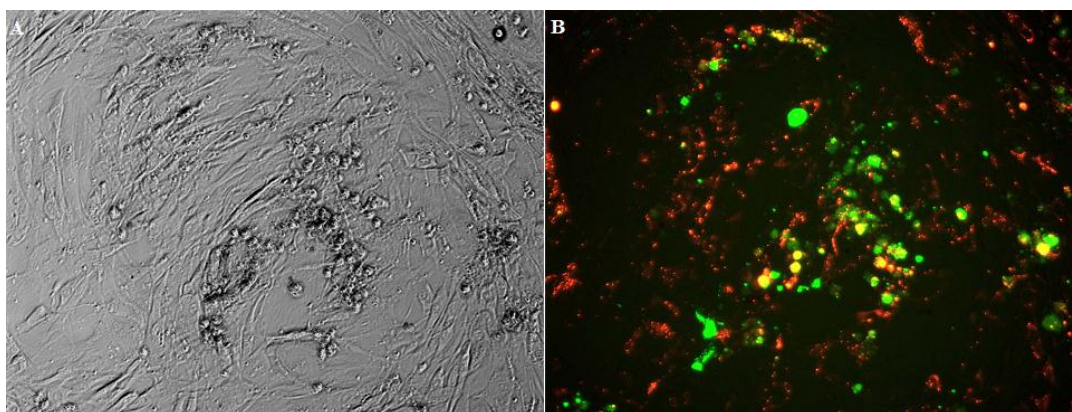


Figure 3.26: hSkMSCs and HUVECs stained with CellTracker™ CM-DiI (Orange) and CFSE (Green), respectively. Samples incubated for 2 days after live cell imaging (A, B).

3.8 Electrophysiological Study

Muscle contraction was observed throughout the entire procedure and the contraction of the multinucleated cells was observed under the phase contrast microscope (Figure 3.27).

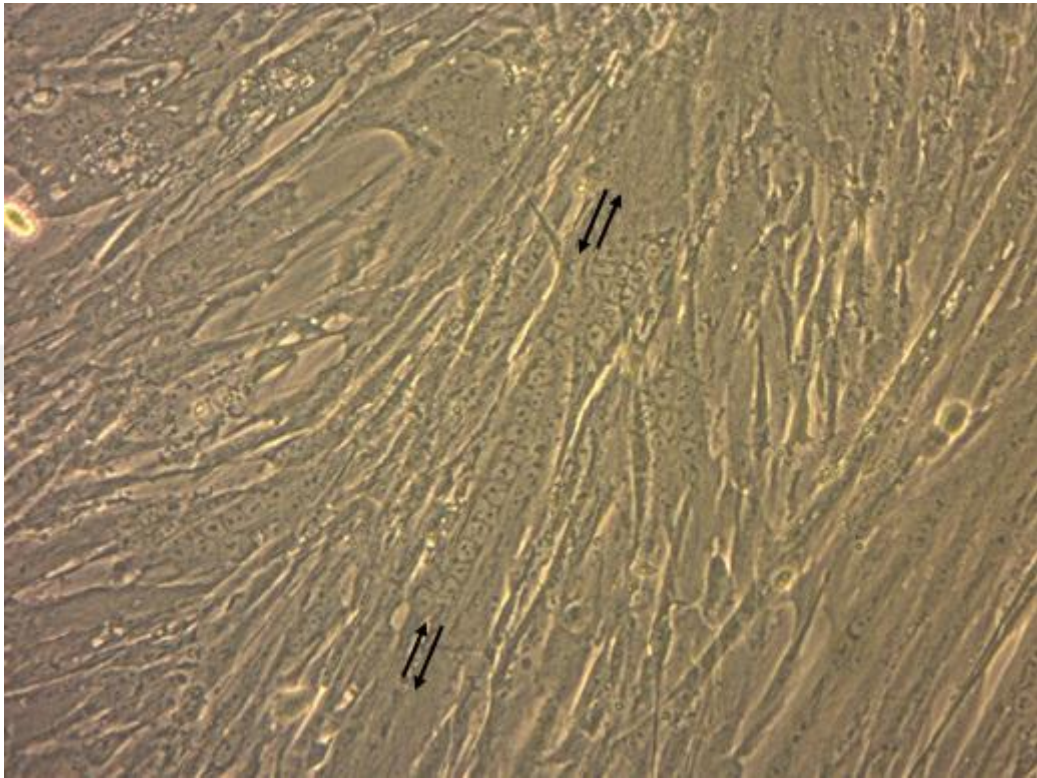


Figure 3.27: Electrophysiological muscle contraction study with the myotubes obtained by fusion of myoblasts. Arrows point the contraction side of the cells (10x).

This study reported for the first time a human skeletal muscle model, containing advanced capillary networks, neurons and myotubes in association with each other, by co-culturing HUVECs, myoblasts and human muscle stem cell derived neuron-like cells. Takahashi et al. (2015) recently reported that capillary network and human induced pluripotent stem cell derived neurons associated with human myoblast sheets when sandwiched in between, but myotube and neuromuscular junction formation between the neurons and myotubes were not indicated in this engineered muscle tissue.



4. CONCLUSIONS

In this study, a complex *in vitro* human skeletal muscle model with capillary networks and interacting myotubes and neuron-like cells was formed. This skeletal muscle model was characterized by confocal microscopy. The best multinucleated myotubes and capillary networks in co-culture of HUVECs and hSkMSCs was obtained in a DMEM/F12 (10% FBS):EGM-2 (2% FBS) (1:1) (D10-E2) mixture. Co-culture of the capillary network, myotubes, and neuron-like cells was successful for 24h in the neural differentiation medium.

Further detailed analyses, such as the determination of the presence and functionality of the neuromuscular junctions by blocking of the AChR (acetylcholine receptor) with nicotinic cholinergic antagonist, (+)-tubocurarine chloride pentahydrate (curare) to investigate its effect on myofiber contractions may be carried out. In the primary culture, heterogeneity and cell content of the hSkMSCs are different as the passage number increases. Investigation of neural differentiation with molecular assays on cells with different passage numbers may give different differentiation results and further analyses may be conducted for future studies.

Furthermore, extension of the co-culture time beyond 24 hours may be carried out. Since primary cultures have a limited time span *in vitro* conditions, our cells may be manipulated for indefinite subcultures through transformation for long term studies. Also, *in vivo* experimentations may be carried out to show the functionality of this model.

Our model has the potential to be employed in the design of accurate *in vitro* physiological models of skeletal muscle tissue for various applications, such as toxicology studies and drug testing. Since we used primary human cells in this study, our model may be use for personalized medicine to customise drug design and dosage prediction. This *in vitro* system which is composed of muscle fibers,

capillaries, and nerves, could also be an effective muscle tissue substitute for both functional treatment and coverage of skeletal muscle defects. This model will be helpful in promoting the regeneration of functional muscle tissue and could eliminate the necessity for any sort of muscle graft transfer in the future.



REFERENCES

- Alessandri, G., Pagano, S., Bez, A., Benetti, A., Pozzi, S., Iannolo, G., ... Parati, E.** (2004). Isolation and culture of human muscle-derived stem cells able to differentiate into myogenic and neurogenic cell lineages, *Lancet.*, 364(9448), 1872-83.
- Alviano, F., Fossati, V., Marchionni, C., Arpinati, M., Bonsi, L., Franchina, M., ... Bagnara, G.P.** (2007). Term amniotic membrane is a high throughput source for multipotent mesenchymal stem cells with the ability to differentiate into endothelial cells *in vitro*. *BMC Dev Biol.*, 7:11.
- Bajard, L., Relaix, F., Lagha, M., Rocancourt, D., Daubas, P., Buckingham, M.E.** (2006). A novel genetic hierarchy functions during hypaxial myogenesis: Pax3 directly activates Myf5 in muscle progenitor cells in the limb, *Genes Dev.*, 20(17):2450-64.
- Barker, J.N., Rocha, V., Scaradavou, A.** (2009). Optimizing Unrelated Donor Cord Blood Transplantation, *Biology of Blood and Marrow Transplantation*, 15(1), 154–161.
- Bartholomew, A., Sturgeon, C., Siatskas, M., Ferrer, K., McIntosh, K., Patil, ... Hoffman, R.** (2002). Mesenchymal stem cells suppress lymphocyte proliferation *in vitro* and prolong skin graft survival *in vivo*, *Experimental Hematology*, 30(1):42–48.
- Behr L, Hekmati M, Lucchini A, Houcinet K, Faussat AM, Borenstein N, et al.** (2009). Evaluation of the effect of autologous mesenchymal stem cell injection in a largeanimal model of bilateral kidney ischaemia reperfusion injury, *Cell Proliferation*, 42(3):284–297.
- Bensinger, W., Martin, P., Storer, B., Clift, R., Forman, S.J., Negrin, R., ... Appelbaum, F.R.** (2001). Transplantation of bone marrow as compared with peripheral-blood cells from HLA-identical relatives in patients with hematologic cancers, *New England Journal of Medicine*, 344(3):175–181.
- Bernardo, M.E., Zaffaroni, N., Novara, F., Cometa, A.M., Avanzini, M.A., Moretta, A., ... Locatelli, F.** (2007). Human bone marrow-derived mesenchymal stem cells do not undergo transformation after long-term *In vitro* culture and do not exhibit telomere maintenance mechanisms, *Cancer Research.*, 67(19):9142–9149.
- Bradley, A., Evans, M., Kaufman, M., Robertson, E.** (1984). Formation of germ-line chimeras from embryo-derived teratocarcinoma cell-lines, *Nature*, 309(5965):255–256.

- Caridade, S.G., Monge, C., Almodóvar, J., Guillot, R., Lavaud, J., Josserand, V., ... Picart, C.** (2015). Myoconductive and osteoinductive free-standing polysaccharide membranes, *Acta Biomater.*, 15:139-49.
- Chirieleison, S.M., Feduska, J.M., Schugar, R.C., Askew, Y., Deasy, B.M.** (2012). Human muscle-derived cell populations isolated by differential adhesion rates: phenotype and contribution to skeletal muscle regeneration in Mdx/SCID mice, *Tissue Eng Part A.*, 18(3-4):232-41.
- Choi, J.S., Lee, S.J., Christ, G.J., Atala, A., Yoo, J.J.** (2008). The influence of electrospun aligned poly(epsilon-caprolactone)/collagen nanofiber meshes on the formation of self-aligned skeletal muscle myotubes, *Biomaterials*, 29(19):2899-906.
- Chou, C.H., Sinden, J.D., Couraud, P.O., Mado, M.** (2014). *In vitro* modeling of the neurovascular environment by coculturing adult human brain endothelial cells with human neural stem cells, *PLoS One.*, 9(9):e106346.
- Christ, B., Ordahl, C.P.** (1995). Early stages of chick somite development, *Anat Embryol (Berl.)*, 191(5):381-96.
- Campeau, P.M., Rafei, M., Francois, M., Birman, E., Forner, K.A., Galipeau, J.** (2009). Mesenchymal Stromal Cells Engineered to Express Erythropoietin Induce Anti-erythropoietin Antibodies and Anemia in Allorecipients, *Molecular Therapy*, 17(2):369–372.
- Castillo, M.D., Trzaska, K.A., Greco, S.J., Ponzio, N.M., Rameshwar, P.** (2008). Immunostimulatory Effects of Mesenchymal Stem Cell-Derived Neurons: Implications for Stem Cell Therapy in Allogeneic Transplantations, *Clinical and Translational Science*, 1(1):27–34.
- Cho, K., Trzaska, K., Greco, S., McArdle, J., Wang, F.S., Ye, J.H., Rameshwar, P.** (2005). Neurons derived from human mesenchymal stem cells show synaptic transmission and can be induced to produce the neurotransmitter substance P by interleukin-1 alpha, *Stem Cells*, 23(3):383–391.
- Chong, M., Chan, J.** (2010). Lentiviral vector transduction of fetal mesenchymal stem cells, *Methods Mol Biol.*, (614):135–147.
- Cutler, C., Giri, S., Jeyapalan, S., Paniagua, D., Viswanathan, A., Antin, J.** (2001). Acute and chronic graft-versus-host disease after allogeneic peripheral-blood stem-cell and bone marrow transplantation: A meta-analysis, *Journal of Clinical Oncology*, 19(16):3685–3691.
- Damjanov, I.** (2005). The road from teratocarcinoma to human embryonic stem cells, *Stem Cell Reviews*, 1(3):273–276.
- De Coppi, P., Delo, D., Farrugia, L., Udompanyanan, K., Yoo, J.J., Nomi, M., ... Soker, S.** (2005). Angiogenic gene-modified muscle cells for enhancement of tissue formation, *Tissue Eng.*, 11(7-8):1034-44.
- de la Fuente, R., Bernad, A., Garcia-Castro, J., Martin, M., Cigudosa, J.** (2010). Retraction Spontaneous human adult stem cell transformation, *Cancer Res.*,(16):6682.

- Defronzo, R.A., Ferrannini, E., Sato, Y., Felig, P., Wahren, J.** (1981). Synergistic interaction between exercise and insulin on peripheral glucose uptake, *J Clin Invest.*, 68(6):1468-1474.
- Delo, D.M., Eberli, D., Williams, J.K., Andersson, K.E., Atala, A., Soker, S.** (2008). Angiogenic gene modification of skeletal muscle cells to compensate for ageing-induced decline in bioengineered functional muscle tissue, *BJU Int.*, 102(7):878-84.
- Dhawan, J., Rando, T.A.** (2005). Stem cells in postnatal myogenesis: molecular mechanisms of satellite cell quiescence, activation and replenishment, *Trends Cell Biol.*, 15(12):666-73.
- Dominici, M., Le Blanc, K., Mueller, I., Slaper-Cortenbach, I., Marini, F., ... Horwitz, E.** (2006). Minimal criteria for defining multipotent mesenchymal stromal cells. The International Society for Cellular Therapy position statement, *Cytotherapy*, 8(4):315–317.
- Dumont, N.A., Wang, Y.X., Rudnicki, M.A.** (2015). Intrinsic and extrinsic mechanisms regulating satellite cell function, *Development*, 142(9):1572-81.
- Eapen, M., Rubinstein, P., Zhang, M.J., Stevens, C., Kurtzberg, J., Scaradavou, A., ... Wagner, J.E.** (2007). Outcomes of transplantation of unrelated donor umbilical cord blood and bone marrow in children with acute leukaemia: a comparison study, *Lancet.*, 369(9577):1947–1954.
- Eberli, D., Soker, S., Atala, A., Yoo, J.J.** (2009). Optimization of human skeletal muscle precursor cell culture and myofiber formation *in vitro*, *Methods*, 47(2):98-103.
- El Beshlawy, A., Metwally, H.G., El Khalek, K.A., Zayed, R.A., Hammoud, R.F., Mousa, S.M.** (2009). The Effect of Freezing on the Recovery and Expansion of Umbilical Cord Blood Hematopoietic Stem Cells., *Experimental and Clinical Transplantation*, 7(1):50–55.
- Emerson, G.G., Segal, S.S.** (1985). Alignment of microvascular units along skeletal muscle fibers of hamster retractor, *J Appl Physiol.*, 82(1):42-48.
- Friedenstein, A., Chailakhyan, R., Latsinik, N., Panasyuk, A., Keiliss-Borok, I.** (1974). Stromal cells responsible for transferring the microenvironment of thehemopoietic tissues. Cloning *in vitro* and retransplantation *in vivo*, *Transplantation*, (4):331–340.
- Gholobova, D., Decroix, L., Van Muylder, V., Desender, L., Gerard, M., Carpentier, G., ... Thorrez, L.** (2015). Endothelial Network Formation Within Human Tissue-Engineered Skeletal Muscle, *Tissue Eng Part A*, 21(19-20):2548-58.
- Gluckman, E., Broxmeyer, H., Auerbach, A., Friedman, H., Douglas, G., Devergie, A., ... Boyse, A.E.,** (1989). Hematopoietic reconstitution in a patient with Fanconi's anemia by means of umbilical-cord blood from an HLA-identical sibling, *New England Journal of Medicine*, 321(17):1174–1178.

- Gotherstrom, C., Ringden, O., Tammik, C., Zetterberg, E., Westgren, M., Le Blanc, K.** (2004). Immunologic properties of human fetal mesenchymal stem cells, *American Journal of Obstetrics and Gynecology*, 190(1):239–245.
- Gronthos, S., Mankani, M., Brahimi, J., Robey, P., Shi, S.** (2000). Postnatal human dental pulp stem cells (DPSCs) *in vitro* and *in vivo*, *Proc Natl Acad Sci U S A.*, 97(25):13625–13630.
- Guenter, L., Brunauer, R., Jamnig, A., Laschober, G., Kassem, M.** (2008). Controversial issue: Is it safe to employ mesenchymal stem cells in cell-based therapies?, *Experimental Gerontology*, 43(11, SI):1018–1023.
- Guo, X., Gonzalez, M., Stancescu, M., Vandeburgh, H.H., Hickman, J.J.** (2011). Neuromuscular junction formation between human stem cell-derived motoneurons and human skeletal muscle in a defined system, *Biomaterials*, 32(36):9602–11.
- Guettier-Sigrist, S., Coupin, G., Braun, S., Warter, J.M., Poindron, P.** (1998). Muscle could be the therapeutic target in SMA treatment, *J Neurosci Res.*, 53(6):663–9.
- Helmy, K., Patel, S., Silverio, K., Pliner, L., Rameshwar, P.** (2010). Stem cells and regenerative medicine: accomplishments to date and future promise, *Ther Deliv.*, 1 (5):693–705.
- Hoebe, R.A., Van Oven, C.H., Gadella, T.W., Dhonukshe, P.B., Van Noorden, C.J., Manders, E.M.** (2007). Controlled light-exposure microscopy reduces photobleaching and phototoxicity in fluorescence live-cell imaging, *Nat Biotechnol.*, 25(2):249–53.
- Horwitz, E., Prockop, D., Fitzpatrick, L., Koo, W., Gordon, P., Neel, M., ... Brenner, K.** (1999). Transplantability and therapeutic effects of bone marrow-derived mesenchymal cells in children with osteogenesis imperfecta, *Nature Medicine*, 5(3):309–313.
- Hosseini, V., Ahadian, S., Ostrovidov, S., Camci-Unal, G., Chen, S., Kaji, H., ... Khademhosseini A.** (2012). Engineered contractile skeletal muscle tissue on a microgrooved methacrylated gelatin substrate, *Tissue Eng Part A.*, 18(23–24):2453–65.
- Hu, P., Geles, K.G., Paik, J.H., DePinho, R.A., Tjian, R.** (2008). Codependent activators direct myoblast-specific MyoD transcription, *Dev Cell.*, 15(4):534–46.
- Izadpanah, R., Kaushal, D., Kriedt, C., Tsien, F., Patel, B., Dufour, J., Bunnell, B.A.** (2008). Long-term *in vitro* expansion alters the biology of adult mesenchymal stem cells, *Cancer Research*, 68(11):4229–4238.
- Janacek, J., Cebasek, V., Kubinova, L., Ribaric, S., Erzen, I.** (2009). 3D visualization and measurement of capillaries supplying metabolically different fiber types in the rat extensor digitorum longus muscle during denervation and reinnervation, *J Histochem Cytochem.*, 57(5):437–447.

- Jaeger, M., Zilkens, C., Bittersohl, B., Krauspe, R.** (2009). Cord Blood-An Alternative Source for Bone Regeneration, *Stem Cell Rev.*, 5(3):266–277.
- Jenq, R.R., van den Brink, M.R.M.** (2010). Allogeneic haematopoietic stem cell transplantation: individualized stem cell and immune therapy of cancer, *Nature Reviews Cancer*, 10(3):213–221.
- Jensen, E.C.** (2012). Use of fluorescent probes: their effect on cell biology and limitations, *Anat Rec. (Hoboken)*, 295(12):2031–6.
- Juhas, M., Bursac, N.** (2014). Roles of adherent myogenic cells and dynamic culture in engineered muscle function and maintenance of satellite cells, *Biomaterials*, 35(35):9438–46.
- Kang, L., Kou, Z., Zhang, Y., Gao, S.** (2010). Induced pluripotent stem cells (iPSCs)-a new era of reprogramming, *Journal of Genetics and Genomics*, 37(7):415–421.
- Kassar-Duchossoy, L., Giacone, E., Gayraud-Morel, B., Jory, A., Gomès, D., Tajbakhsh, S.** (2005). Pax3/Pax7 mark a novel population of primitive myogenic cells during development, *Genes Dev.*, 19(12):1426–31.
- Kern S., Eichler, H., Stoeve, J., Klueter, H., Bieback, K.** (2006). Comparative analysis of mesenchymal stem cells from bone marrow, umbilical cord blood, or adipose tissue, *Stem Cells.*, 24(5):1294–1301.
- Klumpp, D., Rudisile, M., Kühnle, R.I., Hess, A., Bitto, F.F., Arkudas, A., ... Beier, J.P.** (2012). Three-dimensional vascularization of electrospun PCL/collagen-blend nanofibrous scaffolds *in vivo*, *J Biomed Mater Res A.*, 100(9):2302–11.
- Koegler, G., Critser, P., Trapp, T., Yoder, M.** (2009). Future of cord blood for non-oncology uses, *Bone Marrow Transplantation*, 44(10):683–697.
- Kopen, G., Prockop, D., Phinney, D.** (1999). Marrow stromal cells migrate throughout forebrain and cerebellum, and they differentiate into astrocytes after injection into neonatal mouse brains, *Proc Natl Acad Sci U S A.*, 96(19):10711–10716.
- Larkin, L.M., Van der Meulen, J.H., Dennis, R.G., Kennedy, J.B.** (2007). Functional evaluation of nerve-skeletal muscle constructs engineered *in vitro*, *In Vitro Cell Dev Biol Anim.*, 42(3–4):75–82.
- Laumonier, T. and Menetrey, J.** (2016). Muscle injuries and strategies for improving their repair, *J Exp Orthop.*, 3(1):15.
- Le Blanc, K., Rasmuson, I., Sundberg, B., Götherström, C., Hassan, M., Uzunel, M., Ringdén, O.** (2004). Treatment of severe acute graft-versus-host disease with third party haploidentical mesenchymal stem cells, *Lancet.*, 363(9419):1439–1441.
- Levenberg, S., Rouwkema, J., Macdonald, M., Garfein, E.S., Kohane, D.S., Darland, D.C., ... Langer, R.** (2005). Engineering vascularized skeletal muscle tissue, *Nat Biotechnol.*, 23(7):879–84.

- Magatti, M., De Munari, S., Vertua E., Gibelli, L., Wengler, G.S., Parolini, O.** (2008). Human amnion mesenchyme harbors cells with allogeneic T-cell suppression and stimulation capabilities, *Stem Cells*, 26(1):182–192.
- Mauro, A.** (1961). Satellite cell of skeletal muscle fibers, *J Biophys Biochem Cytol.*, 9:493-5.
- McKinnell, I.W., Ishibashi, J., Le Grand, F., Punch, V.G., Addicks, G.C., Greenblatt J.F., ... Rudnicki, M.A.** (2008). Pax7 activates myogenic genes by recruitment of a histone methyltransferase complex, *Nat Cell Biol.*, 10(1):77-84.
- Meng, H., Janssen, P.M.L., Grange, R.W., Yang, L., Beggs, A.H., Swanson, L.C., ... Lawlor, M.W.** (2014). Tissue triage and freezing for models of skeletal muscle disease, *J Vis Exp.*, (89):10.
- Michalczyk, K., Ziman, M.** (2005). Nestin structure and predicted function in cellular cytoskeletal organisation, *Histol Histopathol.*, (2):665-71.
- Moldenhauer, A., Wolf, J., Habermann, G., Genter, G., Kiesewetter, H., Salama, A.** (2007). Optimum storage conditions for cord blood-derived hematopoietic progenitor cells prior to isolation, *Bone Marrow Transplant*, 40(9):837–842.
- Molineux, G., Pojda, Z., Hampson, I., Lord, B., Dexter, T.** (1990). Transplantation potential of peripheral-blood stem-cells induced by granulocyte colony-stimulating factor, *Blood.*, 76(10):2153–2158.
- Moon du, G., Christ, G., Stitzel, J.D., Atala, A., Yoo, J.J.** (2008). Cyclic mechanical preconditioning improves engineered muscle contraction, *Tissue Eng Part A.*, 14(4):473-82.
- Mueller, F.J., Goldmann, J., Loeser, P., Loring, J.F.** (2010). A Call to Standardize Teratoma Assays Used to Define Human Pluripotent Cell Lines, *Cell Stem Cell.*, 6(5):412– 414.
- Mullighan, C., Flotho, C., Downing, J.** (2005). Genomic assessment of pediatric acute leukemia, *Cancer J.*, 11(4):268–282.
- Mullighan, C.G.** (2009). Genomic analysis of acute leukemia, *International Journal of Laboratory Hemat.*, 31(4):384–397.
- Namiki, J., Suzuki, S., Masuda, T., Ishihama, Y., Okano, H.** (2012). Nestin Protein Is Phosphorylated in Adult Neural Stem/Progenitor Cells and Not Endothelial Progenitor Cells, *Stem Cells International.*, ID 430138, 5 pages.
- Nagamori, E., Ngo, T.X., Takezawa, Y., Saito, A., Sawa, Y., Shimizu, T., ... Kino-oka, M.** (2013). Network formation through active migration of human vascular endothelial cells in a multilayered skeletal myoblast sheet, *Biomaterials.*, 34(3):662-8.
- Nauta, A.J., Fibbe, W.E.** (2007). Immunomodulatory properties of mesenchymal stromal cells, *Blood.*, 110(10):3499–3506.

- Neri, M., Maderna, C., Ferrari, D., Cavazzin, C., Vescovi, A.L., Gritti, A.** (2010). Robust Generation of Oligodendrocyte Progenitors from Human Neural Stem Cells and Engraftment in Experimental Demyelination Models in Mice, *PLoS ONE.*, 5(4):e10145.
- Newman, J.M., Dora, K.A., Rattigan, S., Edwards, S.J., Colquhoun, E.Q., Clark, M.G.** (1996). Norepinephrine and serotonin vasoconstriction in rat hindlimb control different vascular flow routes, *Am J Physiol.*, 270(4 Pt 1):E689-E699.
- Olguin, H.C. and Olwin, B.B.** (2004). Pax-7 up-regulation inhibits myogenesis and cell cycle progression in satellite cells: a potential mechanism for self-renewal, *Dev Biol.*, 275(2): 375–388.
- Ostrovidov, S., Hosseini, V., Ahadian, S., Fujie, T., Parthiban, S.P., Ramalingam, M., ... Khademhosseini, A.** (2014). Skeletal muscle tissue engineering: methods to form skeletal myotubes and their applications, *Tissue Eng Part B Rev.*, 20(5):403-36.
- Qu-Petersen, Z., Deasy, B., Jankowski, R., Ikezawa, M., Cummins, J., ... Huard, J.** (2002). Identification of a novel population of muscle stem cells in mice: potential for muscle regeneration, *J Cell Biol.*, 157(5):851-64.
- Partridge, T.A., Morgan, J.E., Coulton, G.R., Hoffman, E.P., Kunkel, L.M.** (1989). Conversion of mdx myofibres from dystrophin-negative to -positive by injection of normal myoblasts, *Nature.*, 337(6203):176-9.
- Pette, D., Sketelj, J., Skorjanc, D., Leisner, E., Traub, I., Bajrovic, F.** (2002). Partial fast-to-slow conversion of regenerating rat fast-twitch muscle by chronic low frequency stimulation, *J Muscle Res Cell Motil.*, 23(3):215-21.
- Pereira, R., Halford, K., O'Hara, M., Leeper, D., Sokolov, B., Pollard, M.D., ... Prockop, D.J.** (1995). Cultured adherent cells from marrow can serve as long-lasting precursor cells for bone, cartilage, and lung in irradiated mice, *Proc Natl Acad Sci U S A.*, 92(11):4857–4861.
- Petersen, B., Bowen, W., Patrene, K.D., Mars, W.M., Sullivan, A.K., Murase, N., ... Goff, J.P.** (1999). Bone marrow as a potential source of hepatic oval cells, *Science.*, 284(5417):1168– 1170.
- Phinney, D.G., Prockop, D.J.** (2007). Concise review: Mesenchymal stem/multipotent stromal cells: The state of transdifferentiation and modes of tissue repair - Current views, *Stem Cells.*, 25(11):2896–2902.
- Pittenger, M., Mackay, A., Beck, S.C., Jaiswal, R.K., Douglas, R., Mosca, J.D., ... Marshak, D.R.** (1999). Multilineage potential of adult human mesenchymal stem cells, *Science*, 284(5411):143–147.
- Powell, C., Shansky, J., Del Tatto, M., Forman, D.E., Hennessey, J., Sullivan, K., ... Vandenberg, H.H.** (1999). Tissue engineered human bioartificial muscles expressing a foreign recombinant protein for gene therapy, *Hum Gene Ther.*, 10(4):565-77.

- Potapova, I.A., Brink, P.R., Cohen, I.S., Doronin, S.V.** (2008). Culturing of human mesenchymal stem cells as three-dimensional aggregates induces functional expression of CXCR4 that regulates adhesion to endothelial cells, *Journal of Biological Chemistry*, 283(19):13100–13107.
- Rameshwar, P.** (2009). Casting Doubt on the Safety of "Off-the-shelf" Mesenchymal Stem Cells for Cell Therapy, *Molecular Therapy*, 17(2):216–218.
- Reimann, V., Koegler, G., Creutzig, U.** (2009). Stem Cells Derived From Cord Blood in Transplantation and Regenerative Medicine, *Deutsches Arzteblatt International*, 106(50):831–836.
- Reinisch, A., Strunk, D.** (2009). Isolation and animal serum free expansion of human umbilical cord derived mesenchymal stromal cells (MSCs) and endothelial colony forming progenitor cells (ECFCs), *J Vis Exp.*, 8:(32):1525.
- Rendl, M.** (2014). *Stem Cells in Development and Disease*. © Academic Press, Hardcover.
- Rossignol, J., Boyer, C., Thinard, R., Remy, S., Dugast, A.S., Dubayle, D., ... Lescaudron, L.** (2009). Mesenchymal stem cells induce a weak immune response in the rat striatum after allo or xenotransplantation, *J Cell Mol Med.*, 13(8B):2547–2558.
- Rubio, D., Garcia-Castro, J., Martín, M.C., de la Fuente, R., Cigudosa, J.C., Lloyd, A.C., Bernad, A.** (2005). Spontaneous human adult stem cell transformation (Retracted article. See vol. 70, pg. 6682, 2010), *Cancer Research*, 65(8):3035–3039.
- Sawada, R., Ito, T., Tsuchiya, T.** (2006). Changes in expression of genes related to cell proliferation in human mesenchymal stem cells during *in vitro* culture in comparison with cancer cells, *J Artif Organs.*, (9(3)):179–184.
- Schultz, S.S., Lucas, P.A.** (2006). Human stem cells isolated from adult skeletal muscle differentiate into neural phenotypes, *J Neurosci Methods.*, 152(1-2):144-55.
- Shandalov, Y., Egozi, D., Koffler, J., Dado-Rosenfeld, D., Ben-Shimol, D., Freiman, A., ... Levenberg, S.** (2014). An engineered muscle flap for reconstruction of large soft tissue defects, *Proc Natl Acad Sci U S A.*, 111(16):6010-5.
- Shandalov, Y., Egozi, D., Freiman, A., Rosenfeld, D., Levenberg, S.** (2015). A method for constructing vascularized muscle flap, *Methods.*, 84:70-5.
- Sinanan, A.C., Buxton, P.G., Lewis, M.P.** (2006). Muscling in on stem cells, *Biol Cell.*, 4: 203- 214.

- Sjøgaard, G., Justesen, J.B., Murray, M., Dalager, T., Søgaard, K.** (2014). A conceptual model for worksite intelligent physical exercise training--IPET--intervention for decreasing life style health risk indicators among employees: a randomized controlled trial, *BMC Public Health.*, 14:652.
- Snijders, T., Nederveen, J.P., McKay, B.R., Joannisse, S., Verdijk, L.B., van Loon, L.J., Parise, G.** (2015). Satellite cells in human skeletal muscle plasticity, *Front Physiol.*, 21(6):283.
- Soleimani, V.D., Punch, V.G., Kawabe, Y., Jones, A.E., Palidwor, G.A., Porter, C.J., ... Rudnicki, M.A.** (2012). Transcriptional dominance of Pax7 in adult myogenesis is due to high-affinity recognition of homeodomain motifs, *Dev Cell.*, 22(6):1208-20.
- Stolzing, A., Jones, E., McGonagle, D., Scutt, A.** (2008). Age-related changes in human bone marrow-derived mesenchymal stem cells: Consequences for cell therapies, *Mech Ageing Dev.*, 129(3):163–173.
- Takahashi, K., Yamanaka, S.** (2006). Induction of pluripotent stem cells from mouse embryonic and adult fibroblast cultures by defined factors, *Cell.*, 126(4):663–676.
- Takahashi, K., Tanabe, K., Ohnuki, M., Narita, M., Ichisaka, T., Tomoda, K., Yamanaka, S.** (2007). Induction of pluripotent stem cells from adult human fibroblasts by defined factors, *Cell.*, 131(5):861–872.
- Takahashi, H., Shimizu, T., Nakayama, M., Yamato, M., Okano, T.** (2015). Anisotropic cellular network formation in engineered muscle tissue through the self-organization of neurons and endothelial cells, *Adv Healthc Mater.*, 4(3):356-60.
- Tamaki, T., Uchiyama, Y., Hirata, M., Hashimoto, H., Nakajima, N., Saito, K., ... Mochida, J.** (2015). Therapeutic isolation and expansion of human skeletal muscle-derived stem cells for the use of muscle-nerve-blood vessel reconstitution, *Front Physiol.*, 6:165.
- Uzel, S.G., Platt, R.J., Subramanian, V., Pearl, T.M., Rowlands, C.J., Chan, V., ... Kamm, R.D.** (2016). Microfluidic device for the formation of optically excitable, three-dimensional, compartmentalized motor units, *Sci Adv.*, 2(8):e1501429.
- Wagner, W., Horn, P., Castoldi, M., Diehlmann, A., Bork, S., Saffrich, R., ... Ho, A.D.** (2008). Replicative Senescence of Mesenchymal Stem Cells: A Continuous and Organized Process, *PLoS ONE.*, 3(5).
- Zeddou, M., Briquet, A., Relic, B., Josse, C., Malaise, M.G., Gothot, A., ... Beguin, Y.** (2010). The umbilical cord matrix is a better source of mesenchymal stem cells (MSC) than the umbilical cord blood, *Cell Biol Int.*, 34(7):693–701.
- Zuk, P., Zhu, M., Mizuno, H., Huang, J., Futrell, J., Katz, A., ... Hedrick, M.H.** (2001). Multilineage cells from human adipose tissue: Implications for cell-based therapies, *Tissue Eng.*, 7(2), 211–228.



APPENDICES

APPENDIX A.1: Chemicals and reagents

AdvanceSTEM Neural Differentiation Medium	Thermo Scientific
AdvanceSTEM Stem Cell Growth Supplement	Thermo Scientific
AEC kit	Invitrogen
Anti-Goat Secondary Antibody	Santa-Cruz
Anti-Mouse Secondary Antibody	Invitrogen
Anti-Rabbit Secondary Antibody	Invitrogen
Beta tubulin-3 primary antibody	Santa-Cruz
bFGF	Roche
CD 105	BD Pharmingen
CD 34	BD Pharmingen
CD 44	BD Pharmingen
CD 45	BD Pharmingen
CD 90	BD Pharmingen
CD31 primary antibody	Invitrogen
cDNA RT-PCR Sensiscript®	Qiagen
CFDA, SE	Thermo Scientific
CM-DiI	Thermo Scientific
Collagenase I	Sigma-Aldrich
DAPI	Sigma-Aldrich
Desmin primary antibody	Santa-Cruz
Dispase	Gibco
DMEM/F12	Life Sciences
DMSO	Sigma-Aldrich
DNA Ladder 100-1000 bp	Fermentas

DNA Ladder 50-1000 bp	Fermentas
DPBS	Life Sciences
EGF	Sigma-Aldrich
EGM-2	Lonza
FBS	Sigma-Aldrich
Gelatin	Sigma-Aldrich
GFAP primary antibody	Santa-Cruz
HBSS	Gibco
HRP immunostaining Kit	Thermo Scientific
Maxima SYBR Green qPCR Master Mix	Fermentas
PBS	Life Sciences
PCR kit	Fermentas
Primary antibody for desmin	Santa-Cruz
PSA	Pan Biotech
RNeasy Mini Kit	Qiagen
Trypsin-EDTA	Sigma-Aldrich

CURRICULUM VITAE



Name Surname : Ayşe Burcu Ertan
Place and Date of Birth : İstanbul, 17.08.1982
E-Mail : ayseburcuertan@yahoo.com

EDUCATION :

- **B.Sc.** : 2005, Haliç University, Faculty of Arts And Sciences, Department of Molecular Biology and Genetics
- **M.Sc.** : 2008, Istanbul Technical University, Graduate School of Science Engineering and Technology, Molecular Biology-Genetics and Biotechnology Programme

PROFESSIONAL EXPERIENCE AND REWARDS:

- 2005-2014, Yeditepe University, Faculty of Engineering, Genetics and Bioengineering, Tissue Engineering Laboratory, Research Assistant
- 2004-2005, Ege University, Faculty of Medicine, Molecular Genetics Laboratory, Microarray Technician
- 2003-2004, Haliç University, Faculty of Arts And Sciences, Department of Molecular Biology and Genetics, Teaching Assistant

PUBLICATIONS, PRESENTATIONS AND PATENTS ON THE THESIS:

- **Ertan A.B.**, Kenar H., Beyzadeoglu T., Kok F.N., Kose G.T. (2017) An *in vitro* human skeletal muscle model: coculture of myotubes, neuron-like cells, and the capillary network, *Turk. J. Biol.*, 41: doi:10.3906/biy-1611-22

OTHER PUBLICATIONS, PRESENTATIONS AND PATENT

- **A.B.Ertan**, P.Yılgor, B.Bayyurt, Ayşe Ceren Çalikoğlu, Ç.Kaspar, F.N.Kök, G.T.Köse, V.Hasirci, Effect of Double Growth Factor Release on Cartilage Tissue Engineering, *Journal of Tissue Engineering and Regenerative Medicine*, DOI: 10.1002/term.509, 2011 (15 cites, 2017)
- 15th International Biomedical Science and Technology Symposium, Biomed, G.T.Köse, **A.B.Ertan**, A.C.Çalikoğlu, P.Yılgor, F.N.Kök, V.Hasirci, Use of Nanospheres in Cartilage Tissue Engineering, [oral presentation], 15th International Biomedical Science and Technology Symposium - BIOMED Güzelyurt, Northern Cyprus, 2009
- Biyomut (14. Biyomedikal Mühendisliği Ulusal Toplantısı), **A. Burcu Ertan**, A. Ceren Calıkoğlu, Pınar Yılgor, Fatma Nese Kok, Gamze Torun Kose and Vasıf Hasirci, Controlled Release of IGF-I Loaded in Nanospheres Improves, *In Vitro* Cartilage Formation, Izmir, 2009, [poster presentation]
- 13. Biyomedikal Bilim ve Teknoloji Sempozyumu, **A.B.Ertan**, P.Yılgor, N.Hasirci, G.T.Köse, V.Hasirci, Use of pH and Temperature Responsive Intelligent Nanobiomaterials in Cartilage Tissue Engineering [poster presentation], Biyomed, Istanbul, Turkey, 2007,
- 3rd Alea Jacta Expertissues **A.B.Ertan**, P.Yılgor, B.Bayyurt, Ayşe Ceren Çalikoğlu, Ç.Kaspar, F.N.Kök, G.T.Köse, V.Hasirci, “Drug Delivery, Targeting and Controlled Release of Growth Factors in Tissue Engineering”, Menorca, Spain, 2006 [poster presentation]
- Organization Committee Member, Cell Culture Appl. on Bone and Cartilage Tissue Engineering Workshop and Summer Course Yeditepe University Institute of Biotechnology, Cell Culture Appl. on Bone and Cartilage Tissue Eng Workshop and Summer Course, 2005